

2004

Online heat transfer measurement and analysis for sugar mill evaporators

David Timothy Solberg

Louisiana State University and Agricultural and Mechanical College

Follow this and additional works at: https://digitalcommons.lsu.edu/gradschool_theses



Part of the [Chemical Engineering Commons](#)

Recommended Citation

Solberg, David Timothy, "Online heat transfer measurement and analysis for sugar mill evaporators" (2004). *LSU Master's Theses*. 2161.

https://digitalcommons.lsu.edu/gradschool_theses/2161

This Thesis is brought to you for free and open access by the Graduate School at LSU Digital Commons. It has been accepted for inclusion in LSU Master's Theses by an authorized graduate school editor of LSU Digital Commons. For more information, please contact gradetd@lsu.edu.

**ONLINE HEAT TRANSFER MEASUREMENT
AND
ANALYSIS FOR SUGAR MILL EVAPORATORS**

A Thesis

Submitted to the Graduate Faculty of the
Louisiana State University and
Agricultural and Mechanical College
in partial fulfillment of the
requirements for the degree of
Master of Science in Chemical Engineering

in

The Department of Chemical Engineering

by
David Timothy Solberg
B.S., University of Natal, Durban, South Africa, 2002
December 2004

ACKNOWLEDGMENTS

The author would like to extend his thanks to Dr Peter Rein for his assistance and experience in undertaking this project and without whose guidance and experience this project would not have succeeded. Thanks are due to other members of Audubon Sugar Institute personnel who assisted with analytical analysis, Brian White and Lee Madsen II your assistance was greatly appreciated. Thanks are also due to those who were around to bounce ideas off and those who have gone through this already, thanks Bruce Ellis!

Appreciation is also extended to the department of chemical engineering who allowed the author to complete the masters program through their department. The coursework required by the department and committee of Dr Valsaraj and Dr Thompson contributed significantly to the authors understanding of a variety of chemical engineering processes.

Special thanks are due to all those at the St James sugar mill and South Louisiana Sugars Cooperative, especially Detlev Schlorke, who allowed the author to set up the project there and assisted financially as well as of their time to ensure the success of this project.

Assistance from Alan Cook of Control Systems who installed the control scheme at St James was also greatly appreciated.

TABLE OF CONTENTS

ACKNOWLEDGMENTS	ii
LIST OF TABLES	vi
LIST OF FIGURES	vii
GLOSSARY OF TERMS	xi
NOMENCLATURE	xii
ABSTRACT	xv
CHAPTER 1. INTRODUCTION	1
1.1 Sugar Mill Overview	1
1.1.1 Process Description	1
1.1.2 Evaporator Overview in the Sugar Industry	4
1.2 Research Objectives	5
CHAPTER 2. REVIEW OF LITERATURE AND BACKGROUND	7
2.1 Evaporators	7
2.1.1 Historical Overview	7
2.1.2 Evaporator Types	9
2.1.2.1 Horizontal-tube Evaporators	9
2.1.2.2 Vertical Short Tube Calandria (Robert or standard) Evaporators	10
2.1.2.3 Long Tube Vertical Evaporators	13
2.1.2.4 Rising Film Plate Evaporators	14
2.1.2.5 Falling Film Plate Evaporators	14
2.1.3 Recovery of Energy	15
2.1.4 Vapor Bleeding	16
2.1.5 Multiple Effect Evaporation	17
2.2 Heat Transfer Coefficients (and Rates of Heat Transfer)	17
2.2.1 What Is the Heat Transfer Coefficient?	17
2.2.2 Why Measure the Heat Transfer Coefficient?	18
2.2.3 Calculation of The Heat Transfer Coefficient	19
2.3 Boiling Processes	19
2.3.1 Pool Boiling	19
2.3.2 Forced Convection Boiling	20
2.4 Scale	21
2.4.1 Scaling and Its Significance	22
2.4.2 Sugar System Scale Components	24
2.4.3 Fouling and Mechanisms that Cause Its Occurrence	26
2.4.4 Modeling of Scale Formation	30
CHAPTER 3. THEORY	31

3.1	Heat Transfer Coefficients.....	31
3.2	Evaporator Model	34
3.2.1	Mass and Energy Balance	34
3.2.1.1	Single Effect Evaporator Balance	34
3.2.1.1.1	Mass Balance	36
3.2.1.1.2	Energy Balance	36
3.2.1.1.3	Temperature Differences	37
3.2.1.1.4	Heat Transfer	39
3.2.1.2	Quadruple Effects	40
3.2.1.2.1	Mass Balances	42
3.2.1.2.2	Energy Balances	44
3.2.1.2.3	Heat Transfer Coefficients	48
3.2.2	Correlations Used.....	50
3.2.3	Microsoft Excel® and Honeywell’s UMC800	50
3.2.4	Microsoft Excel® VBA code.....	54
3.3	Scale Model	57
3.3.1	Initial Model Proposed.....	57
3.3.2	Empirical Model	63
3.3.2.1	Time Dependant Empirical Model.....	63
3.3.2.1.1	McCabe and Robinson & Reitzer	63
3.3.2.1.1.1	Constant ΔT	63
3.3.2.1.1.2	Constant Flux	66
3.3.2.1.1.3	Unsaturated Solutions	67
3.3.2.1.1.4	General Model	68
3.3.2.1.2	Other Models	68
3.3.2.2	Clean Heat Transfer Coefficient	70
3.3.3	Proposed Model for Regression.....	71
CHAPTER 4. MATERIALS AND METHODS		72
4.1	St James Mill Setup	72
4.1.1	Control Scheme and Data Logging.....	72
4.1.2	Measurement Devices	74
4.1.2.1	Mag Flow Meters	74
4.1.2.2	RTD Probes.....	74
4.1.2.3	Microwave Brix Probe.....	76
4.2	Juice Analysis	77
CHAPTER 5. RESULTS AND DISCUSSION.....		79
5.1	Microsoft Excel® Model	79
5.1.1	Microsoft Excel® Model Development.....	79
5.1.2	Microsoft Excel® Model Execution	80
5.1.3	Microsoft Excel® Model Results	81
5.2	Juice and Syrup Analysis.....	89
5.3	Analysis of Heat Transfer Coefficient Data	100
5.3.1	Scaling Rates.....	100
5.3.2	Clean Heat Transfer Coefficient Prediction.....	104
5.4	Scale.....	105

CHAPTER 6. SUMMARY AND CONCLUSION	107
6.1 Recommendations for Future Work	108
REFERENCES	110
APPENDIX A EVAPORATOR MODEL MICROSOFT EXCEL® VBA CODE.....	114
A.1 Evaporator Model Microsoft Excel® VBA Code	114
A.1.1 Startup Macro.....	114
A.1.2 Solver Iteration Code	116
A.2 Code to Run Data After it Has Been Logged and Needs to be Rerun.....	122
APPENDIX B CALCULATION OF BOILING POINT RISE DUE TO HYDROSTATIC HEAD	129
B.1 Calculation of Boiling Point Rise Due to Hydrostatic Head	129
APPENDIX C P&I DIAGRAMS FOR ST JAMES MILL QUADRUPL	
EVAPORATOR TRAIN	131
C.1 P&I Diagrams for St James Mill Quadruple Evaporator Train	131
APPENDIX D CONTROLLER LABEL AND TAG VARIABLES USED AT ST JAMES	142
D.1 Controller Label and Tag Variables Used at St James	142
APPENDIX E SCALE MODEL CODE.....	143
E.1 Scale Model Code	143
E.1.1 Accumulation of Materials in the Evaporators.....	143
E.1.2 Time Dependant Scale Constant Regression.....	147
E.1.3 Clean Heat Transfer Coefficient Regression	149
APPENDIX F PROPERTY CORRELATION EQUATIONS	152
F.1 Property Correlation Equations.....	152
F.1.1 Pressure and Temperature.....	152
F.1.2 Latent Heat.....	154
F.1.3 Steam Enthalpy	156
F.1.4 Juice and Syrup Specific Enthalpy	157
F.1.5 Juice and Syrup Density	158
F.2 Other Correlations Used.....	161
F.2.1 Boiling Point Elevation.....	161
APPENDIX G ELECTROMAGNETIC FLOW METER SIZING AT ST JAMES	164
G.1 Electromagnetic Flow Meter Sizing at St James	164
G.1.1 Sizing the Meters	164
G.1.2 Installation Options of the Electromagnetic Flow Meters:	165
APPENDIX H RTD CALIBRATION.....	167
H.1 RTD Calibration	167
VITA.....	173

LIST OF TABLES

<u>Table</u>	<u>Title</u>	<u>Page</u>
Table 3.1:	Heat transfer coefficients as a function of temperature, Brix and viscosity.....	70
Table 5.1:	Regressed time dependant model constants.....	103
Table 5.2:	Regressed time dependant model constants.....	103
Table 5.3:	Heat transfer coefficients as a function of temperature, Brix and viscosity regressed data.....	105
Table H.1:	The calibration of the calandria RTD's based on saturated steam pressure.....	172

LIST OF FIGURES

<u>Figure</u>	<u>Title</u>	<u>Page</u>
Figure 1.1:	Block diagram of a typical Louisiana sugar cane mill.....	1
Figure 2.1:	The various down comer designs for Robert effects.....	11
Figure 2.2:	The various feed system designs for Robert effects, (a) Central Feed (b) Ring Distribution.....	12
Figure 3.1:	Heat transfer resistances in heat transfer showing the temperature profile in a typical evaporator tube.....	32
Figure 3.2:	A single evaporator effect evaporator diagram.....	35
Figure 3.3:	A quadruple effect evaporator setup for calculation mass and energy balances with no vapor bleeds.....	40
Figure 3.4:	The inputs and outputs data page from Microsoft Excel® simulation.....	52
Figure 3.5:	The model simulation page from Microsoft Excel® simulation.....	53
Figure 3.6:	The iteration option must be on.....	55
Figure 3.7:	The solver library must be loaded in the Visual Basic Editor.....	55
Figure 3.8:	The play macro command in Microsoft Excel ®.....	56
Figure 3.9:	Selecting the macro to run in Microsoft Excel ®.....	56
Figure 3.10:	Mass balance schematic for juice and syrup components.....	62
Figure 4.1:	The measured variables at the St James sugar mill evaporators.....	72
Figure 4.2:	The control loops used at the St James sugar mill evaporators.....	73
Figure 4.3:	RTD probe installation in juice lines at the St James sugar mill evaporators.....	75
Figure 4.4:	RTD probe installation the third effect calandria at the St James sugar mill evaporators.....	76
Figure 4.5:	Final effect Microwave Brix probe at the St James sugar mill evaporators.....	77

Figure 5.1:	Syrup temperatures recorded for the St James evaporators.....	82
Figure 5.2:	Calandria temperatures recorded for the St James evaporators.....	83
Figure 5.3:	Juice and Syrup volumetric flows recorded for the St James evaporators.....	84
Figure 5.4:	Sensitivity analysis of vapor temperature changes.....	85
Figure 5.5:	Differential temperature recorded for each effect at the St James evaporators.....	86
Figure 5.6:	Exit Brix sensitivity analysis.....	87
Figure 5.7:	Computed heat transfer coefficients with flow filtered at the St James evaporators.	88
Figure 5.8:	Computed heat transfer coefficients with flow and heat transfer coefficients filtered at the St James evaporators.....	88
Figure 5.9:	Clarified Juice weekly composite purity.....	90
Figure 5.10:	Syrup weekly composite purity.....	90
Figure 5.11:	Clarified juice weekly composite ash.....	91
Figure 5.12:	Syrup weekly composite ash.....	92
Figure 5.13:	Clarified juice weekly composite refractometer Brix.....	93
Figure 5.14:	Syrup weekly composite refractometer Brix.....	93
Figure 5.15:	Clarified juice weekly composite cation and anion analysis results..	94
Figure 5.16:	Syrup weekly composite cation and anion analysis results.....	94
Figure 5.17:	Clarified juice weekly composite ion analysis results.....	95
Figure 5.18:	Syrup weekly composite ion analysis results.....	95
Figure 5.19:	Clarified juice weekly composite ion analysis results expanded view.....	96
Figure 5.20:	Syrup weekly composite ion analysis results expanded view.....	96

Figure 5.21:	Clarified juice weekly composite ion analysis results expanded view.....	97
Figure 5.22:	Syrup weekly composite ion analysis results expanded view.....	97
Figure 5.23:	Accumulation in the evaporators based on average conditions.....	99
Figure 5.24:	Regression for time dependence of heat transfer coefficients for the first data period.....	101
Figure 5.25:	Regression for time dependence of heat transfer coefficients for the second data period.....	101
Figure 5.26:	Regression for time dependence of heat transfer coefficients for the third data period.....	102
Figure 5.27:	Regression for time dependence of heat transfer coefficients for the fourth data period.....	102
Figure 5.28:	Regression for clean value of the heat transfer coefficients for the first twenty four hours per clean.....	104
Figure 5.28:	Scale in the tubes of the final effect at the end of the season.....	106
Figure B.1:	Pressures and temperatures in the evaporator vessel.....	128
Figure F.1:	Saturated steam pressure related to saturated steam temperatures from steam tables.....	152
Figure F.2:	Error between saturated pressure and temperature for saturated steam correlation used in modeling.....	153
Figure F.3:	Error in latent heat measured value and that computed from steam and water properties at the same saturated temperature.....	154
Figure F.4:	Error in latent heat correlation from equation F.2 as a function of saturated temperature.....	155
Figure F.5:	The fitting of the polynomial in equation F.2 to literature latent heat data.....	156
Figure F.6:	The fitting of the polynomial in equation F.3 to literature vapor enthalpy data.....	156
Figure F.7:	Error in steam enthalpy correlation from equation F.3 as a function of saturated temperature.....	157

Figure F.8:	Boiling point elevation as a function of temperature at a purity of 90%.....	162
Figure F.9:	Boiling point elevation as a function of purity at a temperature of 80°C.....	162
Figure G.1:	Installation of a flow meter to ensure single phase flow on the pipe section containing the meter.....	166
Figure G.2:	Horizontal alignment (left) and vertical alignment (right) for the mag flow meters used at St James.....	166
Figure H.1:	The calibration of RTD's using a heated beaker and calibrated thermometers.....	167
Figure H.2:	The calibration curve of RTD TT-001.....	168
Figure H.3:	The calibration curve of RTD TT-002.....	168
Figure H.4:	The calibration curve of RTD TT-003.....	169
Figure H.5:	The calibration curve of RTD TT-004.....	169
Figure H.6:	The calibration curve of RTD TT-005.....	170
Figure H.7:	The calibration curve of RTD TT-007.....	170
Figure H.8:	The calibration curve of RTD TT-008.....	171
Figure H.9:	The calibration curve of RTD TT-009.....	171

GLOSSARY OF TERMS

<u>Term</u>	<u>Meaning</u>
Billet	A short cut section of a cane stalk.
Brix	Refractometer Brix, an optical measurement related to dissolved solids.
CFD	Computational Fluid Dynamics
HPLC	High Pressure Liquid Chromatography, used to measure the concentration of specific components based on retention times on a stationary phase.
HTRI	Heat Transfer Research Institute
LSU	Louisiana State University
Massecuite	A mixture of sugar crystals and molasses that comes from the pans.
PI	Preparation Index, a measure of the openness of cane bundles after preparation for milling or diffusion.
Pol	Solution sucrose concentration measured using a polarimeter.
ppm	Parts Per Million, a measure of concentration.
RTD	Resistance Temperature Device.
Train	A collection of typically three to five evaporator vessels making up an evaporator station.
VBA	Visual Basic for Applications, a programming extension of visual basic used for programming in applications.

NOMENCLATURE

A subscript i refers to vessel i , where i ranges from 1 to n (where n is the number of effects). A subscript j refers to a component of scale where j ranges from 1 to m (where m is the number of scale components considered).

Symbol	Description	Units
A	Area	m^2
A_{cs}	Cross sectional area	m^2
a to f	Proportionality constants	-
B	Brix	%
B_{avg}	Average mass fraction of solids in vessel (Brix)	%
B_F	Mass fraction of solids in the feed to vessel (Brix)	%
B_L	Mass fraction of solids in the concentrate from vessel (Brix)	%
B_o	Boiling number	-
B_V	Mass fraction of solids in the vapor from vessel (Brix)	%
b	Slope of the solubility curve	-
b	A constant	-
C	Mass flow of condensate from vessel	kg/s
$C_{1 \text{ to } 8}$	Constants	-
C_b	Bulk concentration	kg/m ³
C_{eqi}	Equilibrium concentration of component i	kg/m ³
C_r	Concentration of reacting species	kg/m ³
C_s	Heating surface concentration	kg/m ³
C_{si}	Scale concentration of component i	kg/m ³
C_{ss}	Supersaturated concentration	kg/m ³
C_{sat}	Saturated concentration	kg/m ³
c	A constant	-
c_p	Specific heat of solution	J/kgK
c_{pv}	Specific heat of steam vapor	J/kgK
d	Diameter	m
d	A constant	-
E	Activation energy	J/mol
E_b	Enhancement factor for boiling	-
F	Mass flow of feed to the vessel	kg/s
g	Gravitational acceleration constant = 9.81	m/s ²
G	Mass flux	kg/m ²
H	Vapor enthalpy	J/kg
H_S	Enthalpy of the steam (or vapor) feed to vessel	J/kg
H_V	Enthalpy of the vapor generated in vessel	J/kg
h	Liquid enthalpy	J/kg

h_L	Enthalpy of the concentrated liquid leaving vessel	J/kg
h_C	Enthalpy of the condensate from vessel	J/kg
h_F	Enthalpy of the feed to vessel	J/kg
h_i	Film coefficient, inside tubes	$\text{kW/m}^2\text{K}$
K	A constant	-
k	Overall heat transfer coefficient	$\text{kW/m}^2\text{K}$
k_o	Clean value of the overall heat transfer coefficient	$\text{kW/m}^2\text{K}$
k_d	Combined diffusion-reaction mass transfer coefficient	m/s
k_{pi}	Mass transfer coefficient of component	m/s
k_W	Thermal conductivity, metal wall	kW/mK
k_{LS}	Thermal conductivity, scale (juice side)	kW/mK
k_t	Thermal conductivity	kW/mK
k_f	Thermal conductivity of fouling scale	kW/mK
k_{CS}	Thermal conductivity, scale (steam side)	kW/mK
L	Mass flow of liquid from the vessel	kg/s
L_T	Tube length	m
m	Mass deposited	kg
m	A constant	-
m^*	A constant	kg
n	Number of evaporator effect stages	-
n	Order of scaling process	-
n'	Constant exponent	-
P	Pressure in the boiling liquid	kPa
P_S	Steam (or vapor) pressure heating the effect	kPa
P_V	Pressure in vapor space of vapor generated in effect	kPa
Q	Heat transferred	kW
q	Heat flux (Heat flow per unit area)	kW/m^2
q_r	Radial heat flux	kW/m^2
R	Universal gas constant	J/molK
R_b	Deposit bond resistance	-
R_f	Fouling resistance	Km^2/kW
$R_{f\infty}$	Fouling resistance as $t \rightarrow \infty$	Km^2/kW
R_i	Thermal resistance term	K/kW
S	Mass flow of “steam” (or vapor) to the vessel	kg/s
T	Vessel temperature	K
T	Temperature	K
T^{sat}	Saturated boiling point of water at pressure P	K
T^I	The boiling point of water at pressure	K
T_{boiling}	Temperature of the boiling fluid in the effect	$^{\circ}\text{C}$
$T_{\text{BPR-Bx}}$	Boiling point rise due to Brix effects	$^{\circ}\text{C}$
$T_{\text{BPR-HH}}$	Boiling point rise due to hydrostatic effects	$^{\circ}\text{C}$
T_F	Temperature of the feed	K
T_S	Steam (or vapor) temperature	K

T_V	Vapor temperature	K
T_{juice}	Temperature of the juice	$^{\circ}\text{C}$
T_L	Liquid temperature	K
T_C	Condensate temperature	K
T_W	Wall Temperature	K
t	Time	s
t_c	Characteristic time	s
t_d	Induction time	s
U	Unit step function	-
W	Mass flowrate	kg/s
V	Mass flow of vapor from vessel	kg/s
X_{tt}	Lockhart-Martinelli parameter	-
x	Vapor quality (vapor mass fraction)	-
x_f	Scale deposit thickness	m
z	Height of liquid syrup in the evaporator	m

Other Symbols:

Symbol	Description	Units
α	A constant	-
β	A constant	-
β'	Proportionality constant	-
Δh_v	Latent heat of vaporization	J/kg
ΔT	Differential temperature	K
ΔT_o	Initial (Clean) value of ΔT	K
λ	Latent heat of steam	J/kg
ρ	Density of a solution	kg/m ³
ρ	Density of solid scale	kg/m ³
ρ_f	Fluid density	kg/m ³
ρ_f	Density of scale	kg/m ³
ρ_l	Density of liquid	kg/m ³
ρ_v	Density of vapor	kg/m ³
τ	Shear stress	Pa
ϕ_d	Deposition rate	kgm ⁻² s ⁻¹
ϕ_r	Removal rate	kgm ⁻² s ⁻¹
π	Pi	-
Ψ	Deposit strength	-
μ	Viscosity	Nsm ⁻²
μ_{juice}	Viscosity of juice	Nsm ⁻²
μ_l	Viscosity of liquid	Nsm ⁻²
μ_v	Viscosity of vapor	Nsm ⁻²

ABSTRACT

Fouling and scaling in evaporators has been an area of great interest to raw sugar mills for a number of years and many of the mechanisms causing the scale and the rates of scaling are unknown. In an attempt to quantify the scaling rates and measure the scaling, an online model has been developed to model a system of evaporators. Monitoring the heat transfer coefficient as a function of time enabled measurement of the scaling rate by monitoring the heat transfer coefficient as it decreased with time. It is assumed that the scaling on the juice side of the evaporators with time is the only contributor to the drop in heat transfer and that other effects such as the fouling of the steam side are negligible.

A large problem in the past was reliable measurements of the heat transfer coefficient on evaporators. This was usually because the procedure required multiple measurements that needed to be taken by expensive equipment, which meant large amounts of capital to set up the monitoring systems. Another issue in the past was the iterative nature of the calculations, but with the advancements in computer processing and control systems, it is now possible to setup a control system that requires fewer inputs and low-cost instrumentation to get accurate measurements of the heat transfer coefficient. Utilizing the processing power of the control computer to perform multiple iterations allows for quick convergence to the solution of the heat transfer coefficient for the system.

The scaling rates are measured on a simple quadruple effect evaporator with no vapor bleeds at the St James sugar mill in Louisiana. A model was developed to predict

the scaling rates of the individual effects based on the heat transfer coefficient measurements.

Analysis of the juice and syrup streams to and from the evaporators was performed to quantify the scale components in the scale that accumulates in the evaporators.

The measurement of the heat transfer coefficient shows, as is sometimes seen in practice, that the final effect is the effect that will scale the most and determines the need for the effect to come offline to be cleaned. This information on the degree of scaling is useful for the mills as they can use this to optimize cleaning of the effects.

The measured values of the heat transfer coefficients fell within measured values from other sugar milling countries. The results show that the use of computers enables one to calculate a heat transfer coefficient for a system of evaporators in real time.

CHAPTER 1. INTRODUCTION

1.1 Sugar Mill Overview

1.1.1 Process Description

The process of sugar production from sugar cane (various hybrids of *Saccharum* are used in Louisiana) can be split into a number of separate processes or unit operations. A simplified diagram of a sugar cane mill is shown in figure 1.1 below. The process is described in a little more detail after figure 1.1 below.

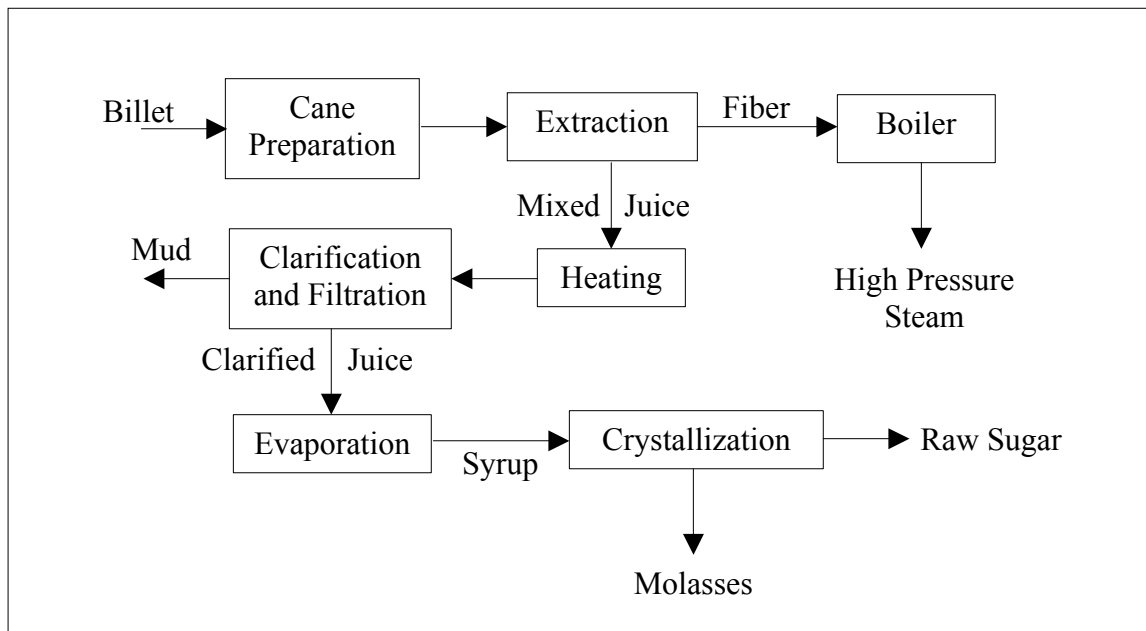


Figure 1.1: Block diagram of a typical Louisiana sugar cane mill

In Louisiana sugar cane is harvested in billet form and the sections of cane range from 46 cm to 56 cm in length (Hoy et al., 2004). In Louisiana the cane is sometimes washed, if it has been harvested after rain before being sent to cane preparation, but this is avoided whenever possible as it results in sugar losses. In cane preparation the cane is shredded, cut with knives and hammered or fiberized to prepare the billets for the next

step of the process of extraction by opening the cane cells. The efficiency of pre-extraction processing is measured by the preparation index (PI), which basically measures the amount of cane cell rupture after cane preparation. The higher the preparation index, the more efficient the extraction step can be.

A large majority of the sugar mills in Louisiana use physical methods in the extraction operation, using large three or four large roll mills to express the juice. Once the cane has been prepared the fiber and sugar matte mix is sent to a milling tandem, a mill will squeeze the sugar juice from the fiber. Usually a tandem of four to six mills will be used to separate the fiber and sugar in the cane. Water is run as imbibition on each mill to aid extraction of sucrose from the fiber mat. Only one of the mills in Louisiana uses a diffuser for cane extraction where the separation process is based on countercurrent solid liquid extraction. The use of a diffuser still requires the use of dewatering mills at the tail end of the process.

The fiber from the process is then sent to the boilers to produce high-pressure steam that is used for later processing operations, electricity production and turbine operation. The exhaust steam (low pressure) from turbines and other processes is used in the pan, heater and evaporator stations for heating and boiling. If fiber is produced in excess of that required for the mill's energy requirements the fiber can be used for a number of possible projects. The options include, producing excess steam and cogeneration of electricity or the fiber could be used to manufacture paper or similar processes requiring fiber.

The juice expressed from the cane in the extraction stage is collected and passed to the next stage of processing. The juice from this section of the mill is called mixed

juice. The mixed juice is heated, limed and clarified to remove solid materials present. The juice in the underflow of the clarifier is filtered and then filtrate is re-circulated back with the mixed juice and re-clarified; any mud from the filters is discarded. The overflow from the clarifier is sent to the evaporator station and is called clarified juice. The clarified juice can have a sugar concentration varying in the range of twelve to sixteen percent by mass, depending on mill operation.

The clarified juice is evaporated in a multiple effect evaporator train heated by exhaust steam and then the concentrated stream, called syrup, is sent to the pans for crystallization. The evaporated water vapor from this unit operation of evaporators is used for heating and condensates from the calandria are recycled within the mill. In the evaporator station the clarified juice is concentrated up to between 60 and 68 Brix by driving off water present in the juice. Brix is the sugar content by mass expressed as a percentage.

In the crystallization operation pans are used to heat the syrup and concentrate it until crystallization begins to occur. The crystallization conditions are carefully controlled to maintain a constant product crystal size. The pan will yield a mixture of crystals and molasses called massecuite. The massecuite is centrifuged in batch or continuous centrifuges depending on the final sugar grade required. The process is repeated in a number of boilings until the molasses formed has low sugar content, and a low purity.

The molasses and sugar products are stored and sold. The sugar is sold to refineries that will purify the sugar from 98.5% to 99.9+% (pol based percentages) pure and the

molasses is typically sold as an animal feed additive. Some other countries use the molasses to produce other products such as ethanol.

1.1.2 Evaporator Overview in the Sugar Industry

An evaporator is a heat transfer operation that heats a fluid to its boiling point, causing it to generate vapor. Heat is supplied to the evaporator by condensing a steam or vapor stream in a calandria. An evaporator contains a calandria where the heating vapor is fed. There is a tube wall separating the fluid and the steam and the heat is conducted through this wall to the juice on the other side.

In Louisiana sugar mills, the evaporators are typically triple or quadruple effects with a pre-evaporator before the train. The pre-evaporator is essentially another first effect in series with the first effect of the mill's evaporator train. Vapor is typically bled from the evaporators to decrease a mill's exhaust steam usage and increase steam efficiency. Other methods to save on exhaust usage include vapor recovery and vapor recompression, which can be mechanical recompression or thermo recompression. In vapor recompression the generated vapor is recompressed using steam ejectors or compressors and fed back into the calandria of the vessel that generated the vapor. Vapor recovery is used to decrease steam consumption. Condensate from a vessel can be flashed at a lower pressure to evolve more lower pressure vapor to be used in the next effect's calandria.

There are a number of different types of evaporator construction and feed distribution systems used. In evaporator designs even the juice flow directions can vary from one type of evaporator to another. The applicability of a particular evaporator is dependant on the duty it has to perform. In sugar mills of Louisiana, where cane is

processed even in bad weather, the juice tends to be fairly dirty and the applicability of plate evaporation technology is difficult if sufficient clarification is not attained. In a large majority of cases in the Louisiana industry the evaporators are Robert types, but some mills are using a few rising plate effects. The description of all the types of evaporators and construction options are extensive and so are described later in this document. All of the mill evaporator trains are forward feed systems, i.e. the vapor and liquid flow in the same direction along the train.

1.2 Research Objectives

A significant drawback to operating evaporators at a sugar mill is the fact that they will foul with time. As the fouling occurs the rate of heat transfer decreases. The rate at which this process of reduced heat transfer occurs can be monitored by measuring the heat transfer coefficient. The aim of the research was to develop an online model for a mill that would compute the heat transfer coefficient on each evaporator effect. This data would alert the mill when a particular effect was dirty and which effects were clean and therefore did not require cleaning. Another aim was to develop a model of scaling to predict when vessels would need to be cleaned over time. The data collected was also used in predicting the heat transfer coefficients of vessels to plan cleaning for design purposes.

The St James sugar mill and Audubon Sugar Institute worked on a joint venture to evaluate the heat transfer coefficients of the St James Nadler quadruple effect evaporator train online during the 2003/2004 season. The evaluation of the heat transfer coefficient for each effect is calculated using the total volumetric flow in and out the quadruple

effect from magnetic flow meters, the Brix out the final effect and a number of temperatures recorded from RTD's in the vessels and interconnecting piping.

The reason for calculating the heat transfer coefficient online is important because the heat transfer coefficients are related to the degree of scaling in the vessels. As a vessel scales up the heat transfer coefficient for that effect drops. Measuring the drop in heat transfer can help the mill determine which vessels require cleaning and when cleaning should be performed. Cleaning only dirty effects when they have dropped below a preset set point can mean that unnecessary cleaning of "clean" vessels is eliminated and the total costs of cleaning the evaporators as well as total downtime for cleaning can be reduced significantly.

The cost saving from reduced downtime and cleaning chemical costs is the main focus for the mills with the project but the extra measurements of flows and Brix can also help mills with refining their mill balances. For Audubon Sugar Institute the data is used to try to predict the scaling characteristics for the evaporator vessels to help in designing evaporator vessels more efficiently and understanding evaporator scaling.

CHAPTER 2. REVIEW OF LITERATURE AND BACKGROUND

2.1 Evaporators

2.1.1 Historical Overview

A thorough review of the history of patents and use of patented equipment is covered by Deerr (1950) and some of the more significant highlights from this source and others are reproduced here. In the early days of evaporation the process typically took place over a direct flame in single open vessels (Deerr, 1950). Some have speculated that heating occurred indirectly by placing heated stones in the liquid to be evaporated, to evolve vapor, but this belief cannot be substantiated. The open vessels were placed in trains around 1657 with the heated air from the single flame source passing under them and became known as a batterie, “Jamaican train” or “copper wall”. It was not until around 1692 that steam was used to heat liquids but the first patents for application to the cane industry only began in the 1817’s and the first use recorded only in 1845. The vessels however remained open until the introduction of vacuum pans in 1813 by Edward Howard. Walker developed the calandria in 1852.

In 1843 (Deerr, 1950) Norbert Rillieux, the son of a slave in Louisiana, is credited with the invention of the horizontal single effect evaporator (Coulson, 1962). It contained a horizontally oriented calandria comprised of tubes, which had steam passing on the inside, and juice passing on the outside of the tubes, this design was particularly prone to fouling. Rillieux also utilized the idea of vacuum evaporation by Howard to successfully develop multiple effect evaporation, which revolutionized the evaporation industry. Attempts had been made previously at multiple heat utilization by William Cleland in

1826 and Degrand in 1833 who worked on double effect evaporation. Later Pecqueur (1834), Derosne (1836) and Rillieux (1843 and 1846) worked on inventing true multiple effect evaporation. Rillieux claimed in 1832 that he had the idea for multiple effect evaporation and had discussed it with Derosne. All of the Rillieux effects only had horizontal calandrias and the only real changes in multiple effect evaporation since those early days are the vessels themselves. It was not until 1880 that Rillieux developed the vapor bleeding system, which is now standard for multiple effect evaporation systems to increase steam usage efficiency. Pauly and Greiner from Germany utilized a pre-evaporator for vapor bleed generation.

Cail, a Frenchman, in 1850 was the first person to patent an evaporator with vertical tubes. After 1870 an Austrian named Jules Robert contributed significantly to what is now known as the Robert evaporator after he had perfected the diffuser he had been working on. Other significant contributions for this vessel at the time came from other Austrians, Welner and Jelinek. The initial design of Robert did not contain a central down comer as seen in more modern vessels and juice flowed up the tubes then around the side of the vessel and down a space between the containment vessel and the calandria. Modern vessels have varied inlet and outlet positions but have tended to use the central down comer, developed by Kasalovsky, as opposed to the outer ring down comer.

Since the invention of the short tube Robert evaporator, modifications were made to invent a long tube, or Kestner, evaporator in 1903. Another advancement for tube evaporators included forced flow to increase tube velocities. The advent of falling film effects had a significant advantage over rising film effect as the overall effective differential temperature for boiling over an evaporator train was increased due to the

falling film effect does not have a boiling elevation caused by a hydrostatic head. This change allowed the possibility of more effects in a train or increasing vapor pressures produced if the number of effects was kept constant.

Plate evaporators are a fairly recent invention and contain no tubes but rather use specially shaped plates to separate the vapor and juice. The plates are designed to ensure good juice distribution without causing blockages in the channels. The plate evaporators come in both falling and rising film modes. All these evaporators are described in more detail in the next section.

Thermo compressors were introduced by the French Engineers Prache and Bouillon (1905 and 1909) but not used until 1920 in a factory.

2.1.2 Evaporator Types

As mentioned previously there are a number of different evaporator configurations and designs that have been used over time. In the next few sections a review of the significant designs will be performed and notes made of any particular advantages and disadvantages with each of them.

2.1.2.1 Horizontal-tube Evaporators

These evaporators were the first closed vessels used in modern multiple effect evaporation. They are particularly prone to fouling as they have steam passing through the inside of the tubes where it condenses. The juice to be evaporated is passed on the outside of the tubes and materials deposit on the tube bundles as it fouts. This particular construction is no longer commonly used because of the fouling issues associated with it. The tubes are typically fairly small being only 2cm to 3cm in diameter (Kern, 1950). The vessels do not transfer heat as efficiently as a horizontal tube setup but require less vessel

vapor space and are easier to bleed incondensable gases from the calandria than the horizontal sets. Even though these vessels were among the first effects used in the sugar industry these vessels are no longer used in the sugar industry because of the major disadvantages they possess.

2.1.2.2 Vertical Short Tube Calandria (Robert or standard) Evaporators

These evaporators are the most common in the sugar industry and were developed after the vertical-tube version. The tubes are short (1.2m to 2.4m) and of a fairly wide diameter (5cm to 10cm) according to McCabe and Smith (1956). The vessels were initially designed with a central calandria and the juice would flow down along the outside of the calandria. Since these effects had a “basket” for the calandria hung in the vessel they were referred to as basket-type evaporators. Modern Robert evaporator vessels have been modified to collect the evaporated juice in a central down comer in the middle of the calandria. Since these effects are so common in the sugar industry they will be focused on the most in these discussions.

There are a number of different designs of down comers and each has reasons for their use. According to Kern (1950) the down comer is typically between half and the same area of the total cross-sectional area of the tubes in the calandria. In a number of Australian designed effects the central down comer does not get piped away and the concentrated juice and feed juice are mixed in the liquid space below the calandria. Different designs of this are shown in figure (2.1). Also depicted in the center of figure (2.1) is the commonly used sealed down comer. The sealed down comer allows complete removal of the evaporated syrup without back mixing with the lower Brix juice fed to the effect. The final illustration in figure (2.1) is that of a semi-sealed central down comer.

The vessel with no down comer requires extra attention in controlling the level. In order to correct the level control some down comers include an overflow around the outside of the down comer tube. This keeps the level constant at the height of the cone in the effect without the use of level control according to Wright et al (2003). Wright et al (2003) believe that the down comer design has an advantage over the system with no down comer as the down comer prevents short circuiting but they argue it has limitations controlling the juice level. The Australians have found that the level of juice in the evaporator affects the heat transfer coefficient. In order to optimize the heat transfer it could therefore be argued that a variable juice level is required. All these three options are shown in figure (2.1).

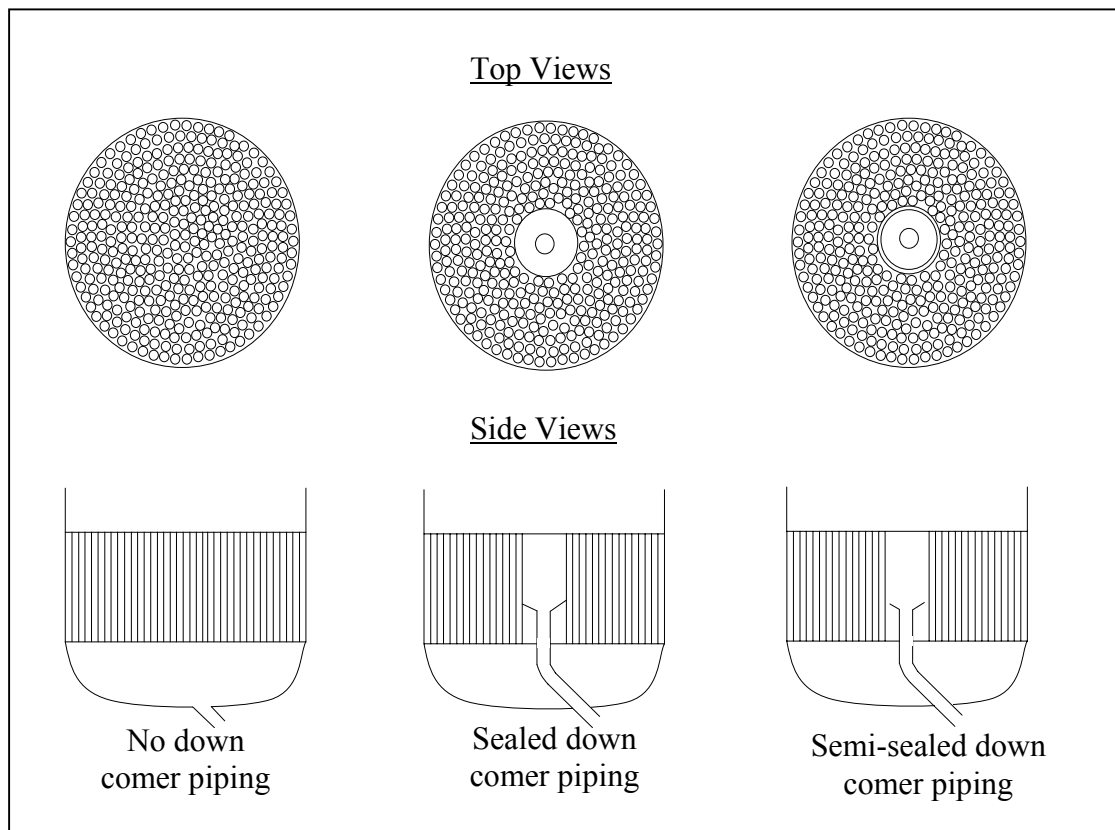


Figure 2.1: The various down comer designs for Robert effects.

The feed arrangements also vary for the Robert effects. The feed arrangement can affect the flow patterns of the juice in the effect. The flow contributes significantly to heat transfer and good feed distribution is essential. The simplest feed arrangement is a single inlet with a feed distribution plate to assist distribution into the vessel. This is however not as efficient as a ring distribution system. These two options are shown in figure (2.2). The mill at St James had a single feed inlet for the 2003/2004 season but have modified the system to a ring distribution system for the 2004/2005 season. Work in Australia has shown (Wright et al, 2003) that an increase in juice flow pattern towards ideal conditions can be realized if the juice is fed as a distributed ring rather than in the centre. It has been calculated that the ring feed system increases the circulation rates and improves the flow patterns, decreasing channeling and recirculation to improve heat transfer using CFD models.

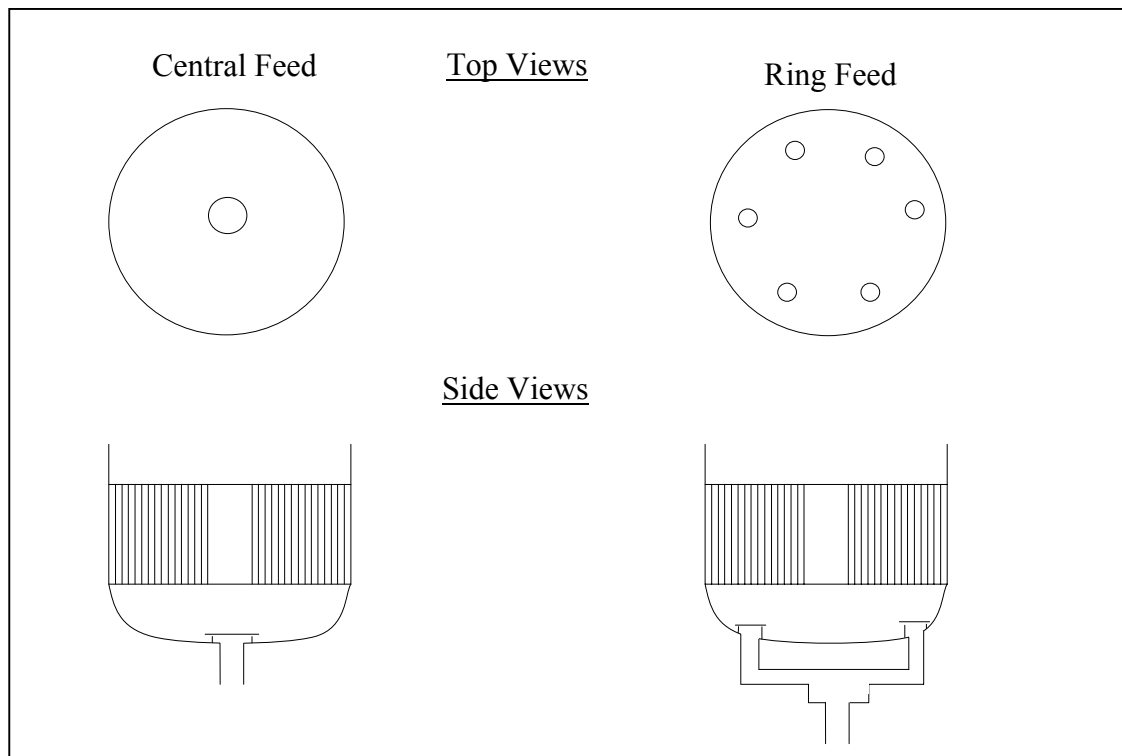


Figure 2.2: The various feed system designs for Robert effects, (a) Central Feed (b) Ring Distribution.

Steam distribution and incondensable vapor buildup in the calandria is an important consideration which cannot be overlooked. To improve steam distribution patterns there is typically a steam belt around the tube bundle and baffles, which direct steam in a specific direction to the bleed positions for incondensable gases. The incondensable vents need to be at the end of the flow pattern for the steam inlet to utilize the most energy and get the best flow pattern. When bleeding the vapor it is important to bleed at the top and bottom of the calandria, as some of the incondensable vapors have a higher density than steam and others have a lower density, so to prevent buildup of either two bleed points are needed.

Forced circulation short tubes are available and are typically used when low retention applications are required and will have smaller tubes than natural circulation effects. The velocities are higher in forced circulation effects. A big advantage for low residence times in the evaporators is the prevention of color formation. The lower the exposure to elevated temperatures the lower the color increase from the evaporation process. The cost involved with operating forced circulation effects is the cost of operation and maintenance on the pumps to force the high flow rates through the units.

2.1.2.3 Long Tube Vertical Evaporators

These evaporators have longer tubes than the Robert effects. They can be forced flow or natural flow systems and can be operated in falling or rising film modes with velocities higher than those found in short tube effects. The tubes are typically of the order of 3.5m to 10m in length and 2.5cm to 5cm in diameter according to McCabe and Smith (1956). Again forced flow systems have high operating costs but because of the

high velocities present the vessels have less of a scaling issue than short tube effects and better heat transfer.

2.1.2.4 Rising Film Plate Evaporators

These evaporators are fairly modern. One of the mills in Louisiana uses a rising film evaporator to boost the second effect evaporator capacity. The use of plate technology requires more stringent feed conditions and control compared to the Robert effects typically found at the mills, but plate technology may provide higher heat transfer coefficients than Robert effects. The beet industry have fairly clean juice compared to the cane industry and so have adopted film technology fairly rapidly, but the cane industry has been slower in adopting plate technology. A major advantage of plate technology is that if extra capacity is required it is simply achieved by adding more plates to the existing pack. The plate effect unit area is also compact when compared to the Robert effects, allowing installation in smaller areas. The major disadvantage with plate technology is the juice distribution, if the juice is not distributed well the plates can have channeled areas that cause bypassing and decrease heat transfer. The plates are specifically designed to try to avoid this problem but if not properly addressed the plate effect may perform poorly.

2.1.2.5 Falling Film Plate Evaporators

The falling film evaporators have the major advantage of negating the boiling point elevation due to hydrostatic head of fluid in the vessel, essentially increasing the available differential temperature across a multiple effect evaporator train. This allows more effects and better quality vapor to be used and produced. The distribution of juice onto the plate packs is an issue and many different distribution systems have been

developed to deal with it. Again these systems typically require more control than traditional evaporator technology.

2.1.3 Recovery of Energy

There are many methods for recovering energy and conserving steam usage, the principle being multiple effect evaporation discussed later in this document. There are however other methods used for vapor recovery that either increase vapor quality or recover energy from condensates produced.

Mechanical vapor recovery involves the compression of vapor produced to increase the energy content of the vapor. The higher energy vapor is then re-circulated back to the calandria of the vessel where the vapor was produced from and used to evolve more vapor. A variation of this recovery is thermo recompression that uses high-pressure steam to upgrade the vapor energy rather than mechanical means. Thermo recompression is basically a steam ejector; the average energy of the steam injected and the vapor to be recompressed is greater than the initial vapor energy thus causing the vapor pressure and temperature of the recompressed vapor to increase.

The flashing of condensates is not a major source of vapor but can assist vapor and steam usage. The condensate from an effect is fed to a knock out vessel where decreasing the pressure flashes off the recovered vapor; this is achieved by pressurizing the knock out vessel with the vapor of that effect which is at a lower pressure than the steam and condensate. The flashed vapor is then mixed with the vapor from the effect and fed into the calandria of the next effect.

2.1.4 Vapor Bleeding

The vapor is bled and used in a number of different ways; the most important vapor bleed in terms of steam conservation from the mills point of view is that of multiple effect evaporation. The vapor of the first effect is used as the heating steam for the next effect and so forth. The steam saving are proportional to the number of effects in this train so steam demands for evaporation are drastically reduced by using multiple effect evaporation.

The next most significant vapor bleed is when the vapor in an effect is bled to the plant for heating as this decreases the steam usage according to the Rillieux principles. The vapor bled is of a slightly lower pressure and temperature than the exhaust steam used in the first effect evaporator. This means that is if the vapor is used for heating in the plant the required heat transfer surfaces need to be slightly larger than they would have been if exhaust steam were used. The capital cost of more heat transfer area is often less in the long term than the operating costs over an extended time period.

The steam calandria also need to have vapor bled from them to prevent incondensable gases building up in the calandria that can blind heat transfer surfaces and reduce heat transfer. It has been noticed by Selman and Plomley (1950) that this requires attention, particularly in design, and typically the bleed lines are undersized. It is recommend to use an area double that of the regular design sizes to ensure this is avoided. They also note that the most incondensable vapors accumulate in the second effect calandria that uses vapor from the first effect.

2.1.5 Multiple Effect Evaporation

Rillieux made the use of multiple effect evaporation famous and a number of evaporator principles are named after him. The steam usage is proportionately decreased with the number of effects in the multiple effect evaporator train. In multiple effect evaporation the vapor generated in an effect is used to heat the juice in the next effect, hence the vapor from a previous effect thus acts as the steam for the next effect. In order for the vapor to be used as steam in the next vessel the vapor generated in the next vessel has to boil at a lower temperature than the previous effect. This process is achieved by having a pressure drop in the vapor space in vessels that will lower the saturated temperature of the vapor, reducing the boiling point.

One would assume that for the best steam economy the best course of action would be to have as many effects in the evaporator train as possible. There is however limitations with the temperature driving forces available for the evaporator set. The higher the initial steam temperature and the lower the vacuum pressure on the final effect the more differential temperature and thus the more effects can be added to a train. In general a sugar mill will have four or five effect in a train and in a few cases as high as six effects are used in evaporator trains, but these cases are rare. The more common range, at least in Louisiana, is a triple or quadruple effect evaporator train.

2.2 Heat Transfer Coefficients (and Rates of Heat Transfer)

2.2.1 What Is the Heat Transfer Coefficient?

The heat transfer coefficient is a measure of the efficiency of the transfer of heat from one medium to another. It includes a temperature differential, surface area and heat transfer dependence. The advantage of using the heat transfer coefficient as opposed to an

evaporation rate per unit area is the fact that it takes into account temperature difference so is a good basis for comparison between effects where operating conditions such as temperature may vary. In general the rate of evaporation purely on a mass flow basis can be improved by increasing the saturated temperature of the condensing steam, but this does not necessarily increase the heat transfer efficiency.

2.2.2 Why Measure the Heat Transfer Coefficient?

There are a number of reasons to measure the heat transfer coefficient online and some of the areas it is perceived that it can assist operations are listed below:

- Optimize evaporator performance and energy utilization.
- Optimize cleaning and maintenance procedures for evaporators.
- Try to understand the formation of scale with time and find ways to reduce its formation.
- Optimum design of multiple effect evaporators.
- Troubleshooting when problems arise with the evaporator sets.
- Highlight under-performing evaporator vessels.
- Evaluate the scale heat transfer coefficient at steady state then record that over time to optimize cleaning time (if all other processes remain constant).
- During design to be able estimate the theoretical time between cleans.
- Optimize cleaning costs.
- Establish how process parameters e.g. Clear juice pH and ion concentration affect scaling.
- Measure effectiveness and cleaning of each individual vessel.
- Measure efficiency of anti-scalants.

2.2.3 Calculation of The Heat Transfer Coefficient

The aim of the project is to obtain an online evaluation of the overall heat transfer coefficient of a set of standard Robert type evaporators. This is evaluated using an online mass and energy balance based model of the system. The main measurements will be temperature based, as it is believed that these measurements will be simpler and cheaper to use than only flows or pressures. The flow of juice feeding and syrup leaving the quadruple effect as well as the Brix of the final syrup will be recorded. The data is inputted into the model online and the overall heat transfer coefficient is evaluated over the grinding season. The full theory of the model is covered in chapter 3.

Work has been done by Truong et al (2002) to develop devices that will measure the fouling of surfaces using heat flux sensors that will record the heat flux. Currently these are only applicable to non-heated surfaces such as pipes and cannot be used in calandria wall surfaces, which is the area of interest for the sugar industry.

2.3 Boiling Processes

The process of boiling can be fairly complicated as there are a number of different types and degrees of boiling. In a tube such as those found in evaporators there may be a number of different boiling processes occurring at different positions of the tube. The various boiling regimes and types are described briefly in the next few sections.

2.3.1 Pool Boiling

The first type of boiling approached is pool boiling; this type of boiling occurs on flat surfaces rather than in tubes. There are a number of boiling regimes, namely free convection boiling, nucleate boiling, transition boiling and film boiling. The boiling

regime in which boiling will occur depends on the difference in temperature between the heating surface and the saturated vapor temperature.

The lowest differential temperatures will tend to cause free convective boiling; during this process if the temperature difference is increased the heat flux increases but no vapor or bubbles are evolved.

Increasing the differential temperature will push the boiling regime into the nucleate boiling regime in which isolated bubbles then jets and columns of vapor are generated. In this regime again an increase in temperature increases the heat flux.

As the temperature difference increases the nucleate boiling range moves into the transition range the heat flux begins to decrease as the differential temperature increases. This is due to the fact that a bubble of vapor begins to blanket the surface, which inhibits heat transfer. This transition is sometime referred to as unstable film boiling.

A further increase in differential temperature will move the process into the film regime, in this process there is a thin film of vapor covering the heating surface and heat is transferred using convective processes to the heated fluid. This process stabilizes the previous regime transition and any further increase in differential temperature will increase the heat flux.

2.3.2 Forced Convection Boiling

This type of boiling occurs in tubes and also is composed of a number of regimes though these differ slightly from these described in the pool boiling section. The processes involve convective as well as bulk fluid movement processes. The heat transfer and heat flux however have similar trends to the pool boiling system and also increase to

a maximum value, decrease sharply then increase slightly further up the tube. The boiling regimes are described starting at the base of a tube and working up the tube.

Initially all the fluid in the tube will contain only liquids and heat transferred will set up convective currents in the fluid. This is the forced convection regime.

As one moves up the tube the differential temperature increases slightly as there is a slightly lower boiling point rise due to the hydrostatic head and bubbles begin to form. The bubbles are initially small in the bubbly regime but begin to coalesce as one moves up the tube into the slug region.

In the annular region a film of juice begins to form at the walls of the vessel where velocities are lower than in the centre of the tube where only vapor is flowing. At this region the heat flux reaches a maximum value.

A transition region begins to occur as the tube length increases and the liquid at the wall begins to dissipate. This causes the heat flux to decrease as one moves up the tube.

Finally the tube is filled with a vapor mist known as the mist region. This region has very bad heat transfer properties and the heat transfer coefficient in this region is extremely low ultimately forming superheated vapor if the tube length is high enough.

2.4 Scale

The topic of scaling and scale modeling is a vast topic in itself and has been studied in great depth for non-boiling systems. For the boiling processes in evaporative systems some of the work done so far is described below but modeling these systems is particularly difficult because there are many mechanisms occurring simultaneously.

2.4.1 Scaling and Its Significance

Scale formation is of interest to the sugar industry and many areas of industry where heat transfer and flows are affected by the formation of this scale. The scale decreases the heat transfer rates in heating media and can cause severely depleted flow through piping if it forms thick scale layers in certain industries. In the sugar industry this scale needs to be removed from heat transfer surfaces to allow the rate of heat transfer to achieve required throughputs. This cleaning means downtime for mills and costs a significant amount of money in chemicals and lost production. Since the scaling causes a reduction in heat transfer efficiency, equipment typically is oversized to account for a certain amount of scaling over time; this increases capital costs of equipment.

The scale can form from a number of scale-forming minerals that are inversely soluble; that is the solubility of the mineral decreases with increasing temperature. Minerals like this include calcium and silicon minerals. Common scale components for water include calcium carbonate, calcium sulfate, calcium phosphate, silica, magnesium silicate, iron-based scales, zinc phosphate and zinc hydroxide.

The solubility and scaling of these components is well known for water systems as these are common problem areas for boilers and much research has been performed to quantify and explain scaling rates in boiler systems.

Calculations can be performed to find the possible deposition of certain minerals by considering their solubility under different conditions in water. Measures of the scale-forming tendency of water that exist include the Langenlier index for calcium scale, the Ryznar Stability index and the Stiff and Davis Index.

In water systems scale inhibition methods include softening with lime or lime/soda, acid treating, scale inhibitors and dispersants as well as surfactants.

A number of references mention that the factors affecting scaling rates include concentration, pH, flow velocity and temperature. This is a broad and general classification and this will need to be refined to decide on model parameters specific to the sugar industry and the evaporator set under consideration. In both the sugar and many other industries pH control is key to reducing scale formation.

The concentration of silica in water is usually in the range 1 to 30 mg/l. Certain elements such as calcium, magnesium, and silica are only moderately soluble in water. As the concentration of calcium, magnesium and silica increase, each one will tend to come out of solution. Calcium and magnesium will come out of solution as carbonates. Silica will come out of solution as a hard dense glass-like material. Calcium carbonate and magnesium carbonate will form a hard substance commonly called limestone. The solubility in sugar solutions is dependant on a number of variables so varies depending on a number of conditions including sucrose content and temperature.

Scale and corrosion are generally thought to be diametrically opposed to one other. Reducing scale build up, for example, increases corrosion and vice versa. This means that a balance needs to be reached between scale reduction and the prevention of corrosion. Lowering the pH in water systems can reduce the scale formation but this increases the likelihood of corrosion. In sugar solutions the inversion of sugars is an important issue when pH changes are made.

Water hardness is associated with the amount of the following $\text{Ca}(\text{HCO}_3)_2$, calcium ions and CaCO_3 , magnesium salts, CaSO_4 , CaCl_2 , MgHCO_3l_2 , MgCO_3 , MgSO_4 , MgCl_2 . The

scale forms insoluble curds in washing processes; magnesium chloride is also corrosive. These are removed using softening treatments. The magnesium scale is not as hard a scale as calcium scale. Sulfates form hard scale if calcium is present and are removed by deionization. Another hard scale former is silica, this is removed by a lime-soda process with the addition of ferric sulfate (cold) or magnesium reagents (cold or hot). If any aluminum is present the silica forms a very hard scale. The problem with these scale and hardness indices, correlations and calculation in the sugar industry is that the sugar solutions modify the characteristics of the minerals and the prediction of scaling from these correlations can be erroneous.

The paper industry also has scaling problems with black Kraft liquor in evaporators used to concentrate the spent pulping liquor. A description of the processes involved is well described in the paper by Fredrick and Grace (1981).

2.4.2 Sugar System Scale Components

Sugar evaporator scale compositions and the evaporator effect where that particular scale component is found are listed below along with cleaning options, this information originates from Honig (1963):

- Phosphates (mainly first effect) can be removed with acid.
- Carbonates (mainly first effect) can be removed with acid.
- Complex organic matter (first effect mainly) remove with caustic.
- Sesquioxides (first and last effects) remove with acid.
- Silicic acid (last effect mainly) remove with concentrated caustic.
- Organic salts (last effect mainly) remove with acid.

ICP analysis has been performed (Published by Godshall and Wartelle, 2002) on some scale from some of the mills in Louisiana; the scale composition of cations has been shown to be as follows:

- Mostly calcium with a composition of 12 to 23 %.
- Phosphorus composition is 2 to 12%.
- Silica compositions vary from 1% to 13%.
- Magnesium is 1 to 5%.

The rest of the cations measured (Sulfur, iron, aluminum, nickel and copper) had compositions of less than 1%. The reason for large variations in compositions is the fact that the scale formed is not uniform along the effects. The calcium for example has a higher concentration in the scale of the first effects compared to the final effects. The main components can be seen to be calcium, phosphorus, silica and magnesium.

The most scale buildup is in the last effect, the next highest scale buildup is the first effect. In the study by Godshall (2002) the final effect of the quad studied had almost 30g/tube of scale and the pre evaporator had about 10g/tube of scale. The first, second and third effect had only about 3g/tube (All about the same amount) of scale in comparison to the 30g in the final effect. Work quoted by Honig (1963) mentions 3.5mg to 7 mg of scale per liter of water evaporated from the first effect, 2mg to 4mg for the second, 1mg to 2mg for the third and 3.5 to 7mg for the final effect.

Scaling rates change over the season since the rate of scaling is a function of composition and so the composition and scale can vary over a season as the pH and concentration of various minerals change in the juice systems fed from the mills due to different cane feed compositions or different operating conditions on the mill.

The main culprits for scale in the final effect have been assumed to be calcium and silica and a number of sugar industries around the world that have measured the scale compositions show these to be significant scale components. The addition of softeners and other scale component removal systems is not very prevalent in the sugar industry. Chemical addition to help prevent the scale forming has been tried to reduce scaling, these include adding minerals or chemicals to modify scale-forming components in the sugar juice to prevent them depositing in the evaporators or by removing them before they get to the evaporators in the clarifiers.

2.4.3 Fouling and Mechanisms that Cause Its Occurrence

For the sugar industry a good outline of fouling literature can be found in a literature review of evaporator fouling performed by Walthew (1994) of the Sugar Milling Research Institute. This paper covers formation, cleaning and reduction of fouling in sugar mill evaporators.

There are a number of different types of fouling mechanisms. These are outlined in the Handbook of Evaporation Technology as well as a paper by Epstein (Somerscales and Knudsen, 1981) and are classed as follows under the following sections:

1. Precipitation fouling
2. Particulate fouling
3. Chemical Reaction fouling
4. Corrosion fouling
5. Biological fouling
6. Solidification fouling

Solidification fouling may occur in evaporators in the form of sugar crystallizing on the evaporator surfaces under consideration. The magnitude of this effect still needs to be determined, to date no papers have been found that quantify the significance of this effect in sugar mill evaporators.

The biological fouling is not significant in the evaporators as in general any “slime” is washed off by juice passing through the tubes and high temperatures mean that only thermophiles could survive. At temperatures above 70°C most organisms (except thermophiles) will be killed.

Corrosion fouling is not noted to be significant in the sugar industry as the products formed on the surface of the tubes are in general not corrosion products of the copper tubes.

Chemical fouling may be occurring in the sugar industry but its significance still needs to be determined.

The particulate fouling does not appear to be a significant mechanism in the evaporators of a sugar mill as shown in Honig (1963) where he mentions that there is no measurable effect on the fouling in the evaporators with the addition or removal of suspended matter in the clarified juice feed.

The precipitation fouling is also referred to as scaling and in the rest of this document the term scaling will refer to precipitation fouling. In the evaporators of the sugar industry scaling is the major fouling forming mechanism encountered. It is described as the deposition of supersaturated inorganic salts on the heating surface of the evaporators. The deposition of the scale component occurs because it is no longer soluble in the juice passing through the evaporator. In the case of inversely soluble materials the solubility

decreases with increasing temperatures, since the fluid at the surface of the tubes in the calandria is hotter than the bulk fluid due to boundary layers setup in the tubes, the deposition due to increased supersaturation is likely at this surface/fluid interface. The normal soluble materials are not left out of the scheme of things however and they also deposit, however this occurs because of a different mechanism. As the fluid passes through the evaporators it is concentrated and this concentration due to water removal causes the solubility of dissolved materials to decrease. The handbook of evaporation also mentions that mixing different streams can cause supersaturated conditions, this is reemphasized in Honig (1963) as he discusses the precipitation of certain minerals by mixing two streams with different pH's.

The scale forms with a number of different stages, firstly it needs to deposit on the surface. This mechanism of adhesion to the surface is known as the adhesion or initiation stage. The use of different materials of construction has been used to extend this period of the mechanism. In general smooth surfaces take longer for the fouling to initiate but once the scaling has initiated they show similar scaling rates to surfaces that are rough initially with short initiation times.

After the surface has an initiated layer of scale on its surface the scaling rate depends on a number of parameters and not all of these parameters are well understood. The scaling component in the juice first needs to be transported from the bulk flow to the deposition surface of the evaporator heating surface. This section of the mechanism is relatively well understood but once it arrives at the surface the mechanism for the deposition onto the surface is not fully known. Even if the material deposits on the surface it is subject to removal due to attrition on the scaling surface as suspended solids

in the juice are passed at reasonable velocities past the heating surface of the evaporator. Solubility of the scale forming compound has a role to play in this section of the mechanism, the solubility of key components determine the equilibrium level of deposition of that component onto the surface.

As the deposited material on the heating surface is exposed to the continuous heating from the calandria the material begins to undergo a transformation. During this aging phase the solid can change its crystal makeup and structure to form crystalline and hard to remove scales. For this reason a number of sugar mills will clean their evaporator trains after about nine days in Louisiana to prevent this hard to remove scale from forming.

For precipitation fouling the important variables have been shown to be:

- Composition of the juice stream.
- Concentration of the juice stream (Brix).
- Temperature of the juice stream.
- The difference in temperature between the juice stream and the vapor heating it.

For particulate fouling, in general, higher fluid velocities reduce scaling.

It was mentioned by Taborek (1972) that increasing the differential temperature in the evaporator decreases the area required for heat transmission but it can increase scaling rates significantly. This would indicate that to reduce scaling mills should operate evaporators at a small a differential temperature as possible whilst still maintaining a reasonable throughput. This is particularly important just after a clean of the evaporator train to reduce the onset of scaling. The introduction of new technology in the form of

plate evaporators, that can operate at lower differential temperatures helps in this area of scale prevention.

Higher velocities which decrease fouling in most cases, and smaller units, can reduce maintenance costs as cleaning does not need to be performed as often but the cost of energy and pumps to pump at higher rates can be expensive.

2.4.4 Modeling of Scale Formation

There are a number of different scale formation modeling techniques that are used, and these are all discussed in greater detail in chapter three. The most important criteria for choosing these models are the applicability of the models. For example HTRI have performed numerous tests and have developed models for heat transfer in heat exchangers, however these cannot be applied to boiling systems, as the mechanisms that govern the processes are vastly different. An extremely complicated model, which only a few people can understand, and use, or a model that will only work under extremely narrow set of conditions may be useless if it is to have broad application in the industry.

CHAPTER 3. THEORY

3.1 Heat Transfer Coefficients

The heat transfer coefficient is a grouped term accounting for a number of heat transfer processes and is calculated from a number of combined heat transfer resistances of media through which heat is transferred. In figure (3.1) the typical media through which heat transfer occurs in a tube are shown in a cross sectional view.

From the tube center line which has the liquid juice flowing through it and moving out to the steam side of the tube the following heat transfer resistances are met; firstly there is a film effect causing a convective heat loss on the juice side close to the wall as less turbulent conditions occur in the fluid phase at the wall. Moving even further out we see the scale formed on the surface of the metal tube which contributes a conductive heat loss, then the transfer of heat through the metal wall of the tube itself also contributes a conductive loss. The scale formation on the steam or vapor side is usually a very thin layer and in most cases can be neglected in the calculations we are considering and is assumed not to contribute significantly to the heat loss due to conduction through it. There is again a film effect causing a convective heat loss on the steam or vapor side close to the wall on the steam side and again this is depicted in figure (3.1).

The overall heat transferred is described by equation (3.1). This heat transfer across these resistance layers can be broken down further into their constituent component as seen in equation (3.2).

$$Q = q_f \cdot A = k \cdot A \cdot (T_s - T_L) \quad (3.1)$$

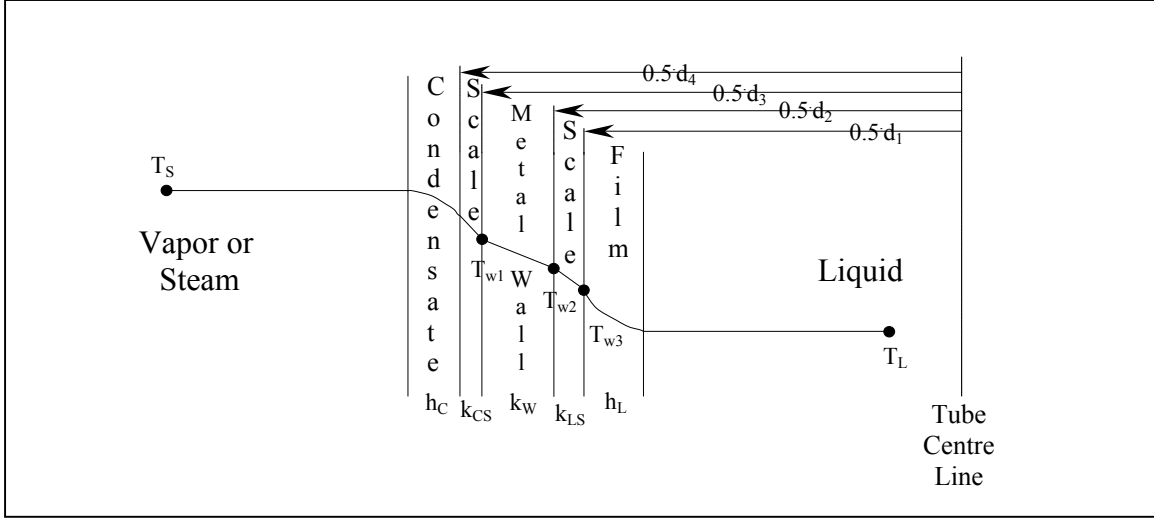


Figure 3.1: Heat transfer resistances in heat transfer showing the temperature profile in a typical evaporator tube.

The overall heat transfer coefficient (k), if we include all the scale and wall conductive losses and all convective losses, can be shown to be as in equation (3.2) based on first principles from heat transfer in Incopera and DeWitt (2002).

$$\frac{1}{k} = A \sum_{i=1}^N R_i = A \left(\frac{1}{h_C \pi L_T d_4} + \frac{\ln\left(\frac{d_4}{d_3}\right)}{2\pi L_T k_{CS}} + \frac{\ln\left(\frac{d_3}{d_2}\right)}{2\pi L_T k_W} + \frac{\ln\left(\frac{d_2}{d_1}\right)}{2\pi L_T k_{LS}} + \frac{1}{h_L \pi L_T d_1} \right) \quad (3.2)$$

Which reduces to equation (3.3) when the appropriate substitutions are made for A . The area used is defined as the outer surface area of the tube between the evaporator tube sheets $A = \pi L_T d_4$ where L_T is the tube length.

$$\frac{1}{k} = \frac{1}{h_C} + \frac{d_4 \ln\left(\frac{d_4}{d_3}\right)}{k_{CS}} + \frac{d_4 \ln\left(\frac{d_3}{d_2}\right)}{2k_W} + \frac{d_4 \ln\left(\frac{d_2}{d_1}\right)}{2k_{LS}} + \frac{d_4}{h_L d_1} \quad (3.3)$$

Our objective in the project is to evaluate the overall heat transfer coefficient (k) and use that to determine scaling rates. The scale on the steam side will be assumed negligible so the equation becomes that shown in equation (3.4).

$$\frac{1}{k} = \frac{1}{h_c} + \frac{d_4 \ln\left(\frac{d_3}{d_2}\right)}{2k_w} + \frac{d_4 \ln\left(\frac{d_2}{d_1}\right)}{2k_{LS}} + \frac{d_4}{h_L d_1} \quad (3.4)$$

Some of the problems associated with trying to find an overall heat transfer coefficient based purely on a theoretical basis includes the fact that many correlations used for values of h_L for example are not applicable to boiling systems. Badger and Banchero (1955) confirm the complexity and lack of data for estimating boiling coefficients. The scale formed is also very specific to the process fluid passing through the tube and a number of physical and chemical changes can occur in the scale with time so a theoretical value for the scale heat transfer resistance is very difficult to predict. Some attempts have been made to model the boiling systems and some of these will be discussed in the scale modeling section.

If the h_c , h_L and k_w values are assumed to be constant, as well as assuming the scale thickness is negligible compared to the tube diameter and there is no scale initially on the tube, the variation of the scale heat transfer resistance can be trended with time and the scale resistance change with time can be evaluated as shown below in equation (3.5). Selamn and Plomley (1950) noted that the scaling on the steam of tubes is not common in any effects but the first and the fouling in the first effect is due to oil deposits from excessive turbine lubrication. This particular problem in the first effect is no longer an issue, as the turbines that have replaced steam engines of the 1950's do not allow lubricants into the steam streams.

$$\frac{1}{k} = \frac{1}{k_o} + \frac{\frac{d_4}{2} \ln\left(\frac{d_2}{d_1}\right)}{k_{LS}} = \frac{1}{k_o} + R_f \quad (3.5)$$

Or in terms of constants, where $Const_1$ and $Const_2$ are constant values, this can be depicted by equation (3.6).

$$\frac{1}{k} = Const_1 + \frac{Const_2}{k_{LS}} \quad (3.6)$$

Using the data obtained from St James the value of the fouling resistance (R_f in equation (3.5)) as a function of time can be evaluated and used in the models described in a later section.

3.2 Evaporator Model

3.2.1 Mass and Energy Balance

The model proposed is based on a mass and energy balance over a quadruple effect evaporator train but let us begin with the heat transfer and mass balance equation calculations for a single evaporator effect before moving on to the quadruple effect calculation.

3.2.1.1 Single Effect Evaporator Balance

A single effect will consist of a feed stream, steam input, condensate outlet, vapor outlet and concentrate outlet as seen in figure 3.2. The list of variables used is shown in the nomenclature section of this document.

There are a number of assumptions that need to be made in the development of a mass and energy balance for the system and these are listed below:

- Steady state conditions prevail for all stream flows.
- The solute is non-volatile ($B_V = 0$) and all dissolved solids (Brix) remain in the concentrated product stream.
- No sub cooling of condensate occurs ($T_S = T_C$).

- Saturated steam/vapor is used ($T_S = T_S^{\text{sat}}$) and the saturated temperature (T_S) is found from saturated pressure conditions (P_S). In the simulation all exhaust steam and vapor used is assumed not to be superheated. Note that if superheated steam is used this needs to be account for this in the balance if significant superheating has occurred. The vapor evolved on heating the feed is also assumed to be saturated and not superheated.
- If the steam temperature is saturated ($T_S = T_S^{\text{sat}}$) and the and the condensate temperature is the same as the steam temperature ($T_C = T_S^{\text{sat}}$) then the difference in enthalpy of the steam and condensate is the latent heat of vaporization ($H_S - h_C = \lambda$) of steam at the saturated steam temperature (T_S^{sat}).
- There is no loss of steam on condensing to condensate ($S = C$).

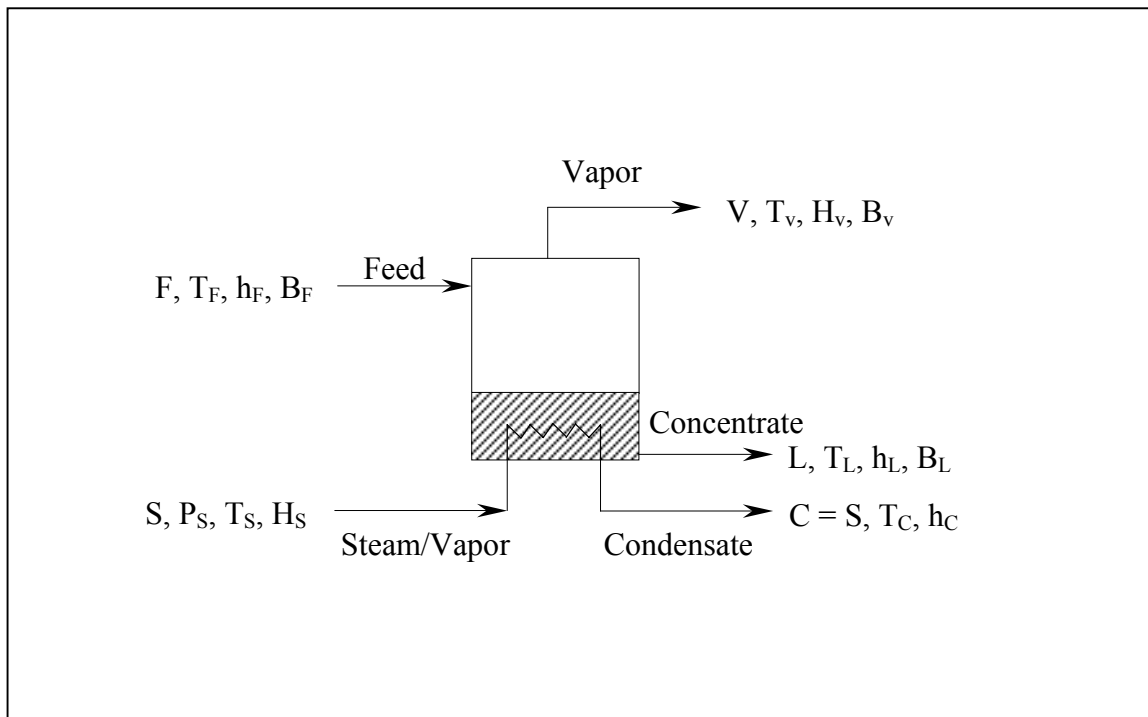


Figure 3.2: A single evaporator effect evaporator diagram.

3.2.1.1.1 Mass Balance

The overall mass balance of the total juice side flows is given by equation (3.6) below, (assuming that there is no loss of steam on condensing the steam mass balance is trivial, $S = C$):

$$F = L + V \quad (3.6)$$

So rearranging results in,

$$V = F - L \quad (3.7)$$

The solute (Brix) balance is then given by equation (3.11) below assuming no Brix loss to the vapor line ($B_V = 0$):

$$F \cdot B_F = L \cdot B_L \quad (3.8)$$

So rearranging results in,

$$L = (B_F/B_L) \cdot F \quad (3.9)$$

So we can rearrange equations (3.6) and (3.8) into the form of equations (3.7) and (3.9). These equations are equally valid for each vessel of the multiple effect set and will be used in those calculations also.

3.2.1.1.2 Energy Balance

The energy (enthalpy) balance is computed for a single effect as below in equation (3.10), and by applying the assumptions for the system the equation can be reduced to the form shown in equation (3.11).

$$F \cdot h_F + S \cdot H_S = V \cdot H_V + L \cdot h_L + C \cdot h_C + \text{Losses} \quad (3.10)$$

$$F \cdot h_F + S \cdot \lambda = V \cdot H_V + L \cdot h_L + \text{Losses} \quad (3.11)$$

Where the terms in equation (3.11) are described below,

$$\lambda = H_S - h_L \quad (3.12)$$

$$T_S^{\text{sat}} = T_S^{\text{sat}}(P_S^{\text{sat}}) \quad (3.13)$$

Equation (3.12) defines the latent heat of vaporization for steam/vapor, and this term is a function of the saturated steam temperature and pressure. Equation (3.13) implies that if saturated pressure is known the temperature can be computed, this calculation is also reversible so a saturated vapor pressure can be computed for a saturated vapor temperature.

3.2.1.1.3 Temperature Differences

A boiling point rise occurs due to the solutes (sugar and impurities) in the water solvent and due to a hydrostatic head pressure on the boiling solution. Both of these effects can be calculated based on the Brix of the solution and the liquid level height in the vessel.

The boiling point rise due to Brix can be calculated from a simple correlation (Honig,1963) as in equation (3.14) below:

$$T_{BPR-Brix} = \frac{2B_{avg}}{100 - B_{avg}} \quad (3.14)$$

There is a more complicated looking correlation given in the Sugar Technologists Manual for technical sugar solutions as seen below in equation (3.15) to equation (3.18). Equation (3.15) is used in the model but when compared with the results of equation (3.14) very little difference was noted until high Brix solutions were faced (As seen in Appendix F), so both can be used and have similar accuracy for the first effects but the last effect requires equation (3.15). The term w_{ds} in equation (3.15) is replaced with the average Brix (B_{avg}) of the solution in the simulation. The terms a, b and c include a term

accounting for the purity of the fluid, equations (3.16) to equation (3.18) are derived for a Brix between 0% and 60%, in this case $k = 40$ and q is the purity of the juice.

$$T_{BPR-Brix} = aw_{ds}^2 \frac{(273+t)^2}{(374.3-t)^{0.38}} [b(w_{ds}-k)^2 + c] \quad (3.15)$$

$$a = 1.59515 * 10^{-4} - 2.00092 * 10^{-6} * q + 8.01933 * 10^{-9} * q^2 \quad (3.16)$$

$$b = 1.84440 * 10^{-6} - 3.04380 * 10^{-8} * q + 1.72958 * 10^{-10} * q^2 \quad (3.17)$$

$$c = 1.08062 * 10^{-3} + 2.89645 * 10^{-6} * q - 3.01416 * 10^{-9} * q^2 \quad (3.18)$$

The boiling point rise due to hydrostatic head is calculated from the Antoine equation (As shown in Appendix B) for saturated steam and using half the hydrostatic head height for an average boiling temperature elevation due to this effect can be calculated as in equation (3.19) below:

$$T_{BPR-HH} = 46.13 - \frac{3816.44}{-18.3036 + Ln\left(\frac{P_v + \rho g(z/2)}{0.1333224}\right)} - T_v \quad (3.19)$$

To find the boiling point of the solution the boiling temperature of water at a pressure (P_v) the vapor temperature (T_v) is found from saturated conditions then correct for by adding the total boiling point rise that is a function of Brix, liquid height, purity and vapor pressure (or temperature). This corrected temperature is the average solution boiling temperature and used in the computation of the heat transfer coefficient. The boiling point rise effects are combined to compute the overall average boiling temperature of the solution as below in equation (3.20):

$$T_{avg} = T_v + T_{BPR-Brix} + T_{BPR-HH} \quad (3.20)$$

Other research and computations to perform online heat transfer computations by Snoad (1997) makes the assumption that the average Brix in an effect is the same as the

outlet Brix. This is not assumed to be true for the St James mill the author computed the data for, the average Brix is assumed to be the geometric average of the inlet and outlet Brix values. The work by Snoad (1997) also assumes a constant boiling point elevation, which is not true if the Brix varies or if the level changes.

3.2.1.1.4 Heat Transfer

The heat transferred from steam or vapor to the feed stream is then calculated as in equation (3.21) and equation (3.22).

$$Q = S(H_S - h_C) - \text{Losses} = S\lambda(T_S) - \text{Losses} \quad (3.21)$$

$$= k \cdot A \cdot \Delta T_{\text{mean}} \quad (3.22)$$

The value of the steam flow is found from the energy balance (coupled with the mass balance) using equation (3.23). The heat transferred is evaluated (assuming only latent heat of the steam is lost and no sub cooling occurs) then equation (3.22) is used to compute the value of the heat transfer coefficient. If correlations are used to compute the specific enthalpy values of each stream the values are used to compute the steam flow (assuming no sub cooling of the condensate) by rearranging equation (3.11) and substituting in equation (3.7) for the vapor flow into the form shown in equation (2.23).

$$S = ((F-L)H_V + L \cdot h_L - F \cdot h_F + \text{Losses})/\lambda \quad (3.23)$$

The steam economy of a single effect can be calculated as seen in equation (3.24).

$$\text{Steam economy} = V/S \quad (3.24)$$

From equations (3.21) and (3.22) equation (3.25) can be deduced and the heat transfer coefficient can be solved for as shown in equation (3.26). The mean differential temperature (shown in equation (3.22)) is the difference between the steam temperature and the average boiling temperature of the fluid as in equation (3.25).

$$Q = k \cdot A \cdot \Delta T_{\text{mean}} = k \cdot A \cdot (T_S - T_{\text{avg}}) = S \lambda \quad (3.25)$$

$$k = [S \lambda (T_S)] / [A (T_S - T)] \quad (3.26)$$

3.2.1.2 Quadruple Effects

A typical quadruple effect evaporator setup with no vapor bleeds is shown in Figure 3.3, this is the same system as that used at St James and will be used to describe the calculations occurring in the simulation for a multiple effect evaporator train. The calculations will need to consider the energy and mass balance for the multiple effect train. The list of variables used is shown in the nomenclature section of this document.

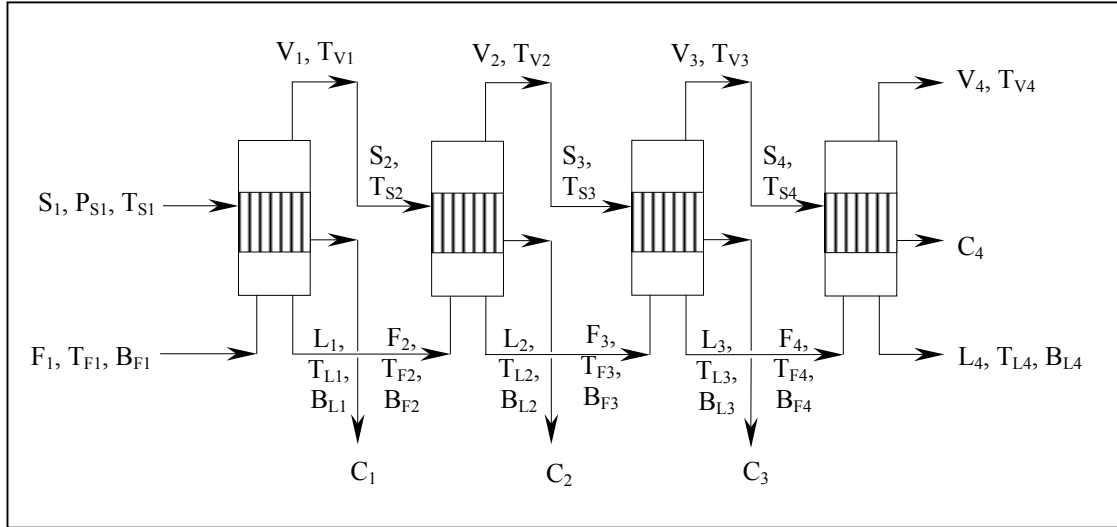


Figure 3.3: A quadruple effect evaporator setup for calculation mass and energy balances with no vapor bleeds.

There are a number of assumptions that need to be made in the development of a mass and energy balance for the system and these are listed below:

- Steady state conditions prevail for all streams.
- The solute is non-volatile and all dissolved solids (Brix) remain in the concentrated product stream and the Brix in vapor lines is zero.

- The boiling point of the liquid in the tubes is the generated vapor temperature plus the boiling point rise due to Brix and a hydrostatic head effects.
- The vapor generated on boiling is not superheated; it is saturated. ($T_V = T_V^{\text{sat}}$).
- All steam or vapor utilized in heating is saturated not superheated, also condensate leaves at the same temperature as the steam inlet and is not sub cooled so $T_S = T_S^{\text{sat}}$ and $T_C = T_S^{\text{sat}}$, then also $H_S - h_C = \lambda$ (latent heat of vaporization at T_S^{sat}).
- Heat loss across the calandria is assumed to be 1.5% of the energy in the steam or vapor in the calandria. (Honig 1963)
- Any other energy losses are accounted for by comparing the temperature of the vapor in the vapor line (T_{Vi}) to the temperature in the calandria of the next effect ($T_{S\ i+1}$) and are accounted for as a pressure loss in the vapor space to prevent the energy loss error accumulating in the computation.

In order to perform the computation a number of variables need to be recorded and these are listed below.

- **Flows and compositions**

F_1 (volumetric), L_4 (volumetric), B_{L4}

- **Temperatures**

T_{F1} , T_{L1} , T_{L2} , T_{L3} , T_{L4} , T_{S1} , T_{S2} , T_{S3} , T_{S4}

- **Other values required**

The area for heat transfer, level measurements in the vessels and purities of the streams are also required inputs but are all inputted manually and not on a continuous basis from the controller.

From this data the boiling point rises, intermediate flows and compositions can be found when full mass and energy balances are performed.

3.2.1.2.1 Mass Balances

The overall total mass balance is given in equation (3.27).

$$F_1 + S_1 = C_1 + C_2 + C_3 + C_4 + L_4 + V_4 + \text{Vapor Bleeds} \quad (3.27)$$

If we assume no condensate mass loss, then $S_1 = C_1$ (In general $S_i = C_i$) and that there are no vapor bleeds (Vapor Bleeds = 0) the equation simplifies to equation (3.28)

$$F_1 = C_2 + C_3 + C_4 + L_4 + V_4 \quad (3.28)$$

From our assumptions we also can see that the following are true:

$$V_1 = S_2 = C_2 \quad (3.29)$$

$$V_2 = S_3 = C_3 \quad (3.30)$$

$$V_3 = S_4 = C_4 \quad (3.31)$$

The overall solute (Brix) balance yields equation (3.32), assuming no sugar is lost to vapor lines. Although the flows for the feed and concentrate are volumetric from the controller, they can be converted to mass flows by using a density correlation based on Brix, purity and temperature.

$$F_1 B_{F1} = L_4 B_{L4} \quad (3.32)$$

So rearranging equation (3.32) we can solve for the inlet Brix flow (B_{F1}):

$$B_{F1} = (L_4 B_{L4}) / (F_1) \quad (3.33)$$

Also from the overall total mass balance for the juice:

$$F_1 - L_4 = V_1 + V_2 + V_3 + V_4 \quad (3.34)$$

In order to compute the mass balances on each effect the vapor flow from each effect is required. In the model this is calculated iteratively from the energy balance but

for the purposes of describing the calculations we will approximate the vapor flows by using the Rillieux principles. This approximation is performed as a first approximation in the model for the vapor flow and then the value is calculated from the energy balance to refine the balance later.

$$V_1 = V_2 = V_3 = V_4 = (F_1 - L_4)/4 \quad (3.35)$$

Also by considering an overall mass balance around the first effect we see that:

$$F_2 = L_1 = F_1 - V_1 \quad (3.36)$$

Similar equations exist for the other effects (corrections need to be made for vapor bleeds where necessary, if they exist). When vapor is bleed for a stream the flow to the next vessel is simply the calculated stream flow minus the bleed value and the calculation proceeds.

$$F_{i+1} = L_i = F_i - V_i \quad (3.37)$$

After the intermediate feed, liquid and vapor flow have been computed the intermediate Brix values can be calculated based on these values. The Brix is calculated from a Brix balance on the effect and assuming that the Brix is non-volatile.

$$B_{L1} = (L_4 \cdot B_{L4}) / (F_1 - V_1) \quad (3.38)$$

$$B_{L2} = (L_4 \cdot B_{L4}) / (F_1 - V_1 - V_2) \quad (3.39)$$

$$B_{L3} = (L_4 \cdot B_{L4}) / (F_1 - V_1 - V_2 - V_3) \quad (3.40)$$

If it is assume that initially the vapor and steam flow rates are equal ($S_1=V_1$) which is one of the Rillieux principles then a starting framework based on assumed steam and vapor flows has been set up. All that is required now is to use the energy balance to calculate the steam and vapor flows for each effect to get the true flows and use those instead of assumed values.

3.2.1.2.2 Energy Balances

The first step of the energy balance is to calculate the temperatures at the various points in the system. The known temperatures are: T_{F1} , T_{L1} , T_{L2} , T_{L3} , T_{L4} , T_{S1} , T_{S2} , T_{S3} and T_{S4}

The boiling point rise due to Brix in the exit stream from each effect is calculated to convert each of the readings of T_{Li} to the vapor generated temperature T_{Vi} . This temperature (T_{Vi}) is then used to find the average temperature of the boiling solution by adding the boiling point rise due to hydrostatic head and Brix in the vessel (B_{avg}) to its value.

Boiling point rises occur due to solute (sugar and other dissolved solids) in the water solvent and due to hydrostatic head pressure on the boiling solution. Both of these effects can be calculated based on Brix and height measurements in the vessels. The purity and temperature of the juice or syrup may need to be evaluated when considering certain correlations. For the boiling point rise a number of correlations exist. The equation in the Sugar Technologists Manual gives equation (3.42) as the boiling point rise where as Honig (1963) suggests equation (3.41). The validity of these equations was checked against charts and tables of boiling point rise in Appendix F to see which was more appropriate but both give fairly similar results for low Brix systems but differed at very high Brix. In the simulation w_{ds} is replaced by the Brix.

$$BPR = \frac{2B}{100 - B} \quad (3.41)$$

$$T_{BPR-Brix} = aw_{ds}^2 \frac{(273 + t)^2}{(374.3 - t)^{0.38}} [b(w_{ds} - k)^2 + c] \quad (3.42)$$

For the hydrostatic head an average boiling point rise can be calculated. The hydrostatic head pressure can be calculated from the equation given below from Honig (1963).

$$P_{\text{Pressure}} = P_{Vi} + \rho g(z_i/2) \quad (3.43)$$

The height (z) that is used is the liquid height in the evaporator vessel. The liquid height is halved in order to evaluate the temperature increase due to the hydrostatic pressure exerted on the fluid in the vessel at an average liquid level. The pressure of saturated vapor (P_{Vi}) is calculated using correlations from steam tables (assuming vapor temperature is T_{vi}) then the extra pressure due to the liquid head is calculated. The pressure at the mid point of the boiling syrup calculated, this pressure is then converted back to a temperature (T_{pressure}) using steam table correlations. The change in temperature from the vapor space (T_{vi}) to this new temperature (T_{pressure}) is the boiling point rise. The derivation of equation (3.45) is shown in Appendix B.

$$T_{\text{BPR} - \text{Hydrostatic head}} = T_{\text{pressure}}(P_{Vi}, z/2) - T_{vi} \quad (3.44)$$

$$T_{\text{BPR} - \text{Hydrostatic head}} = 46.13 - \frac{3816.44}{-18.3036 + \ln\left(\frac{P_{Vi} + \rho_i g(z_i / 2)}{0.1333224}\right)} - T_{vi} \quad (3.45)$$

So now one must find the saturated boiling point of solution (water) (T_{vi}^{sat}) then correct for the boiling point rises, which are a function of Brix and hydrostatic pressure. The corrected temperature is the solution boiling temperature.

The feed temperature (T_F) is assumed to be the same as the exit temperature from the previous effect (T_L). It is assumed no heat is lost in the small stretch of piping from the exit of one vessel to the entrance of the next.

Now all the temperatures are defined the energy balance can be calculated. The use of correlations from steam table values is incorporated. These are also tested in a similar manner to the boiling point rise correlations in Appendix F to find the best correlations for various regions of the saturated steam regions. The correlations can produce latent heat and enthalpy for streams based on their saturated temperatures. The latent heat of vaporization is simply the steam enthalpy minus the water enthalpy at a given temperature (and thus pressure). The equation is shown below:

$$\lambda = H_S - h_C \quad (3.46)$$

The overall energy (Enthalpy) balance for the i^{th} effect is calculated as below, noting that all the specific enthalpies are related to temperature and sometimes composition:

$$F_i h_{Fi} + S_i \lambda = V_i H_{Vi} + L_i h_{Li} \quad (3.47)$$

H_{Vi} and λ can be found from saturated steam table correlations and are a function of the saturated steam temperature. The correlations for h_{Fi} and h_{Li} come from correlations for sugar solutions from the sugar technologist manual, and require purity of the solution as well as the Brix and temperature.

To calculate the enthalpy, assuming negligible heat of dilution (for sugar) one could also use the heat capacity to calculate enthalpy as in equation (3.48).

$$h = c_p(T - T_o) \quad (3.48)$$

It is common to set $T_o = 273.15\text{K}$ and c_p is the specific heat of solution. The values of the heat capacity (c_p) are correlated for sugar solutions in the Sugar Technologist Manual (1995) but one error that is included is the fact that equation (3.48) is an approximation of an integral to calculate the enthalpy. Since the heat capacity is a function of temperature

some deviation from the true enthalpy occurs if the approximation of equation (3.48) is used.

If correlations are used for the enthalpy and latent heats then a corrected vapor flow can be computed as in equation (3.49). This is where an iterative solution is required since a change in the vapor flow computed from equation (3.49) is different from the guessed vapor flow based on one of the Rillieux principles. The corrected vapor flow changes the Brix as a differing amount of vapor is evolved, this change affects the boiling point elevations and also the temperatures out the effect. This temperature change affects the enthalpy that in turn affects the energy balance and vapor flow! The process is iterated until a stable unique solution is obtained for the measured variables.

$$V_i = (F_i h_{Fi} + S_i \lambda - L_i h_{Li}) / H_{vi} \quad (3.49)$$

So from an assumed steam flow the vapor flow can be calculated. The true vapor flows for the effects is calculated sequentially starting at the first effect, then the liquid flow out that effect is calculated by subtracting the vapor generated from the feed flow. Corrections are made when vapor is bleed and the flow to the next calandria is lower by the value of the bleed vapor. The next effect now has different flows of vapor, steam and feed but all other parameters are assumed constant. The calculation proceeds until all the flows have been recalculated. The Brix and thus boiling point rise are recalculated and the steps repeated if necessary. The calculate function in Microsoft Excel® can perform these iterative calculations.

Once all vessels have been calculated the outlet Brix from the mass and energy balance will differ from the measured value so the assumed steam flow is varied and the process repeated until the desired Brix is obtained out the final vessel. This requires

another iterative process looping on top of the inner iterations occurring with the calculate function.

Microsoft Excel® has a built in solver, which can be used to perform this outer iterative calculation. The challenge was to automate this function, it required some VBA programming and the use of macro's. The function only has to be run once per evaluation of the heat transfer coefficient at sampled conditions. The measurements of flow, temperature, Brix and heat transfer coefficients are stored at one-minute intervals. Some of the data had to be filtered before processing, this type of correction and calculation may take up a lot of processor usage depending on the manipulations required but a computer with a fairly fast Intel Pentium 4 processor and a few hundred megabytes of RAM was used for the calculations and did not significantly affect the computer performance.

Once the values have been calculated the steam economy of the system can be calculated from the equation (3.50).

$$\text{Steam economy} = (V_1 + V_2 + V_3 + V_4)/S_1 \quad (3.50)$$

3.2.1.2.3 Heat Transfer Coefficients

One of the assumptions made was that the steam loses only its latent heat of vaporization so the energy supply by the steam or vapor fed to the calandria is only its latent heat of vaporization. This means the heat supplied to an effect can be calculated:

$$Q_1 = k_1 A_1 \Delta T_1 = S_1 \lambda - \text{Losses} \quad (3.51)$$

In general for the i^{th} effect the equation becomes:

$$Q_i = k_i A_i \Delta T_i = S_i \lambda - \text{Losses} \quad (3.52)$$

The area A_i for each effect is known by calculations using the tube sizes and number of tubes. For these calculations the ΔT we refer to is the steam (or heating vapor) temperature minus the boiling point of the liquid as seen from equation (3.53).

$$\Delta T_i = T_{si} - T_{avg_i} \quad (3.53)$$

In these equations the value of ΔT_i is known and the overall ΔT for the train can be found as in equation (3.54).

$$\Delta T = \sum_{i=1}^4 \Delta T_i = T_{s1} - T_{v4} (Known) \quad (3.54)$$

The available ΔT for boiling is slightly less than the overall ΔT due to boiling point rises and the total available ΔT for heating is the overall ΔT as calculated above minus all the boiling point rises in each effect.

In the Microsoft Excel® model the definition of the average boiling point of the liquid as seen in equation (3.53) is a corrected value. The boiling point elevation due to hydrostatic effects is ignored, this is done so that the data produced can be compared with other literature data where heat transfer coefficients corrected for Brix are typically computed. The reason why hydrostatic effects are sometimes neglected is because in the past some of the data required for these calculations were not readily available to be used and so only Brix effects were corrected for (Kern, 1950). Although it is fairly simple to compute the hydrostatic effects at the present, the corrected convention has stuck for a number of sugar milling countries. The heat transfer coefficients calculated and presented in the results sections all heat transfer coefficient values are corrected for Brix only. In pan boiling even the boiling point elevation due to Brix effects is ignored and the computed heat transfer coefficient is referred to as an apparent heat transfer coefficient.

In computing the differential temperature used for apparent heat transfer coefficients the difference between the steam and vapor space temperatures are used without any boiling point rise correction.

From equation (3.52) the overall heat transfer coefficient can be calculated for each effect as in equation (3.55).

$$k_i = (S_i \lambda - \text{Losses}) / (A_i (T_{Si} - T_{avg_i})) \quad (3.55)$$

The losses can be assumed to be 2% of the steam supply energy according to Hugot (1960).

3.2.2 Correlations Used

The terms for the energy balance such as enthalpy and latent heat need to be evaluated to allow the computation of the value of the heat transferred (Q). Some of the correlations are described in the section of energy balance sin multiple effect evaporation but a complete list of the correlations, their decencies and correlation checks is shown in Appendix F.

An extra note on correlations, if the steam is superheated steam tables need to be used to account for the extra enthalpy in the steam or a correlation of the form $H_V \approx H_V(T_V^{\text{sat}}) + c_{pv}(T_V - T_V^{\text{sat}})$ (Steam tables can be used to find heat capacity (c_{pv}) values for the vapor) can be used. c_{pv} is the heat capacity of steam at the average temperature $(T_V + T_V^{\text{sat}})/2$ or an integral form of the equation could be used as well if the temperature dependence of the heat capacity is known.

3.2.3 Microsoft Excel® and Honeywell's UMC800

The simulation is performed in Microsoft Excel®, an attempt was made to perform the calculation in the control builder program built in the Honeywell control

software but the calculation is very iterative and the code for the control builder software cannot handle the number of iterations necessary for the process.

In Appendix A of this report the code and explanations of what each line of code does is detailed. This section gives a general overview of the computation and the user interface in the Microsoft Excel® spreadsheet.

To begin with the volumetric flows in and out of the effect of juice and syrup are inputted into the Microsoft Excel® spreadsheet from the UMC800 Honeywell controller along with the Brix of the syrup. The mass flows of juice and syrup to the effects are computed and the juice Brix fed to the set calculated. The difference between the flow in and out the set in the form of juice and syrup is the water evaporated in the set, as a first assumption this difference is divided by four to compute the steam flow to the first effect and vapor flow from each effect.

A mass and energy balance on the first effect is used to find the flows to the second effect and then consecutive vessels by repeating the calculation. The temperature data for each effect is sent to the simulator in Microsoft Excel® from the controller. Once these calculations are preformed (an iterative, looped process) the final effect Brix is computed, this value is compared with the actual Brix recorded out the final effect and is corrected by using solver. The solver function minimizes the sum of squares of the difference in computed Brix out the final effect and the mass flow out the final effect. The solver varies the steam flow and iterates until the computed mass and Brix out the final effect that are calculated match up with the measured data.

The heat transfer coefficient and “error” (the sum of squares error mentioned in the previous paragraph is logged to check no errors are occurring in the computation)

values are then sent to the controller and stored as a set point value. A set point value is used for logging, as it is difficult to send a numerical value back to the controller for data logging as an analogue input unless it is inputted as an electrical signal of 4 to 20 mA or 0 to 5 V. It is however easy to send a numerical value to the controller as a set point without the need for a true analogue input to be sent to the controller.

The inputs and outputs to and from the controller are sent to the first page of the Microsoft Excel® workbook, a copy of this page and its underlying commands are shown in figure (3.4). Any data needed for the simulation and any information sent to the controller is sent via this page, any data sent to the spreadsheet is sent to this worksheet then when needed in the simulation the cell reference refers to this page for the inputs.

	A	B	C	D
2		Recalculation time set:	60 secs	
4		Input Description	Value	
5		JUICE INLET TEMP.	=C:\Honeywell\client\xls\dataex\mede.xls!getpointvalarray(1,"localhost","TT-001","PV","V")	
6		1st BODY STEAM TEMP.	=C:\Honeywell\client\xls\dataex\mede.xls!getpointvalarray(1,"localhost","TT-002","PV","V")	
7		2nd BODY STEAM TEMP.	=C:\Honeywell\client\xls\dataex\mede.xls!getpointvalarray(1,"localhost","TT-003","PV","V")	
8		3rd BODY STEAM TEMP.	=C:\Honeywell\client\xls\dataex\mede.xls!getpointvalarray(1,"localhost","TT-004","PV","V")	
9		4th BODY STEAM TEMP.	=C:\Honeywell\client\xls\dataex\mede.xls!getpointvalarray(1,"localhost","TT-005","PV","V")	
10		1st BODY JUICE TEMP.	=C:\Honeywell\client\xls\dataex\mede.xls!getpointvalarray(1,"localhost","TT-006","PV","V")	
11		2nd BODY JUICE TEMP.	=C:\Honeywell\client\xls\dataex\mede.xls!getpointvalarray(1,"localhost","TT-007","PV","V")	
12		3rd BODY JUICE TEMP.	=C:\Honeywell\client\xls\dataex\mede.xls!getpointvalarray(1,"localhost","TT-008","PV","V")	
13		4th BODY JUICE TEMP.	=C:\Honeywell\client\xls\dataex\mede.xls!getpointvalarray(1,"localhost","TT-009","PV","V")	
14		INLET JUICE FLOW	=C:\Honeywell\client\xls\dataex\mede.xls!getpointvalarray(1,"localhost","FT-001","PV","V")	
15		OUTLET SYRUP FLOW	=C:\Honeywell\client\xls\dataex\mede.xls!getpointvalarray(1,"localhost","FT-002","PV","V")	
16		OUTLET BRIX OF SYRUP	=C:\Honeywell\client\xls\dataex\mede.xls!getpointvalarray(1,"localhost","BT-001","PV","V")	
18		Outputs	k [kW/m²K]	
19		Heat Transfer Coefficient Vessel 1	=Model\F34	
20		Heat Transfer Coefficient Vessel 2	=Model\L34	
21		Heat Transfer Coefficient Vessel 3	=Model\R34	
22		Heat Transfer Coefficient Vessel 4	=Model\X34	
24		Error Value	=Model\X74	
26		Outputs	Sent Data	
27		Heat Transfer Coefficient Vessel 1	=C:\Honeywell\client\xls\dataex\mede.xls!PutPointVal_Number("LOCALHOST","HTCV1","SP",C19)	
28		Heat Transfer Coefficient Vessel 2	=C:\Honeywell\client\xls\dataex\mede.xls!PutPointVal_Number("LOCALHOST","HTCV2","SP",C20)	
29		Heat Transfer Coefficient Vessel 3	=C:\Honeywell\client\xls\dataex\mede.xls!PutPointVal_Number("LOCALHOST","HTCV3","SP",C21)	
30		Heat Transfer Coefficient Vessel 4	=C:\Honeywell\client\xls\dataex\mede.xls!PutPointVal_Number("LOCALHOST","HTCV4","SP",C22)	
32		Error Value	=C:\Honeywell\client\xls\dataex\mede.xls!PutPointVal_Number("LOCALHOST","ERROR","SP",C24)	

Figure 3.4: The inputs and outputs data page from Microsoft Excel® simulation

The data is sent from this page to the “Model” sheet where the simulation calculation is performed. The model spreadsheet is shown in figure (3.5). A full description of the code behind the calculations on this spreadsheet is shown in Appendix A.

Inputs from the controller are in the green filled cells; cells in purple fill are assumed values (iterated for) and cells in yellow fill are values returned to the controller for logging. Cells in light blue and pink fills are user inputs (manual user inputs required for the computation). Cells computed next to cells with a tan fill are values computed from a correlation based on a number of parameters. Cells in grey fill are cells that are manipulated when initial guesses and the “startup” macro are run, they are initially numerical guesses then later replaced by computed values, at the end of the simulation calculation they will be computed values based on the mass and energy balance not numerical guesses.

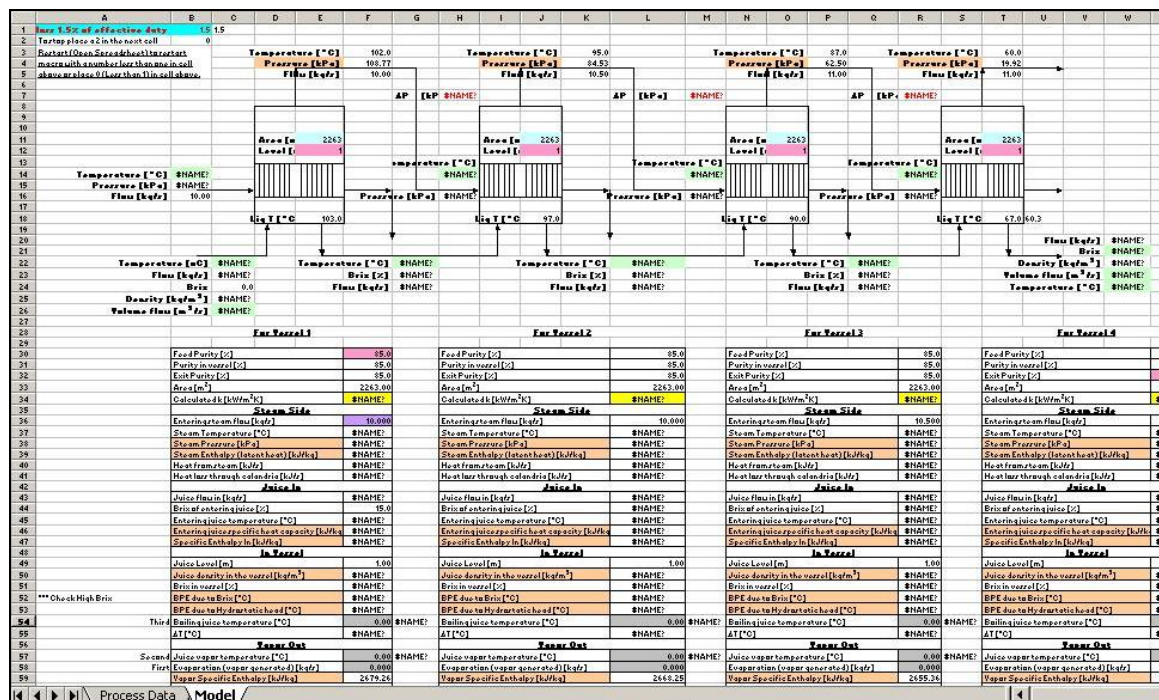


Figure 3.5: The model simulation page from Microsoft Excel® simulation.

The model has a number of Macros built into the spreadsheet. When the sheet is first opened the sheet will have errors on it due to the iterative procedure used (There will be circular cell references that cannot be solved for as they have no initial guesses). For this reason there is a macro called “Startup” which needs to be run to initiate initial guesses for the simulation and remove the erroneous cell references.

Once the erroneous cell references have been removed the automatic simulation macro can be initiated, this is performed by placing a “0” (Or any number less than 1) in cell B2. Once this is performed the spreadsheet will continue iterating the simulator to a solution that cause the mass and energy balance to converge. The simulation will continue to iterate until a “2” (Or any number greater than 1) is placed in cell B2 to stop the macros code and come out of the solver solution loop.

3.2.4 Microsoft Excel® VBA code

VBA was used for the calculation this section describes the code in detail and explains the calculation methods employed for the process. When opening the Microsoft Excel® spreadsheet Microsoft Excel® will ask if you will allow macros to be enabled, macros must be enabled for the simulator to operate.

Before the code can be used there are two important settings that need to be set in Microsoft Excel®. Some of these may already be set but if not they are as mentioned in the next few paragraphs.

Firstly, iteration calculations must be selected, this can be set under the menu Tools, Options. The calculation tab should have iteration selected as shown in figure (3.6).

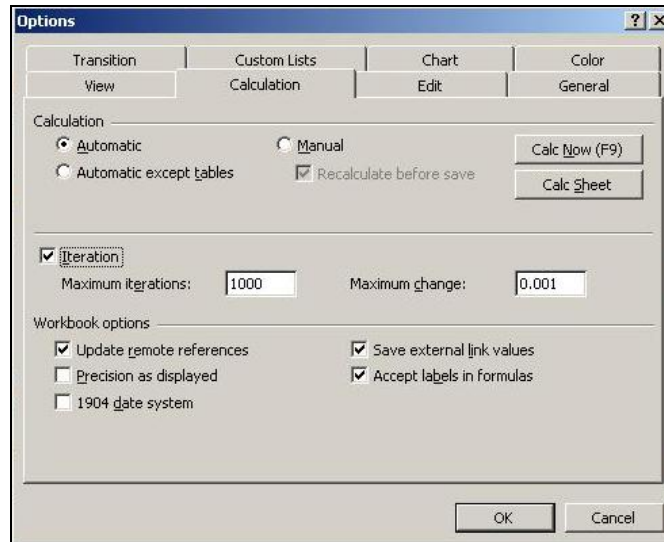


Figure 3.6: The iteration option must be on.

Secondly, in the visual basic editor (Tools, Macro, Visual Basic Editor) the solver library must be loaded. To do this, choose the Tools menu, then References, under the list of libraries the solver option must be selected as in figure (3.7).

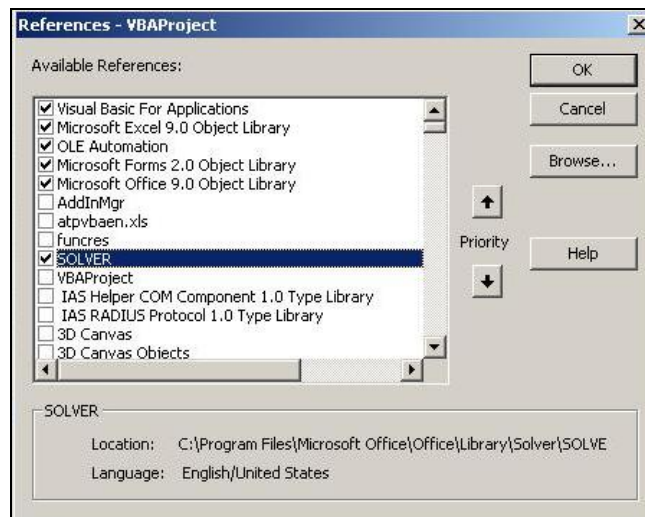


Figure 3.7: The solver library must be loaded in the Visual Basic Editor.

Once these settings have been set the code for startup can be run. The code is run by choosing tools, Macro, run macro and running the macro named startup. This code gives initial guesses for a number of variables then creates circular references to iterate to

a stable solution for the simulation. The code is described as in Appendix A; the code is found in the module section of the VBA project. In the code comments are in green.

To run this code the macro play command must be selected from the tools menu, as shown in figure (3.7), selecting to play the macro then brings up figure (3.8) as the display menu. To run the macro simply select the macro named “startup” and click on the run command.



Figure 3.8: The play macro command in Microsoft Excel ®.

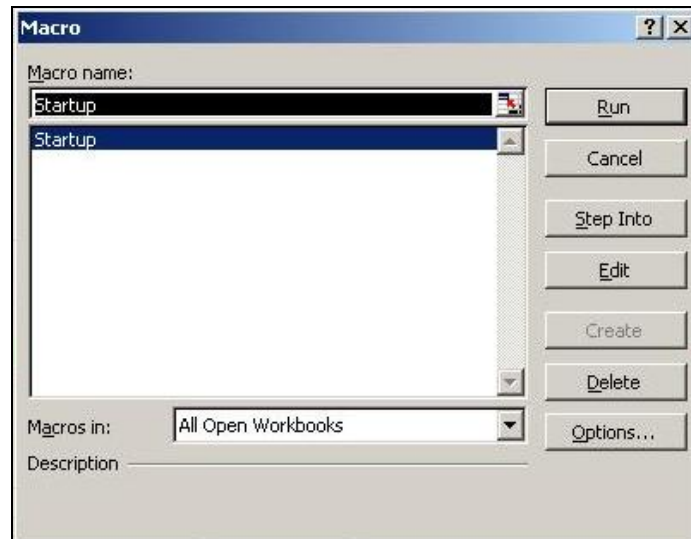


Figure 3.9: Selecting the macro to run in Microsoft Excel ®.

This will have initiated the spreadsheet and the calculations of the heat transfer coefficient can begin.

In order for the heat transfer coefficient to be computed the solver function must be kept running to keep the solution converged. This section of code can be turned “on”

or “off” by changing the value of cell B2, when this cell has a value greater than one the code will exit its loop but if the value is less than one the code will be executed and loop infinitely until interrupted. The solver code can be interrupted by placing a value greater than one in cell B2 or by pressing the “Ctrl” and “Pause/Break” keys simultaneously.

The code (found in the Microsoft Excel® Objects, This Workbook section of the VBA project) continually scans cell B2 to check for changes to the cell when running to see if it needs to exit the computation or keep running. The code also scans cell B2 if there are any changes made to the sheet, so if the value in B2 is changed to initiate the code the code detects a change in the workbook and checks if it is in B2 then initiates the code if B2 is changed to the “on” status.

There is a five second delay between each of the iterations of the solver routine in the code. The code uses the timer function for the delay of five seconds and this is shown in Appendix A.

3.3 Scale Model

3.3.1 Initial Model Proposed

The initial model proposed was based on the model presented by Taborek et al (1972) and is modified to account for the various processes occurring in evaporators. The model by Taborek et al was developed to try to systematically combine a number of different ideas on scaling into a single reference source. This model accounts for removal and deposition terms for the rate of change of change of the fouling resistance. The initial starting equation is shown in equation (3.56) below:

$$\frac{d(x_f k_f)}{dt} = \rho_f k_f \frac{dR_f}{dt} = \phi_d - \phi_r \quad (3.56)$$

where

$$R_f = \frac{1}{k} - \frac{1}{k_o} \quad (3.57)$$

The next step in developing the model is to find the terms for deposition and removal. We will begin with the deposition term. The initial model term proposed by Taborek et al has to be modified to account for boiling processes, Oufer et al (1993) showed that a modification to boiling systems is possible. Oufer et al have used the model with reasonable success to predict reaction fouling under sub-cooled and saturated boiling. The deposition term is assumed to be caused by the mass transfer diffusion and deposition of the scale components in the juice onto the tube surface. As a starting point the driving force for this process is assumed to be the difference in concentration between the bulk fluid at equilibrium conditions and the concentration at the tube surface of a specific component. The solution is supersaturated so it could easily be conceived that a difference in concentrations would be a large driving force for the deposition. The choice for this model selection is based on the fact that Reitzer (1964) and Oufer (1985) used this form to describe deposition of saturated solutions in evaporators. This can be described as below for each species fouling the surface in equation (3.58). There is typically an induction period for scaling so the deposition and removal terms should be able to account for these using a step function $U(t-t_d)$, this function is zero up to time t_d then has a value of one.

$$\phi_d = U(t-t_d) \sum_{i=1}^m E_b k_{pi} (C_{eqi} - C_{si}) = U(t-t_d) E_b \sum_{i=1}^m k_{pi} (C_{eqi} - C_{si}) \quad (3.58)$$

The term E_b is an enhancement factor to account for saturated boiling occurring in the tubes and is a function of two dimensionless variables, the Lockhart-Martinelli

parameter (X_{tt}) and the boiling number (B_o). Gungor, et al (1986), describe all these equations below for a system, the equations are derived to cover both sub cooled boiling and saturated boiling conditions. Gungor et al. (1986) claim that the following correlation is simpler to use and more accurate than previous correlations.

$$E_b = 1 + 24000B_o^{1.16} + 1.37 \left(\frac{1}{X_{tt}} \right)^{0.86} \quad (3.59)$$

$$B_o = \frac{\left(\frac{Q/A}{\Delta h_v} \right)}{\left(\frac{m/A_{cs}}{\lambda G} \right)} = \frac{q}{\lambda G} \quad (3.40)$$

$$\frac{1}{X_{tt}} = \left(\frac{x}{1-x} \right)^{0.9} \left(\frac{\rho_l}{\rho_v} \right)^{0.5} \left(\frac{\mu_v}{\mu_l} \right)^{0.1} \quad (3.41)$$

There are a number of other possible deposition factors that could account for reaction rate controlled deposition or gravity controlled settling of solids. It was decided to keep the model as simple as possible initially then increase the complexity as needed. Initially a diffusion process is assumed to be dominant and if this is insufficient to describe the process the then other deposition model extensions could be incorporated.

For the removal term, the scale is assumed to be removed by shear forces due to the fluid passing the surface, this term is described by Taborek et al as follows:

$$\phi_r = U(t - t_d) C_2 \frac{\tau}{R_b} = U(t - t_d) C_2 \frac{\tau}{\Psi} x_f^m \quad (3.42)$$

Where τ is defined by Tabork et al and Kern (1959) as below in equation (3.43)

$$\tau = C_6 \frac{1}{\rho_f} \left(\frac{W}{A_c} \right)^2 = \frac{2fv^3\rho}{4g} \quad (3.43)$$

And

$$R_b = \psi \left(\frac{1}{x_f} \right)^m \quad (3.44)$$

So the equation becomes:

$$\phi_r = U(t - t_d) C_3 \frac{1}{\rho_f} \left(\frac{W}{A_c} \right)^2 \frac{(x_f)^m}{\psi} \quad (3.45)$$

Using the assumption that the fouling resistance is proportional to scale thickness, $R_f = C_4 x_f$ and substituting all the equations into (3.56) we have the following result:

$$\rho_f k_f \frac{dR_f}{dt} = U(t - t_d) E_b \sum_{i=1}^n k_{pi} (C_{eqi} - C_{si}) - U(t - t_d) C_5 \frac{1}{\rho_f} \left(\frac{W}{A_c} \right)^2 \frac{(R_f)^m}{\psi} \quad (3.46)$$

Taborek et al found that for evaporation under the conditions similar to those found in a sugar mill the value of $m=1$ is a fair assumption. There are a number of problems when trying to implement this model, the value of the rate of change of fouling resistance with time can easily be determined from experimental measurements of the heat transfer coefficient and the removal term ϕ_d can be calculated. The values of the thermal conductivities of individual components are fairly easy to locate in books like Perry, Frantz and other heat transfer books. The biggest problem comes when trying to evaluate the equilibrium concentration of each component, even if the component concentration is recorded in the bulk phase one would think it is simply a matter of using the equilibrium coefficients to relate the bulk concentration to the equilibrium concentration as in equation (3.47).

$$\rho_f k_f \frac{dR_f}{dt} = U(t - t_d) E_b \sum_{i=1}^n k_{pi} \left(\frac{C_{bi}}{K_{ieq}} - C_{si} \right) - U(t - t_d) C_5 \frac{1}{\rho_f} \left(\frac{W}{A_c} \right)^2 \frac{(R_f)}{\psi} \quad (3.47)$$

The problem is trying to fit a mathematical function to equilibrium data, for example the data shown in Walthew (1994) will initially show an increase in solubility with temperature to a certain temperature then the solubility decreases below this temperature above it. The ceiling solubility temperature changes with Brix and to describe the solubility as a function of just two parameters, temperature and Brix is incredibly difficult. Another problem is that much of the solubility data is for only set temperatures (25°C for example in Meade and Chen) and the evaporators are operating at higher temperatures (around 100°C to 60°C). The literature data also has a problem in that the solubility is in “technical” sucrose solutions or other idealized systems, which are very far from reality in real syrup and juice solutions. Initially the plan was to regress the experimental data for the model to obtain the solubility coefficients but to formulate the mathematical form of the solubility curve is challenging. Another mathematical calculation that is difficult to perform is the vapor fraction in the boiling enhancement factor, because boiling is such a complicated process the vapor fraction varies along the tube of an evaporator and is fairly difficult to compute without making assumptions about the zones that various boiling regimes occur in.

The other model constants can be found as described in Part 2 of Taborek et al’s (1972) paper.

Other models that try to describe scaling are discussed in the paper by Taborek et al, these include the Kern-Seaton model, Watkinson-Epstein model, Reitzer model and the Beal model. A number of these models were developed for heat exchanger design work so are not applicable to the evaporators under consideration also some of the

theoretical models such as the model by Kern and Seaton do not fit literature data available.

An overall mass balance of juice compositions needs to be performed over the evaporator set to determine how much mass accumulates in the set with time in order to use this model. Assuming that the components of interest are non volatile and that there is no entrainment in the vapor phase it is possible to perform a mass balance. The formulation of this balance for each effect can be shown assuming a system of flows similar to those shown in figure (3.10).

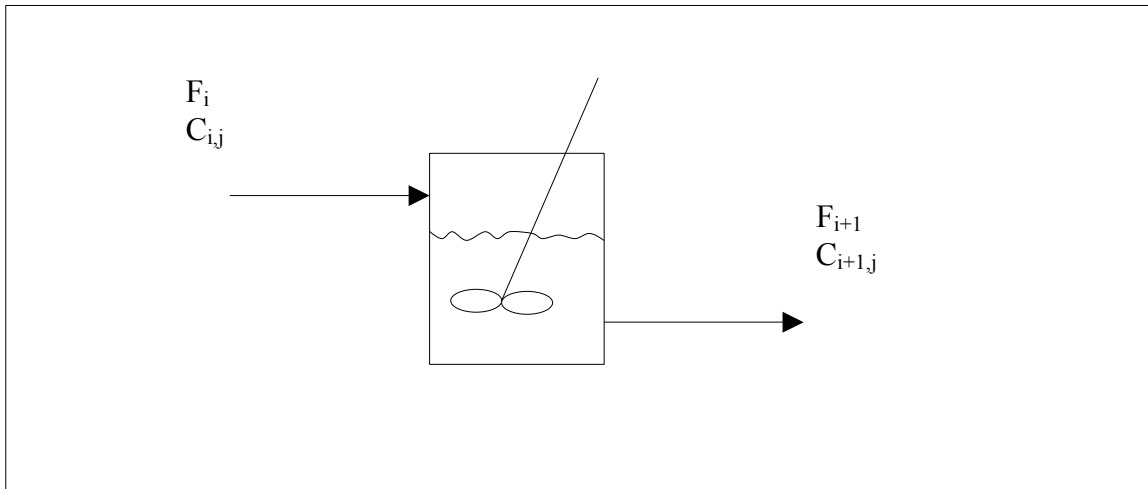


Figure 3.10: Mass balance schematic for juice and syrup components.

A balance occurs if:

$$\text{Accumulation} = \text{Input} - \text{Output} + \text{Generation} - \text{Removal} \quad (3.48)$$

So for each individual effect I, with component j:

$$\frac{dVc_{i,j}}{dt} = F_i c_{i,j} - F_{i+1} c_{i+1,j} \quad (3.49)$$

And for the overall balance (when there are four effects):

$$\frac{dVc_j}{dt} = F_1 c_{1,j} - F_5 c_{5,j} \quad (3.50)$$

By taking samples of the cane juice fed to the evaporators and the syrup leaving the effects the major scaling components can be analyzed and their accumulation in the system studied.

3.3.2 Empirical Model

Because of the difficulties of the initial model proposed one turns to empirical formulations of clean heat transfer coefficients as a function of Brix, temperature, viscosity and other important parameters when the vessel is clean then correcting for the scaling by adding a time dependence term accounting for scaling. This two part model is described next.

3.3.2.1 Time Dependant Empirical Model

The next few pages show some models to allow for the computation of a time dependant model of the heat transfer coefficient and the resistance-fouling rate of change, which would have been needed if the initial modeling from first principles were implemented.

3.3.2.1.1 McCabe and Robinson & Reitzer

3.3.2.1.1.1 Constant ΔT

The earliest model for scaling includes the work by McCabe and Robinson (1924) who proposed a model for scale formation on the following assumptions.

- Constant differential temperature across the calandria
- Constant velocity of fluids in the tubes
- Feed is to enter at a temperature close to that of the boiling liquid in the vessel i.e. no flash or sub cooling of the feed fluid (This is not entirely true in multiple effect evaporators)

- Scale deposition rate is proportional to the evaporation rate
- Scale does not crack or flake off and remains on the surface until cleaned
- Thin enough scale deposits to assume that the heat transfer area is constant and the scale deposits do not significantly affect the velocities of fluids by reducing the cross sectional area for flow (In Robert evaporators in the sugar industry this assumption is for the most part valid)

The original text had a few errors in the derivation so it is recalculated below and some of the assumptions and formulations expanded on. It is assumed that the evaporation rate is proportional to the heating rate so the scale thickness is proportional to the heat flux (Only true for thin scale deposit thicknesses) is shown in equation (3.51).

$$\text{Scale thickness} = a.q \quad (3.51)$$

In the above equation a is a proportionality constant and q is the heat flux (heat transferred per unit of heat transfer area). The heat transfer equation governing the heat transfer between the heating stream and the fluid to be heated is shown below:

$$\frac{dq}{dt} = k\Delta T \quad (3.52)$$

We make the assumption that the value of the overall heat transfer coefficient is the addition of the reciprocals of the layer resistances yielding the equation below.

$$k = \frac{1}{\alpha + \beta q} \quad (3.53)$$

Equation (3.53) can be proved by considering the fact that we know that equation (3.54) holds and manipulations can reduce this to equation (3.53).

$$\frac{1}{k} = \frac{1}{h_0} + \frac{1}{h_{0d}} + \frac{d_1 \ln\left(\frac{d_1}{d_2}\right)}{2k_w} + \frac{d_1}{d_2} \left(\frac{1}{h_i} + \frac{1}{h_{id}} \right) \quad (3.54)$$

Scale on the steam side we will assume is negligible so the equation becomes:

$$\frac{1}{k} = \frac{1}{h_0} + \frac{d_1 \ln\left(\frac{d_1}{d_2}\right)}{2k_w} + \frac{d_1}{d_2} \left(\frac{1}{h_i} + \frac{1}{h_{id}} \right) \quad (3.55)$$

If it is further assumed that the values of k_w , h_0 , h_i , d_1 and d_2 are constant (Constant operating conditions) and the equation becomes:

$$\frac{1}{k} = \alpha + \beta' \left(\frac{1}{h_{id}} \right) \quad (3.56)$$

Where α and β' are constants. We made the assumption that the scale resistance ($1/h_{id}$) is proportional to scale thickness then substituting (3.51) into (3.56) yields:

$$\frac{1}{k} = \alpha + \beta' a q \quad (3.57)$$

Combining the constants β' and a into a new constant β equation (3.53) results.

Rearranging (3.53) to solve for q results in the following.

$$q = \frac{1}{\beta k} - \frac{\alpha}{\beta} \quad (3.58)$$

ΔT is assumed to be constant in (3.52) so substitute (3.58) into (3.52) to find an integral version of the equation and solve for k . Note that α and β are constants so the term (α/β) falls from the equation. The manipulations are shown below:

$$\frac{d\left(\frac{1}{\beta k}\right)}{dt} = k \Delta T \quad (3.59)$$

$$-\frac{dk}{\beta k^2 dt} = k \Delta T \quad (3.60)$$

Place in integral form:

$$-\int \frac{1}{k^3} dk = \int \beta \Delta T dt \quad (3.61)$$

This yields the following solution:

$$\frac{1}{k^2} = 2\beta \Delta T t + \text{const.} = ct + d \quad (3.62)$$

Where c and d are constants. This model was checked with data from Kerr (Bulletin 149 of the Louisiana State University) and found to be applicable for a quad evaporator set.

The model presented above was also derived by Reitzer (1964), his proof shows the constant d to be the inverse of the initial (clean) overall heat transfer coefficient squared (As would be expected). Reitzer also derived the equation in such a way as to define the constant c, as below:

$$c = \frac{2bk_d \Delta T}{\rho k_t h_i} \quad (3.63)$$

Where all the variables in this equation are shown in the nomenclature. The summarized equations are shown in equations (3.64) and equation (3.65).

$$\frac{1}{k^2} = \frac{1}{k_o^2} + \frac{2bk_d \Delta T}{\rho k_t h_i} t \quad (3.64)$$

$$\Delta T = \Delta T_o \quad (3.65)$$

3.3.2.1.1.2 Constant Flux

Reitzer (1964) also extended the model to a system with constant flux as opposed to constant differential temperature. This results in the following result with less restrictive assumptions:

$$\frac{1}{k} = \frac{1}{k_o} + \frac{k_d}{\rho k_t} \left(\frac{b}{h_i} \right)^{n'} (q)^{n'} t \quad (3.66)$$

The model described by equation (3.66) can be used to show how ΔT should increase as scaling occurs over time to maintain a constant flux. This is also linear with time and is shown below:

$$\Delta T = \Delta T_o + \frac{k_d}{\rho k_t} \left(\frac{b}{h_i} \right)^{n'} (q)^{n'+1} t \quad (3.67)$$

3.3.2.1.1.3 Unsaturated Solutions

In evaporators and heaters in general Reitzer (1964) notes that there is usually a delay time before scaling occurs. He attributes this to the fact that the solution is not necessarily saturated in the bulk phase but as one moves closer to the heating surface the concentration increases and eventually becomes supersaturated and nucleation spots begin to occur. This gradient of concentration is assumed to be linear in Reitzers derivation.

$$\frac{1}{k} = \frac{1}{k_o} + \frac{k_d}{\rho k_t} \left((C_{sat} - C_b) + \frac{bq}{h_i} \right)^{n'} t \quad (3.68)$$

And for the temperature difference the profile can be described with:

$$\Delta T = \Delta T_o + \frac{k_d q}{\rho k_t} \left((C_{sat} - C_b) + \frac{bq}{h_i} \right)^{n'} t \quad (3.69)$$

These models will describe and model the heat transfer coefficient with time. This coefficient can be related back to the scale thickness with time using equations (3.51) and (3.53). Since the scale thickness is assumed to be directly proportional to the scale resistance the scale resistance with time can be computed. The data will have to be checked against these models to determine which processes describe the operating conditions most closely. It is important to ensure that the right equations are used to

describe the processes occurring in the evaporators if any reproduction of, or predictive modeling from, the results is to be achieved.

3.3.2.1.1.4 General Model

All these models show a trend of the form of equation (3.70).

$$\frac{1}{k^n} = \frac{1}{k_o^n} + a_o t \quad (3.70)$$

$$\Delta T = \Delta T_o + a_o t \quad (3.80)$$

3.3.2.1.2 Other Models

There are a number of other models for fouling behavior the paper by Epstein on fouling in heat exchangers reviews some of these models and includes a number of models described from other sources. This paper is the same as that presented by the same author in the book on fouling of heat transfer equipment by Somerscales and Knudsen. The models presented show exponential behavior and a common equation that show up in a number of references for mass deposition onto surfaces as a function of time is as in equation (3.81).

$$m = m^* \left(1 - e^{-\frac{t}{t_c}} \right) \quad (3.81)$$

Bott (1997) supports this equation but adds a further modification and takes into account dead time which if assumed to be small will reduce his equation to that shown in equation (3.91). [This also assumes that m is proportional to R_f and Bott recommends that this proportionality constant is 5000 kgW/m^4]

$$R_f = R_{f\infty} \left(1 - e^{-\frac{t-t_D}{t_c}} \right) \quad (3.91)$$

In the paper by Oufer and Knudsen the equation derived was almost exactly the same as (3.81) and an equation similar to (3.91) is derived, the only difference is that in order to apply the equations to a boiling system the Enhancement factor is multiplied by the mass transfer coefficient to account for enhanced mass transfer due to boiling. This enhancement factor equation is dependant on two dimensionless numbers the Lochart-Martinelli parameter and the Boiling number as described previously.

Among the thirteen deposition models presented in the paper by Epstein the most applicable models to evaporators are those by McCabe and Robinson and the model by Reitzer.

The deposition model by Reitzer (1964) is as below:

$$\frac{dm}{dt} = K(C_c - C_s)^n \quad (3.92)$$

For constant differential temperature the model is reduced to:

$$\frac{dm}{dt} = C_7 k^n \quad (3.93)$$

For constant heat flux the model simplifies to:

$$\frac{dm}{dt} = C_8 \quad (3.94)$$

Epstein also comments that the value of n for sugar boiling evaporator systems is one. This simplifies the model computations somewhat compared to higher order models.

Both Kern (1959) and Taborek suggest equations of the form of equation (3.95) for scale modeling.

$$R = R^* (1 - e^{\beta t}) \quad (3.95)$$

3.3.2.2 Clean Heat Transfer Coefficient

There are a number of different models to determine the heat transfer coefficient as a function of many variables, the various models found from literature are included in table 3.1.

Some equations in the table such as the Dessin formula in Honig, which are used to compute mass flow rather than heat transfer, may be useful to get the form of a heat transfer coefficient value; some resemblance for example is seen to Guo et al's form.

Table 3.1: Heat transfer coefficients as a function of temperature, Brix and viscosity

<u>Equation</u>	<u>Source</u>	<u>Literature constants</u>
$k_o = K \frac{Q^a k_j^b}{\eta^c}$	Madsen (1996)	a = 0.63 to 0.5 b = 0.5 c = 0.22 to 0.33
$k_o = K(100 - B)^a T_b^b$	Guo et al. (1983)	a = 0.4 b = 0.25
$k_o = K\mu^a$	Guo et al. (1983)	a = -0.13
$k_o = K(100 - B)^a (T - 54)^b$	Honig (1963)	a = b = 1
$k_o = K \frac{T_j}{B}$	Van der Pol et al (1998)	K = 0.5
$k_o = K \frac{T_{avg}}{B_{avg}}$	Heluane et al. (2001)	K = 6.51
$k_o = KT_s - a$	Smith and Taylor (1981)	K = 0.034 a = 1.13
$k_o = K(1 - aB)^b (1 + cT)^d (1 + eV)^f$	Hussey (1973)	K = 49.093 a = 15.6 b = 0.776 c = -8.998x10 ⁻³ d = 0.4 e = 0.2518 f = 1.036

The first 24hrs of heat transfer coefficient data will be assumed to be clean and regressed for in the form of the above equations to find the best form of the equation.

3.3.3 Proposed Model for Regression

The final regressed model should be able to predict the heat transfer coefficient as a function of time for the St James sugar mill based on the “clean” conditions at the mill and the regressed time dependant model parameters. The final model will have the following form:

$$\frac{1}{k^n} = \frac{1}{k_o^n} + a_o t \quad (3.96)$$

The value of n to be chosen should be 2 as work presented by Epstein (1978) showed that for natural circulation evaporators n=2. The value of a_o will depend on the effect chosen. The value of k_o will depend on the initial operating conditions after a clean and will be a function of many variables:

$$k_o = f(Brix, viscosity, temperature,) \quad (3.97)$$

The choice of the best model for the initial heat transfer coefficient values are critical and the models found for this purpose will be regressed for and checked for their applicability. These values will be regressed for using the first twenty four hours of data after each clean and regressed to deduce these values as a function of Brix, viscosity, temperature, heat flux or other important parameters from the empirical models.

CHAPTER 4. MATERIALS AND METHODS

4.1 St James Mill Setup

The St James mill contains a control computer for the logging of data but a large majority of the control loops are pneumatic stand-alone loops and not actually run through the controller computer. A full diagrammatic depiction of the control scheme is shown in figure (4.1) and all the recorded variables are labeled with the tags they use in the controller.

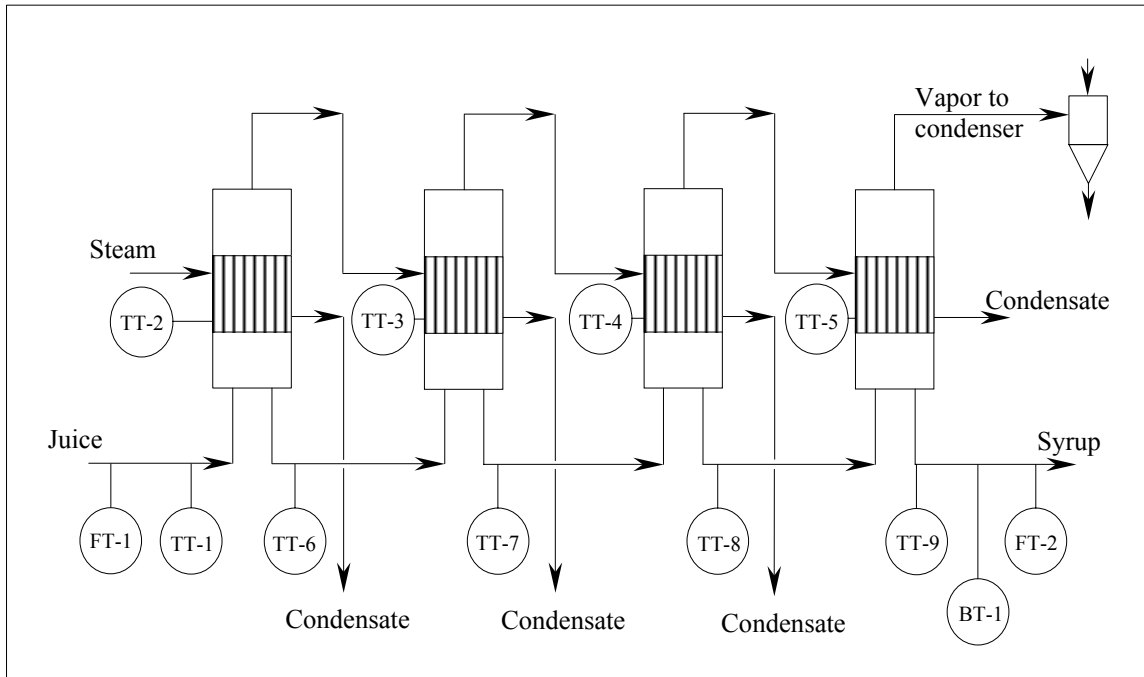


Figure 4.1: The measured variables at the St James sugar mill evaporators.

4.1.1 Control Scheme and Data Logging

There are level control loops for each effect using the feed flow as a manipulated variable to control the level in each effect. This causes a large variability in the flow to each effect as the valve control causes rapid changes to the feed valve position to control the level. The level of the juice supply tank controls the steam supply valve percentage

opening. The Final Brix out the final effect is controlled by a three-way valve, which recalculates syrup to the final effect if the Brix is too low. There are disadvantages to this particular loop, the most crucial being the possible creation of color by prolonged residence times of the syrup in the evaporator station particularly in the final effect. The control loops for the mill are shown in figure (4.2).

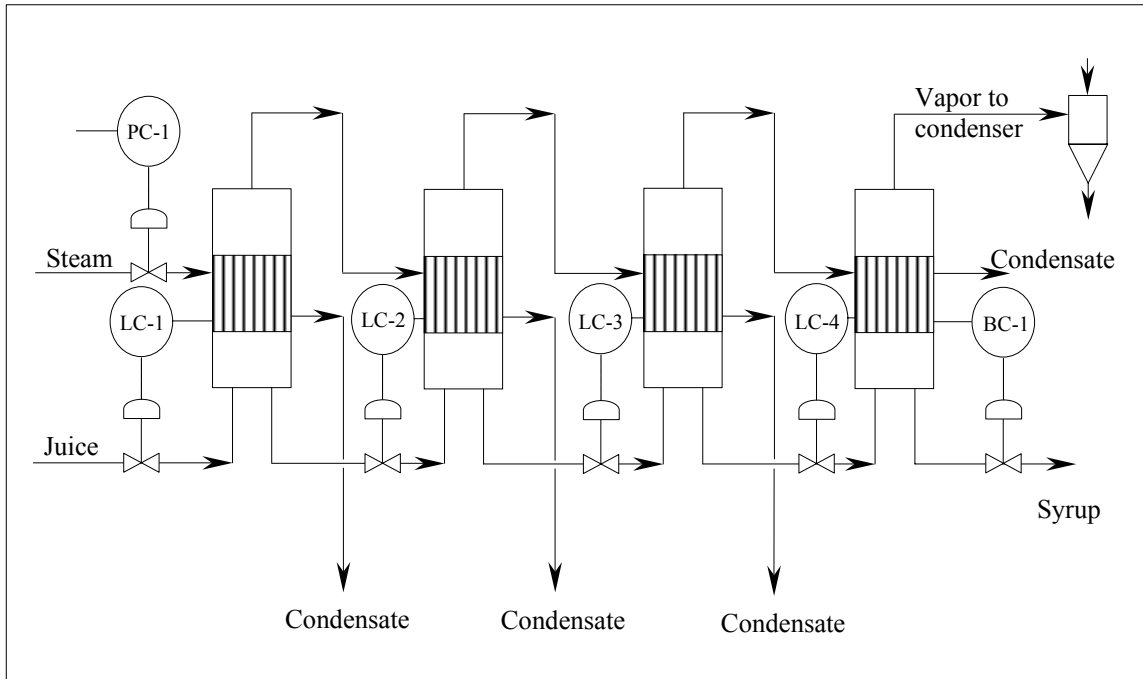


Figure 4.2: The control loops used at the St James sugar mill evaporators.

Data is logged on a personal computer running a control program called Plantscape supplied by Honeywell. This software logs the measured variables as well as passing these variables on to Microsoft Excel® where the heat transfer coefficients for each effect are computed. After being computed the calculated heat transfer coefficients are passed back to the Plantscape software and are also logged by the Honeywell software. The history log times for the data is one minute for the data and then averages of six and thirty minutes up to an hour or day can be computed if required.

4.1.2 Measurement Devices

There are a number of measuring devices used to compute the heat transfer coefficients at St James and they are described briefly in the following sections. To see where these are setup at the mill refer back to figure (4.1).

4.1.2.1 Mag Flow Meters

The flow meters used for the juice flow to the evaporators and the syrup flow out the effects is measured using a magnetic flow meter. The meters chosen are Ultra Mag® electromagnetic flow meters, made by McCrometer. These meters use magnetic coils to generate an electric field in the instrument, as a conducting fluid passes through the instrument it disturbs the generated magnetic field resulting in an induced voltage. The instrument has electrodes that measure this disturbance and relate this to the velocity of fluid passing through the unit, which can be converted to a volumetric flow. The unit outputs a volumetric flow signal which is converted to m^3/s by the controller. The sizing of these units for the St James mill is shown in Appendix G. The sizes of the meters used were the 8" unit for the juice and the 4" meter for the syrup. The meters have an accuracy rated at 0.5% of the actual flow according to the suppliers. The juice meter for the flow to the first effect was installed horizontally and the syrup flow meter was installed vertically.

4.1.2.2 RTD Probes

The Resistance Temperature Devices (RTD) probes installed have an extremely high accuracy. The probe accuracy was checked and found to be very good and although there was a slight hysteresis effect the RTD's were in general accurate to within a fraction of a percent. See Appendix H for the calibration curves for each probe. The

slight hysteresis effect may be due to a small lag in the system but in general the probes were extremely accurate.

The RTD probes were installed in the concentrated juice lines from each effect and in the feed line to the first effect. The probes were fully inserted in the juice lines as seen in figure (4.3). The length of each RTD probe is 20cm but then also have the connection housing installed at the end of them.



Figure 4.3: RTD probe installation in juice lines at the St James sugar mill evaporators.

The installation in the steam calandria required a little more thought as the probes need to be positioned in a place where they will record the saturated temperature of the steam in the calandria. Since there are two steam inlets to each calandria the probes were installed midway between each inlet and half way up the calandria wall to ensure temperature measured was sat not a super heated one but the saturated condensing temperature. There were some problems with these probes not being able to be fully inserted into the calandria because of the tubes being in the way, these issues are

discussed in the discussion and results section of this document. A picture of the probe in the third effect calandria is shown in figure (4.4). In this setup only about 3cm of the probe is actually in the calandria and the rest of the probe is in the insulation section, it was repositioned for the 2004/2005 season to more fully insert it.



Figure 4.4: RTD probe installation the third effect calandria at the St James sugar mill evaporators.

4.1.2.3 Microwave Brix Probe

A microwave Brix probe measures the water content in a sample. The probe can be calibrated to measure Brix or dissolved solids. Typically mills are interested in Brix and the probes will be calibrated against samples of Brix, but will be more accurate if calibrated against moisture. The microwave Brix probes instruments compete with hydrostatic head measurement Brix measurements which compute density, which is back computed to Brix using tables. The Brix probe at St James is shown in Figure (4.5), it is

pipled in such a way that it can be isolated during cleaning. or if it needs to be worked on without disturbing the evaporators while online.



Figure 4.5: Final effect Microwave Brix probe at the St James sugar mill evaporators.

4.2 Juice Analysis

The juice and syrup from the evaporators were analyzed on an HPLC system. In HPLC there is a stationary and mobile phase, the phase material is chosen based on the chemicals of interest to be studied. The samples are injected under pressure into a column that contains the stationary phase, with time the chemicals exit the column. The times various chemicals exit the column is based on the size of chemicals of interest and their affinity for the column stationary phase. As a chemical exits the column it is detected by a detector, the response of the detector gives an indication of the concentration of the compound. Standards are used to calibrate the response of the detector.

HPLC was run to analyze cation and anion components present in the juice and syrup. These are performed on two separate instruments setup specifically for cation and anion determination.

CHAPTER 5. RESULTS AND DISCUSSION

5.1 Microsoft Excel® Model

5.1.1 Microsoft Excel® Model Development

The advancement of computers and their integration to control schemes as well as their speed in performing computations are the only reason a project such as this can be performed. As noted by Hoekstra (1981) the calculation of an unknown heat transfer coefficient from known data is complicated, iterative and computationally intensive. The work performed by Hoekstra was performed in a number of modules and run as a stand-alone program, although there were aspirations to incorporate the program into the factory overall mass and energy balances. Although the modeling may appear to be linear in nature the system is nonlinear because of the boiling point elevation terms, which depend on Brix and temperatures.

In developing the model, the code for executing the computations would have been neatly packaged if the calculations could be included in the software used by Honeywell for the controller. There is a control builder software package with Plantscape that can perform control and computational manipulations on analogue and digital input signals. The mathematical manipulations are very rudimentary and the large number of iterations required to perform the mass and energy balances make the coding problematic. An attempt to use control builder to perform the computations was aborted when the complexity of equations and vast number of iterations required were realized. The data was then sent to Microsoft Excel® where the iterations and complex correlations are

more easily manipulated and performed. The calculated heat transfer coefficients are then sent back to the controller for logging.

The use of spreadsheets have made the excessive amounts of coding a thing of the past and the built in code in spreadsheets such as Microsoft Excel® make the application of the mass and energy balance solver that much simpler to derive and tailor to individual mill needs. Urgan et al. (1999) mention that when boiling point elevations are considered some non-linear solution techniques fail. The equations can be linearized and Urgan proposed solution techniques for simulation purposes but the systems are fairly time intensive to program and the use of spreadsheets have negated a large majority of this intensive programming, as much of it is hard coded into the spreadsheet programs.

The transfer of data to and from Microsoft Excel® is simply performed using the Microsoft Excel® data exchange plug in that is incorporated with the Honeywell software.

5.1.2 Microsoft Excel® Model Execution

Urgan et al. (1999) mentions for initial guesses that the vapor flow is that calculated from Rillieux's principle and initial temperatures from an even split of the available differential temperature. This principle is applied to the Microsoft Excel® model to initiate the model as initial guesses before the iterative true solution is performed. A full listing of the VBA code used is included in Appendix A.

The model makes a number of assumptions, such as assuming that heat losses in lines negligible, a similar assumption was made by Abdulmuin et al. (1985) in a model derived to describe steady and non steady state evaporator operation. They also made the

assumption that the input steam is saturated. All these assumptions are described fully in the theory section of this document

The initialization of the spreadsheet is achieved by running a macro that makes initial guesses for flows and temperatures then systematically reinserts calculations to iterate to the correct solution for the system. After the spreadsheet has been initialized a macro can be run that will converge the input data to the steady state solution for the system. The code to converge the solution can be turned on or off by the user by changing the value of a cell reference.

There were issues with operators closing the Microsoft Excel® spreadsheets, to ensure this was less likely to occur when the Microsoft Excel® code is running, the Microsoft Excel® application is hidden from the screen and does not show up on the taskbar (the application does still appear in the task manager list though). The application makes itself visible every two minutes or so for about five seconds to allow users to break the computational loop if desired.

A full list of the model development in terms of the correlations used is shown in Appendix F.

5.1.3 Microsoft Excel® Model Results

The Microsoft Excel® model was developed to show how the computed heat transfer coefficient changed with time. The data collected can however be used to see some trends in other measured variables. Some of these trends are observed because of the way the mill operates and how the control of the effects is performed. In figure (5.1) the temperatures of the syrup exiting each effect is trended. The final effect has a constant temperature, due to the fact that the evaporator train has a constant vacuum applied to the

final effect. The final effect is also forced to produce a constant Brix product and levels are kept constant in the final effect. This means that the saturated vapor temperature is fixed by the constant vacuum, and since the Brix and level are constant the boiling point elevation both due to Brix and hydrostatic effects are constant the exit temperature should be constant. The other effects have continuously increasing steam and vapor temperatures due to the current control scheme so will exhibit an increased syrup temperature. The gaps in the data are clean out periods in which the vessels were taken offline to chemically clean them. There are other periods in which stops on the mill or other operational glitches caused the temperatures to change, but these take place over fairly small time periods so are not visible on the scale of time seen in the figure.

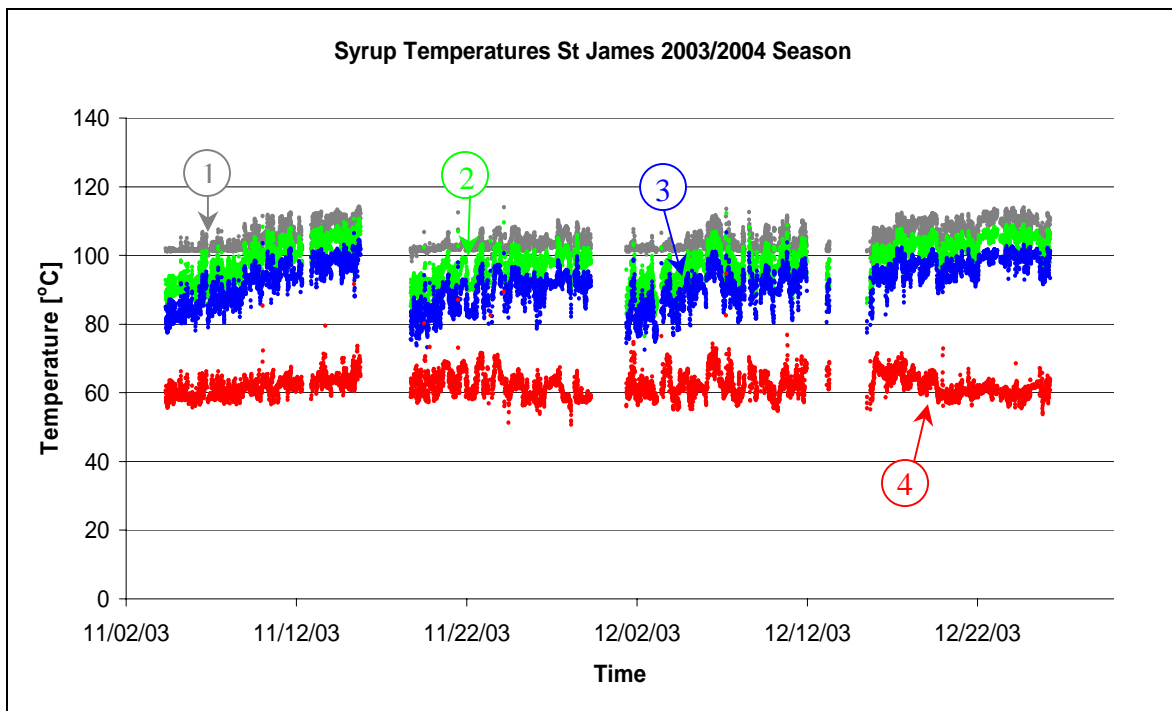


Figure 5.1: Syrup temperatures recorded for the St James evaporators.

In figure (5.2) the steam temperatures are plotted for collected data at the mill. The mill controls the pressure of the exhaust steam applied to the first effect using a level

control from the juice tank; as more throughput is required by the evaporator train, the pressure of the exhaust steam in the first effect is increased. The effect ripples through the effect as an increase in the pressure of the first effect vapor results, which increases the pressure and temperature of the calandria of the second effect and so on.

The data presented in figure (5.2) is corrected data as it was found that a conductive error was occurring in the third effect calandria. The conductive error occurs because a majority of the probe is exposed to lower temperatures than the calandria steam as it was not fully inserted into the calandria. The ambient air cools the probe and heat is conducted away from the probe tip causing a lower temperature to be recorded at the tip of the probe. This error of 1.4°C caused the computed heat transfer coefficient to be erroneous. The offset of this error was added to the temperature data for the third effect calandria temperature readings and the data remodeled and the heat transfer coefficient correctly computed.

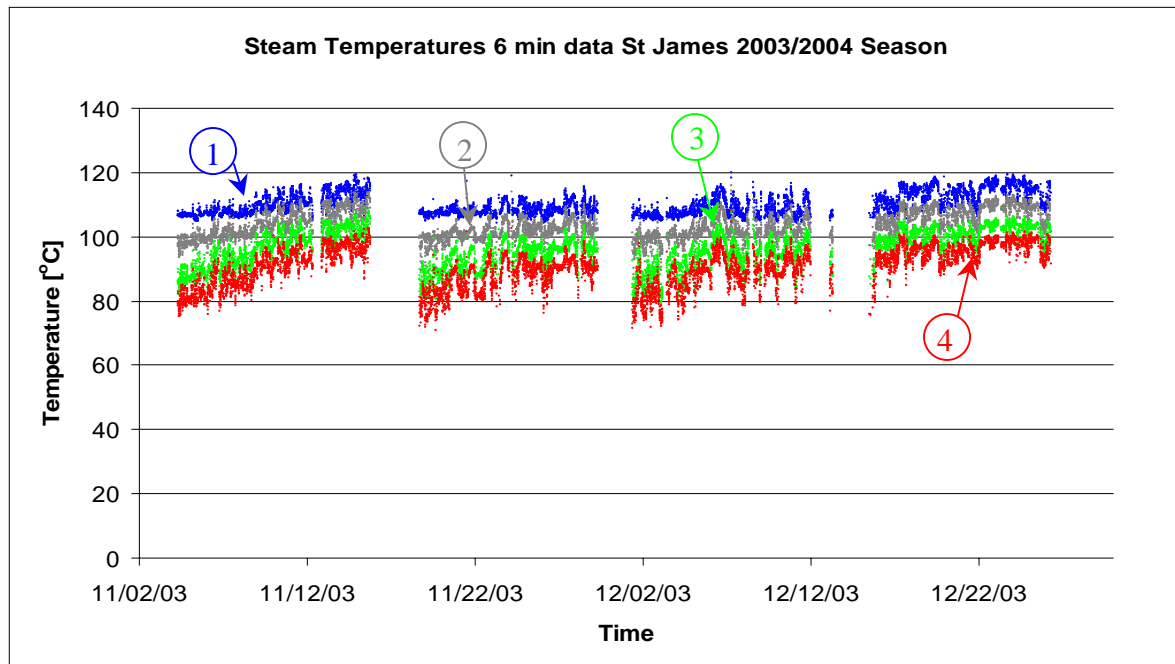


Figure 5.2: Calandria temperatures recorded for the St James evaporators.

The results from the checking of the calandria temperatures and the RTD probe accuracy is shown in Appendix H.

The next figure (5.3) shows the volumetric flows to and from the evaporator train. The flows are very “noisy” and needed to be filtered. The filtering was justified by the fact that the “noise” is generated by the control of the levels in each effect. A valve on the inlet line to each effect controls the level of each effect, the control is set up to have an accurate level control, and this however causes surges in flow. The average flow is of more interest than the high and low surges for our mass and energy balance, which is based on steady state conditions and requires steady inputs. The flow is filtered for a few seconds by the Honeywell control software but a larger filter time is required for real time data collection.

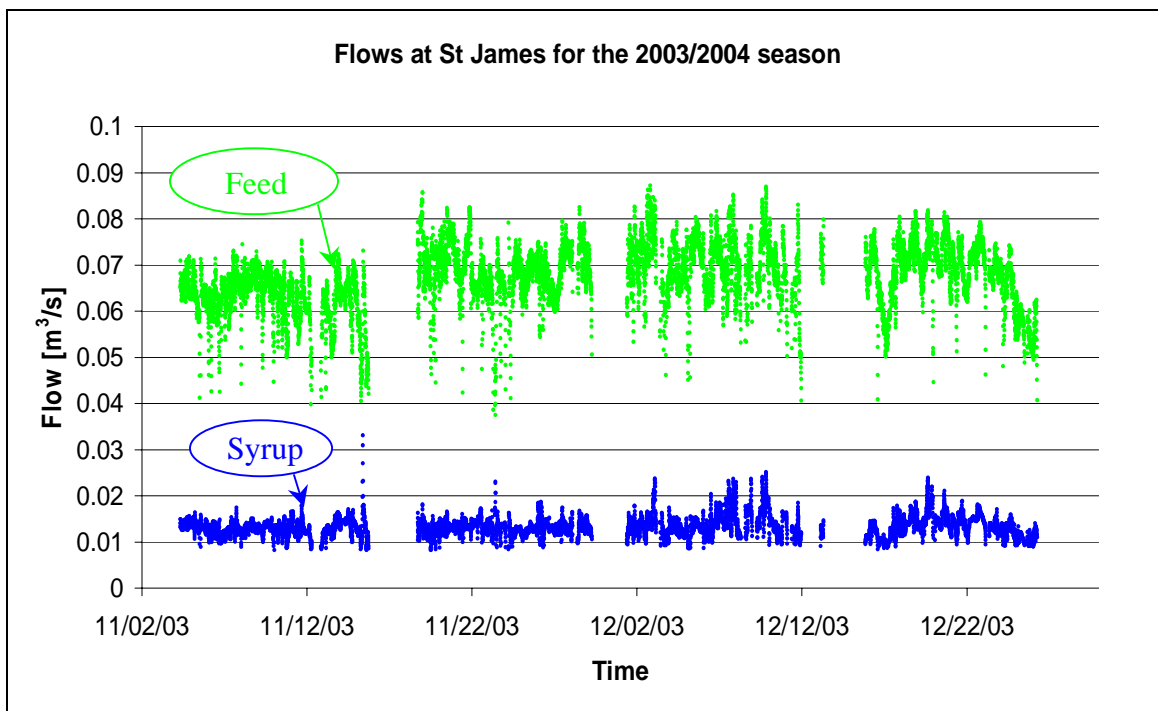


Figure 5.3: Juice and Syrup volumetric flows recorded for the St James evaporators.

The last effect is least affected by temperature measurements across the calandria and syrup, as the total differential is fairly large. The findings of temperature sensitivity being more significant in the first few effects was seen in a sensitivity analysis of the model performed before the start of the season. Figure (5.4) shows how drastically the computed heat transfer coefficient changes when small variations in the first effect calculated vapor temperature are made. The heat transfer coefficient is computed by dividing the heat transferred through the calandria by the area of the calandria and differential temperature across it. Since the differential temperatures are so small, the effect of even small changes in temperature can result in vast changes in the heat transfer coefficient. This underlies the importance of accurate and well-positioned temperature measuring devices.

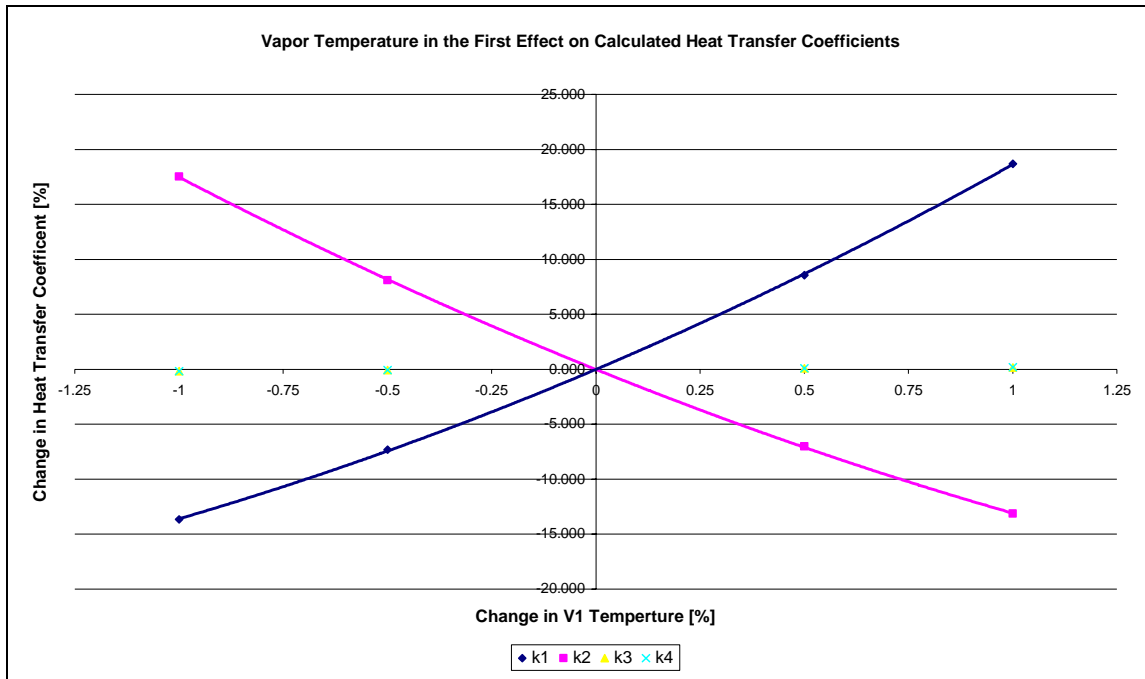


Figure 5.4: Sensitivity analysis of vapor temperature changes.

The differential temperature across each effect is computed as this has a significant effect on the computed heat transfer coefficient. Figure (5.5) shows the

differential temperature in the effects. The differential temperature for the first three effects is fairly small and remains constant.

There is an increase in the last effect differential temperature because the temperature of the heating vapor increases but the vacuum (and thus vapor temperature) remains constant resulting in an overall increase in differential temperature with time.

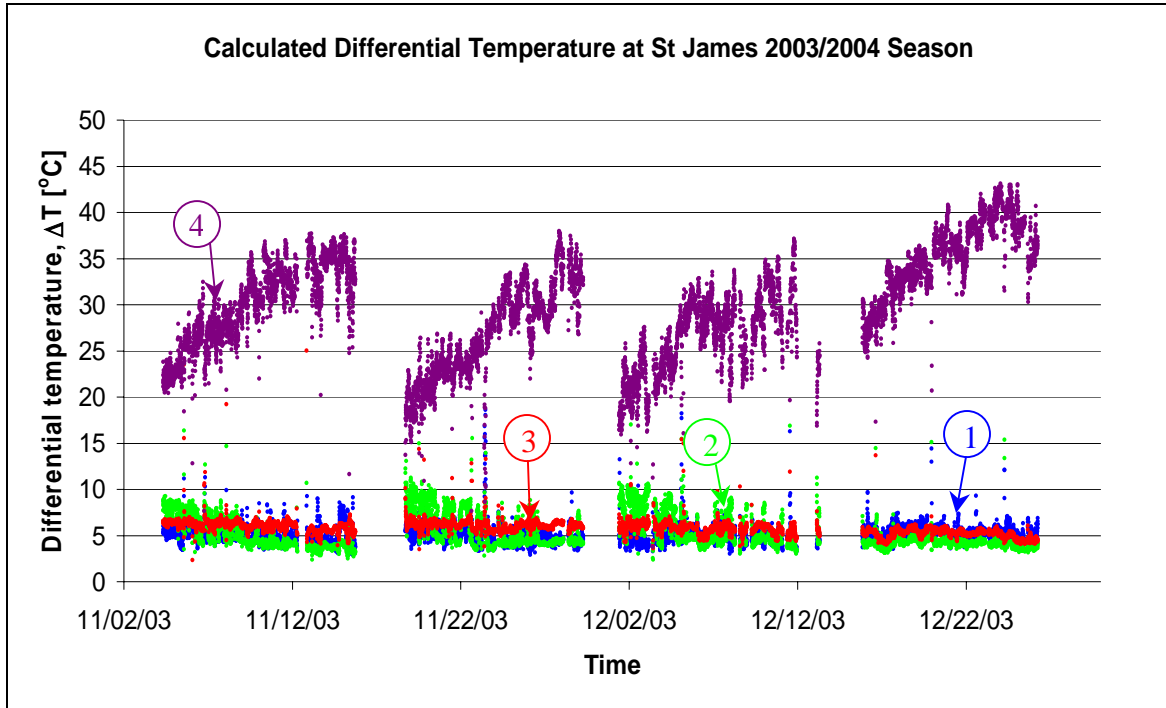


Figure 5.5: Differential temperature recorded for each effect at the St James evaporators.

There was a problem with the installed microwave Brix probe that caused the ceramic tip on the unit to crack, and syrup passed through the ceramic tip and shorted out the delicate electronics in the transmitter. The mill had a spare unit but a similar problem occurred so the measured laboratory Brix values needed to be used for the syrup Brix. These values had to be manually entered into the computer and run with the collected data when the season was over. Sensitivity analysis on the model indicated that the accuracy loss by using these slightly less accurate values is not significant. The results of

the sensitivity analysis depicted in figure (5.6) show that a change of around ten percent in the measured Brix value would only change the measured heat transfer coefficient value by about five percent.

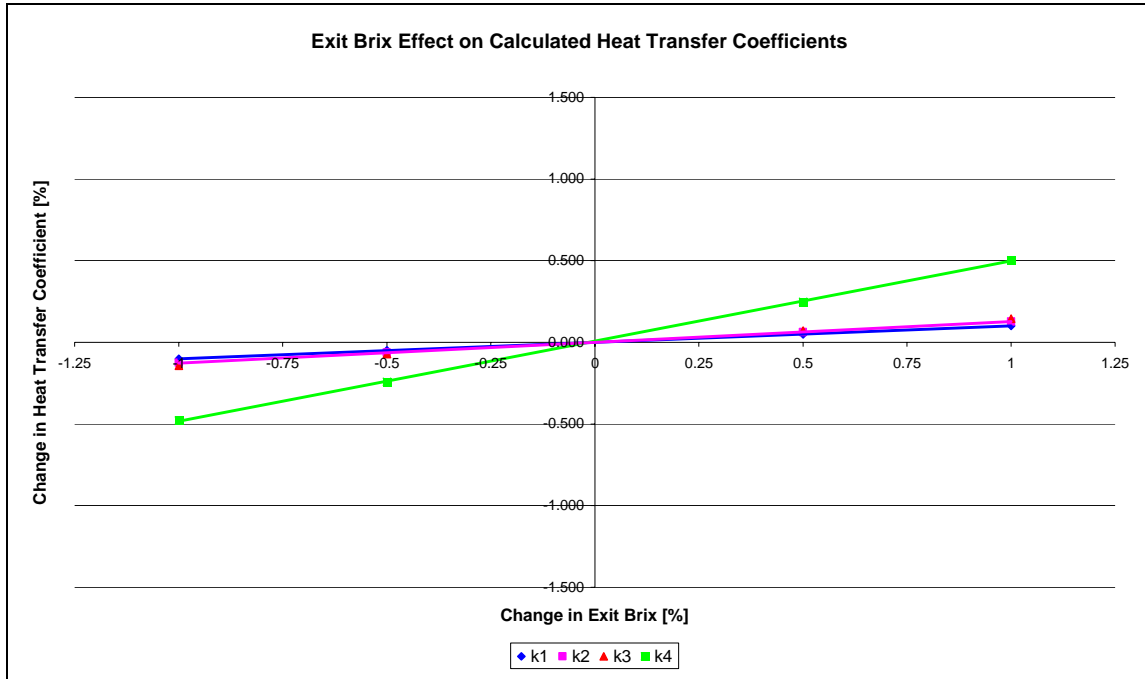


Figure 5.6: Exit Brix sensitivity analysis.

The heat transfer coefficient results are shown in figure (5.7). These results are calculated by re-running the data with a smoothed flow. The flows are smoothed using exponential smoothing to get the results shown. The results were a little hard to decipher trends from, so the calculated heat transfer coefficients are smoothed and re-plotted in figure (5.8). The noise due to shut downs and upsets cause the scatter and noise so are filtered out to show true trends in the values.

As can be seen there is little significant change in the heat transfer coefficients for the first few effects, but the last effects shows a steady decline in the heat transfer coefficient. These conclusions will be discussed further in the evaluation of heat transfer coefficient data later in this chapter.

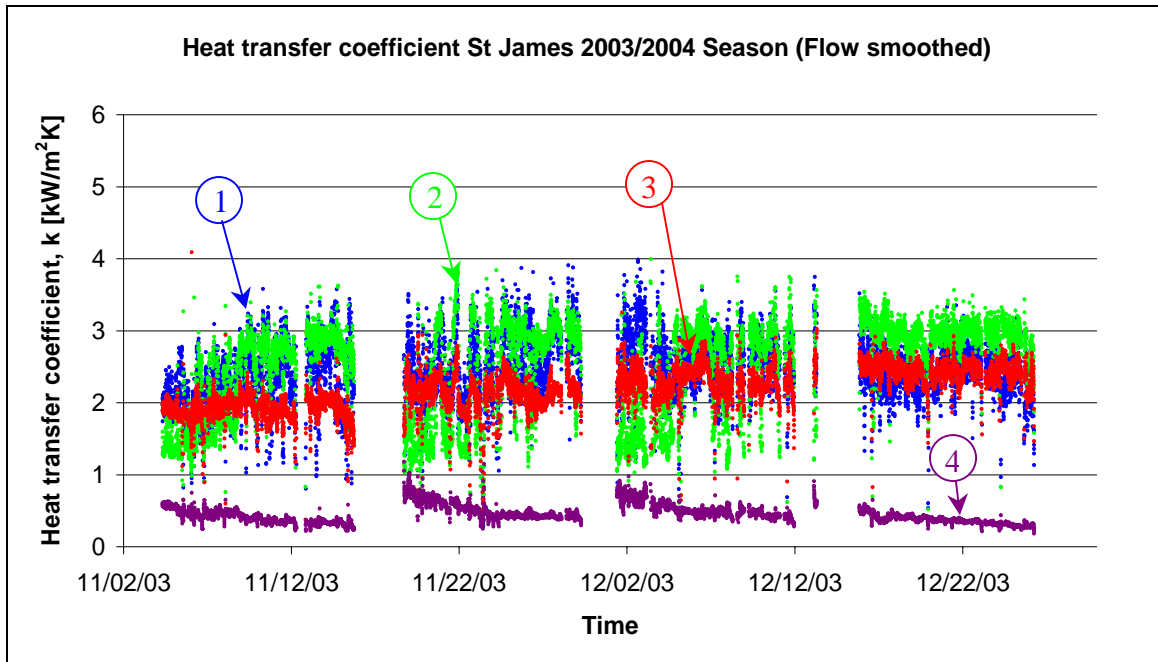


Figure 5.7: Computed heat transfer coefficients with flow filtered at the St James evaporators.

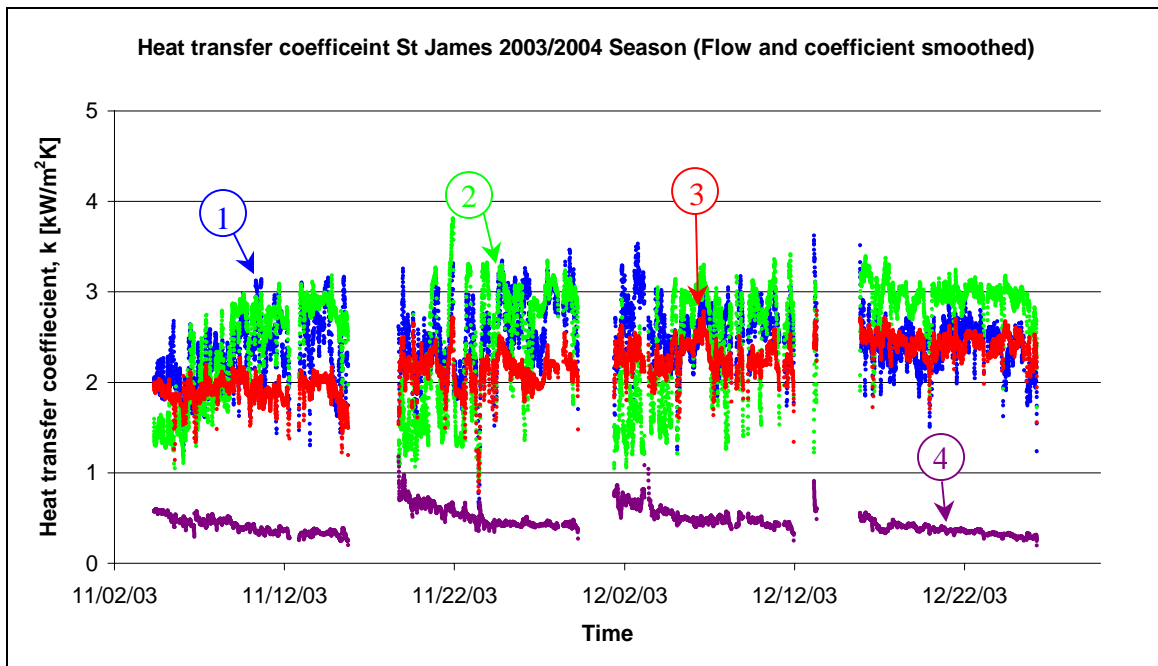


Figure 5.8: Computed heat transfer coefficients with flow and heat transfer coefficients filtered at the St James evaporators.

An interesting point to note is that the last effect was not cleaned properly in the second to last clean. This resulted in the heat transfer coefficient not returning to a high

“clean” condition but rather staying low, as the scale material was not removed adequately. This increases further the usefulness of the Microsoft Excel® model as it will show if a particular effect is scaled or not and how efficient cleans were.

Similar work by Snoad (1997) showed that the heat transfer coefficients cycled with the changes in the vacuum in the last effect as this changes the overall differential temperature available for the train to operate on. Snoad (1997) who was performing measurements on a five effect evaporator train found a heat transfer coefficient of $2.5 \text{ kW/m}^2\text{K}$ for the third effect (Snoad noted this value to be 20% more than the heat transfer coefficient data compiled by Watson in 1986) and 1.5 to $1 \text{ kW/m}^2\text{K}$ for the forth effect and the final effect operated at around 0.6 to $0.7 \text{ kW/m}^2\text{K}$. He also made the same observation that the second and third effects show practically no scaling trends and scaling in the first effect is only slight.

5.2 Juice and Syrup Analysis

The clarified juice fed to the evaporators and the final syrup from the last effect was collected as a weekly composite from the mill. The samples were run on the HPLC to analyze the samples for specific cations and anions. The Brix, purity, ash and sucrose were also determined for the samples based on HPLC sucrose concentrations in the samples. The purity values were used in the model as some of the correlations require a purity value to compute the values in the model. These values of each components concentration were fairly stable as seem in figures (5.9) and (5.10).

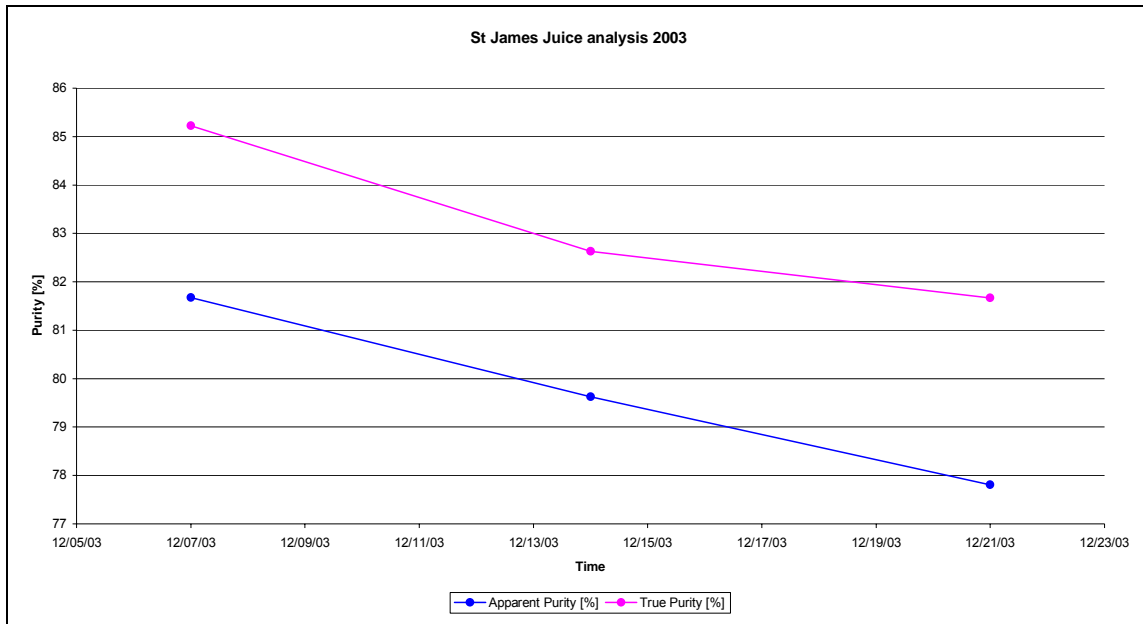


Figure 5.9: Clarified Juice weekly composite purity.

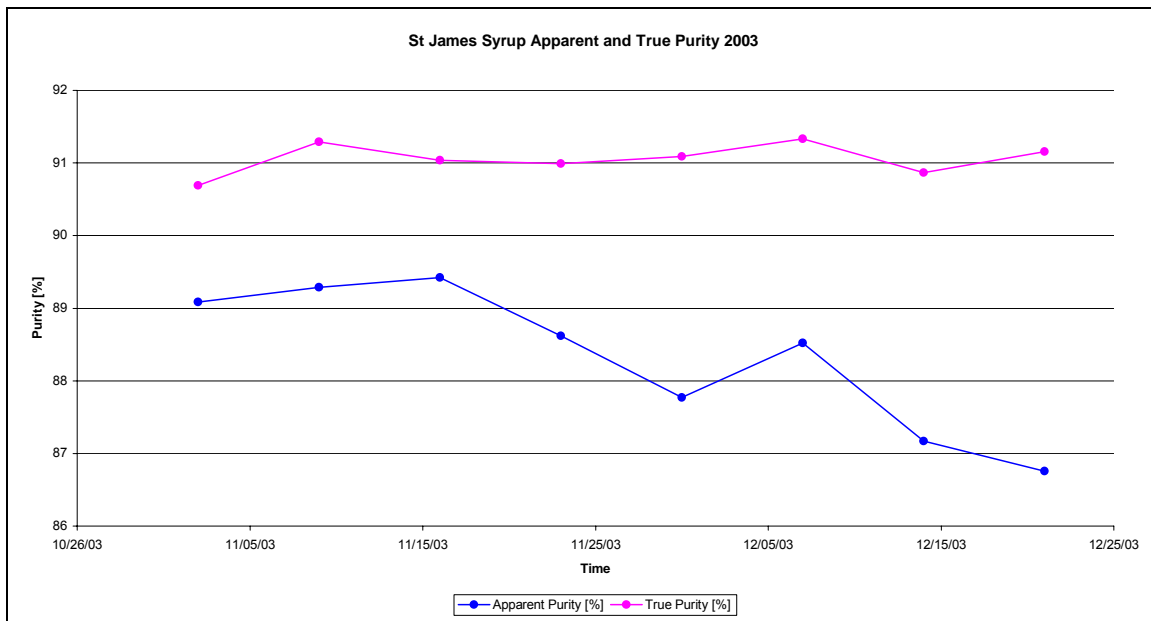


Figure 5.10: Syrup weekly composite purity.

As can be seen from the results there are less juice sample results than syrup results, this was because there were problems with storing the juice samples, as the juice samples are collected they typically have a preservative added and then are frozen at minus 70°C to ensure that the samples do not degrade with time. The freezer for this

application was shipped late and only arrived towards the end of the season. The syrup samples with a higher sucrose concentration are less likely to degrade due to microbial activity and can be stored in a fridge with no preservative. This meant that syrup results were collected for the majority of the season but only a few juice samples were collected.

The ash results for juice and syrup is shown in figures (5.11) and (5.12) respectively. The results show very little ash content change over the period sampled except for the single peak in the one sample of the syrup, but it returned close to the average value the next week.

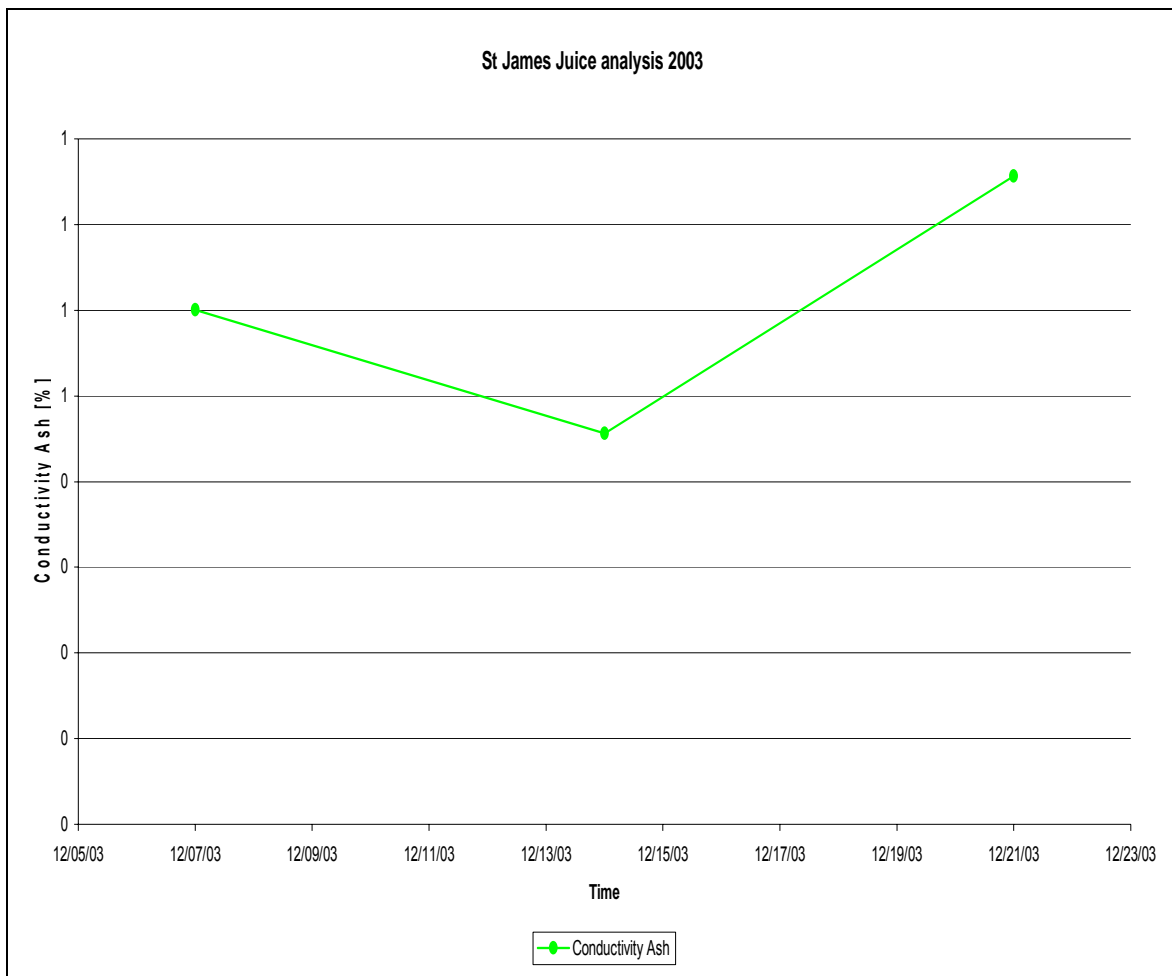


Figure 5.11: Clarified juice weekly composite ash.

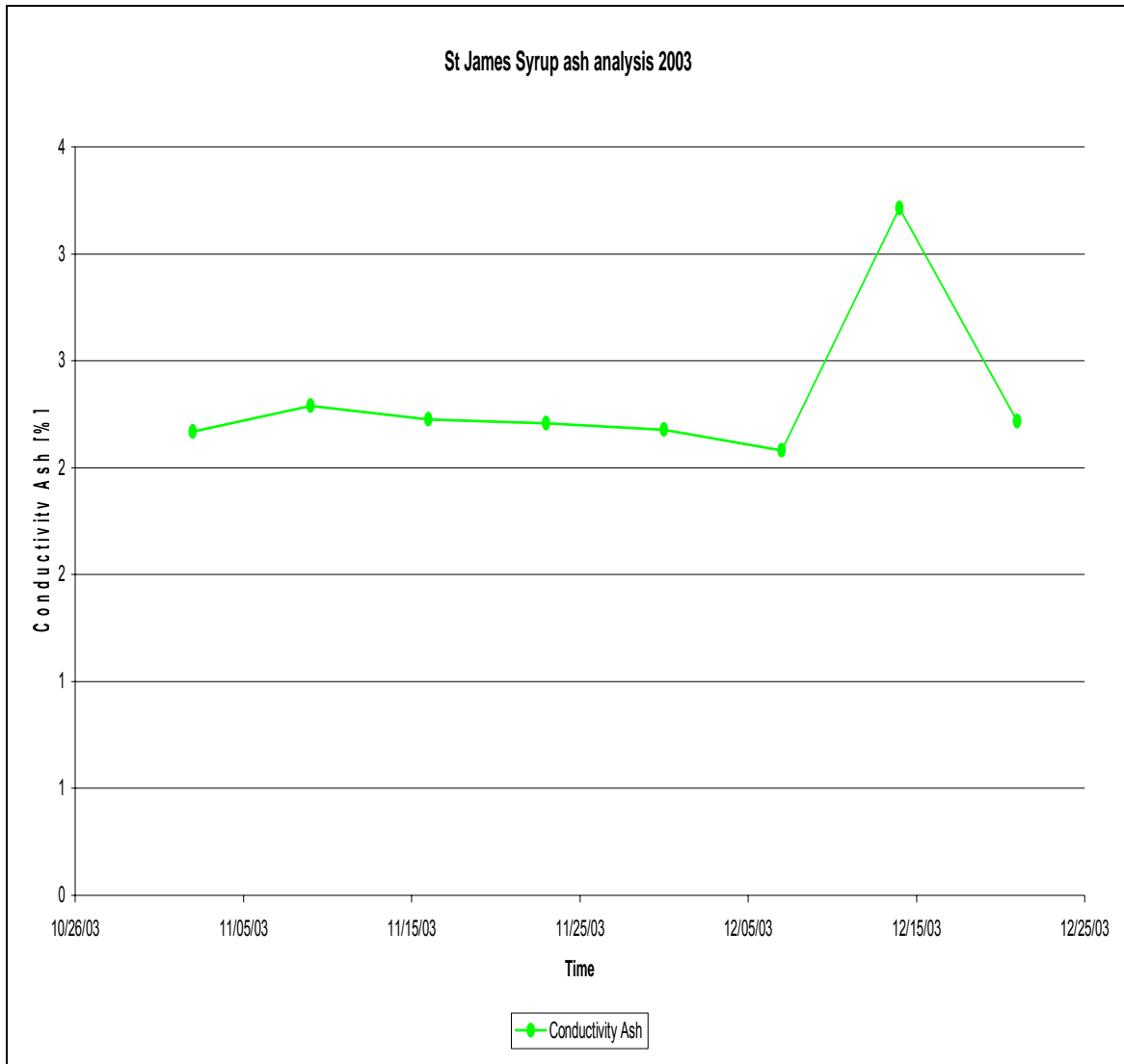


Figure 5.12: Syrup weekly composite ash.

The Brix content are shown in figures (5.13) and (5.14) for juice and for syrup. The results seem to indicate that there is a fairly steady Brix out the evaporators until the end of the season even though the clarified juice Brix is increasing. One possible explanation is that with the final effect of the evaporators fouled, the evaporators may not have been able to maintain the throughput required and maintain a high Brix product so in order to maintain throughput the Brix needs to be lowered.

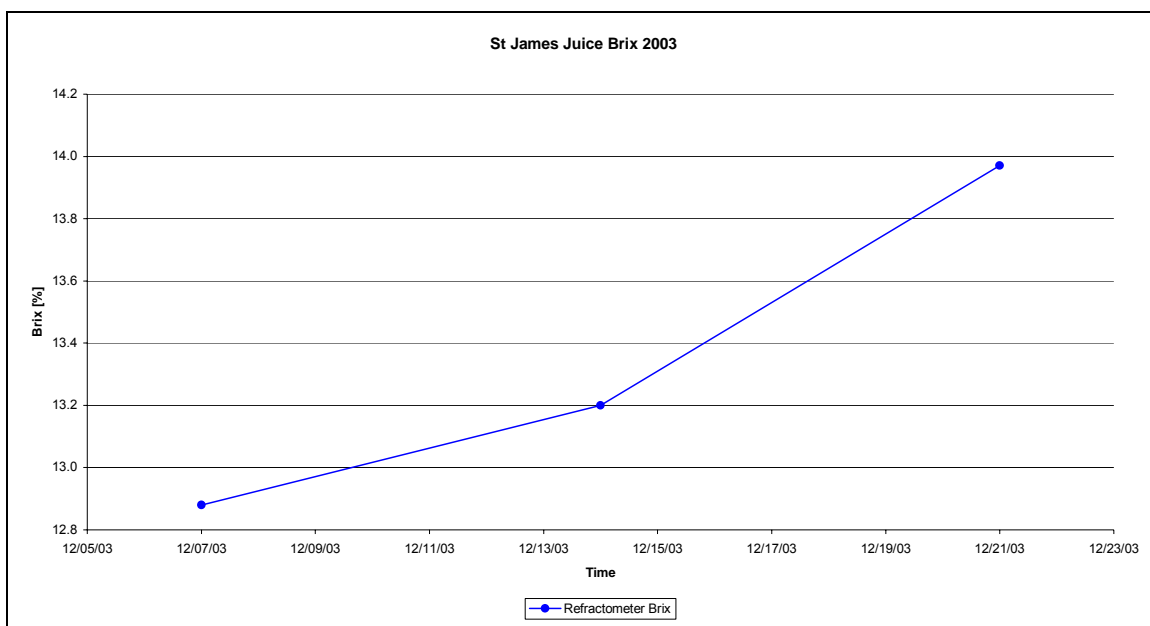


Figure 5.13: Clarified juice weekly composite refractometer Brix.

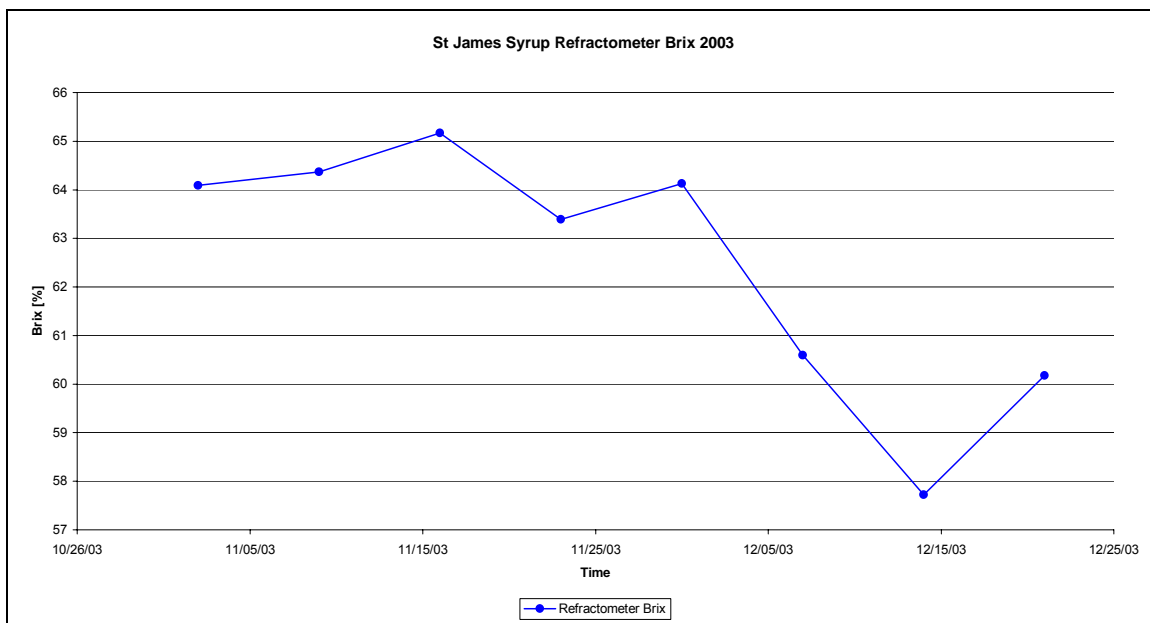


Figure 5.14: Syrup weekly composite refractometer Brix.

The juice and syrup samples analyzed for cations and anions are shown in the next few figures. Figure (5.15) shows the ions in the clarified juice, and figure (5.16) shows the ions in the syrup for all ions except potassium, chlorine and aconitate. Figure

(5.17) shows the potassium, chlorine and aconitate ions in the clarified juice, and figure (5.18) shows the potassium, chlorine and aconitate ions in the syrup.

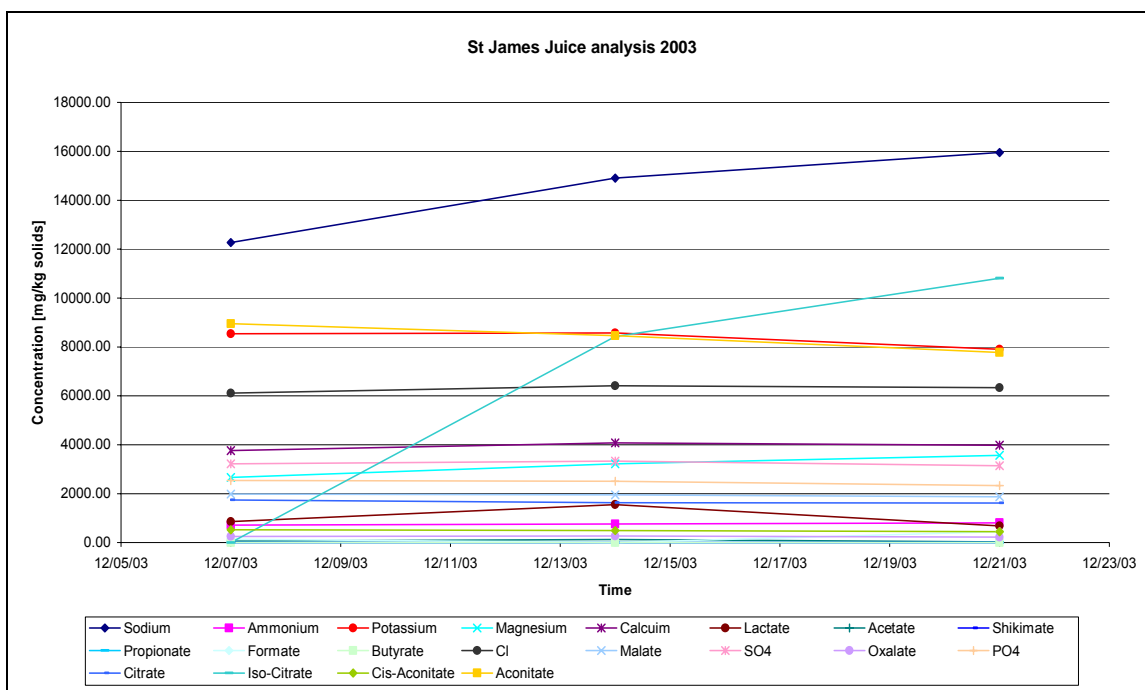


Figure 5.15: Clarified juice weekly composite cation and anion analysis results.

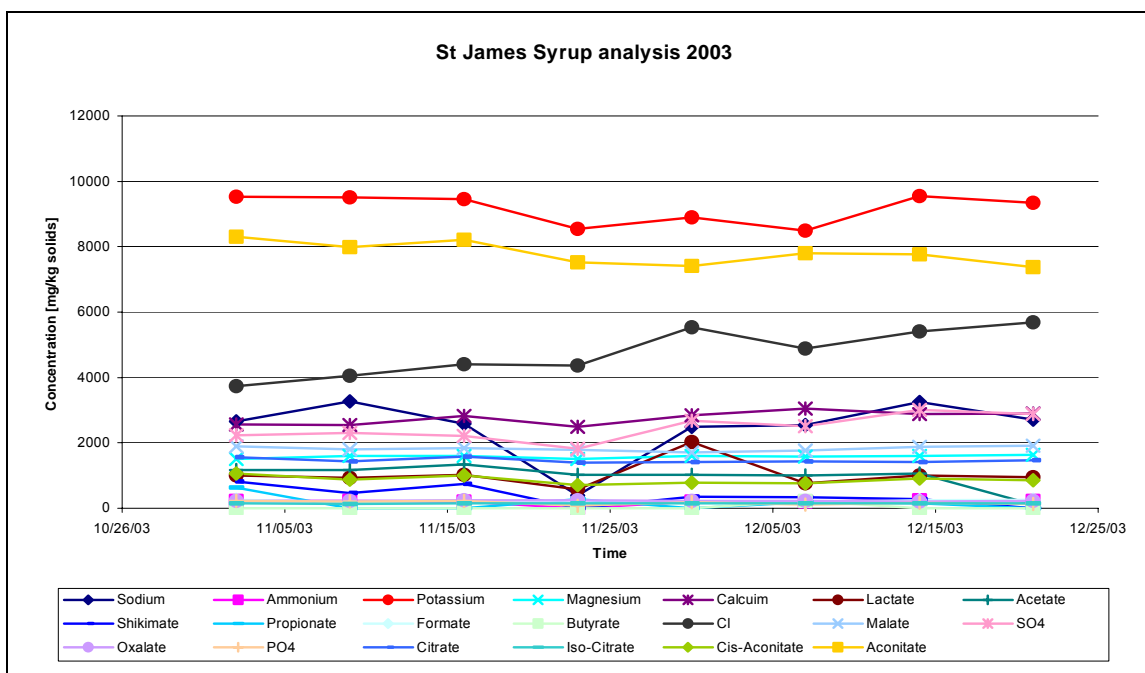


Figure 5.16: Syrup weekly composite cation and anion analysis results.

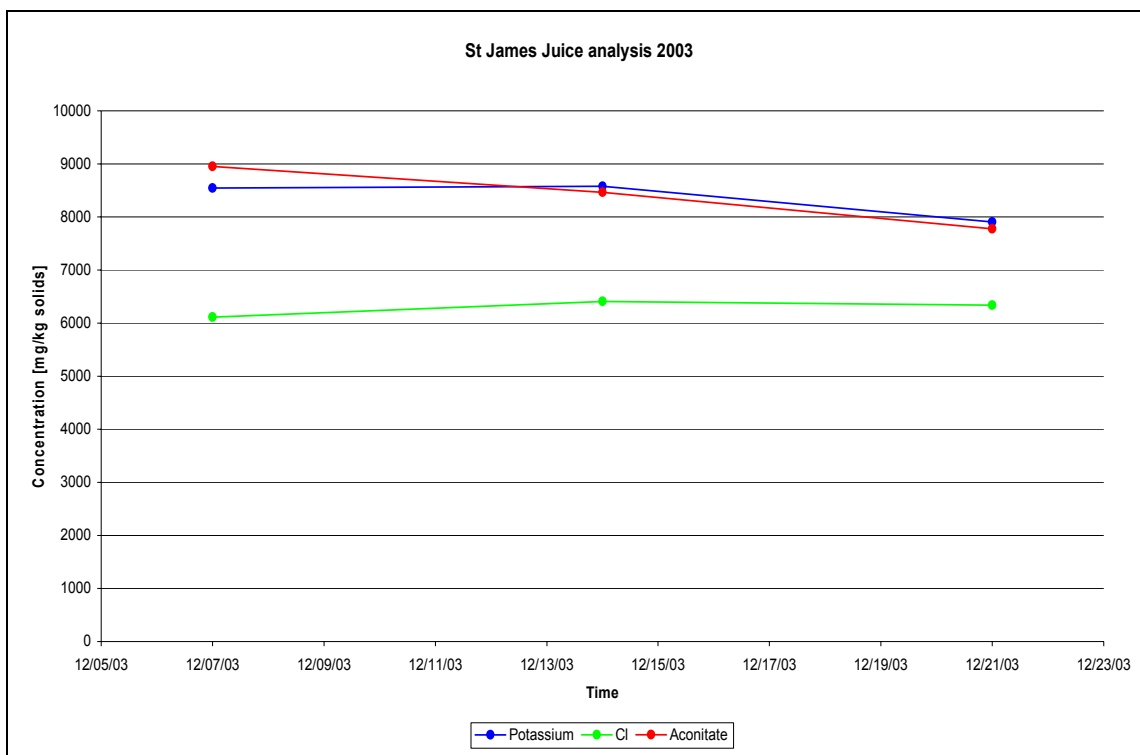


Figure 5.17: Clarified juice weekly composite ion analysis results.

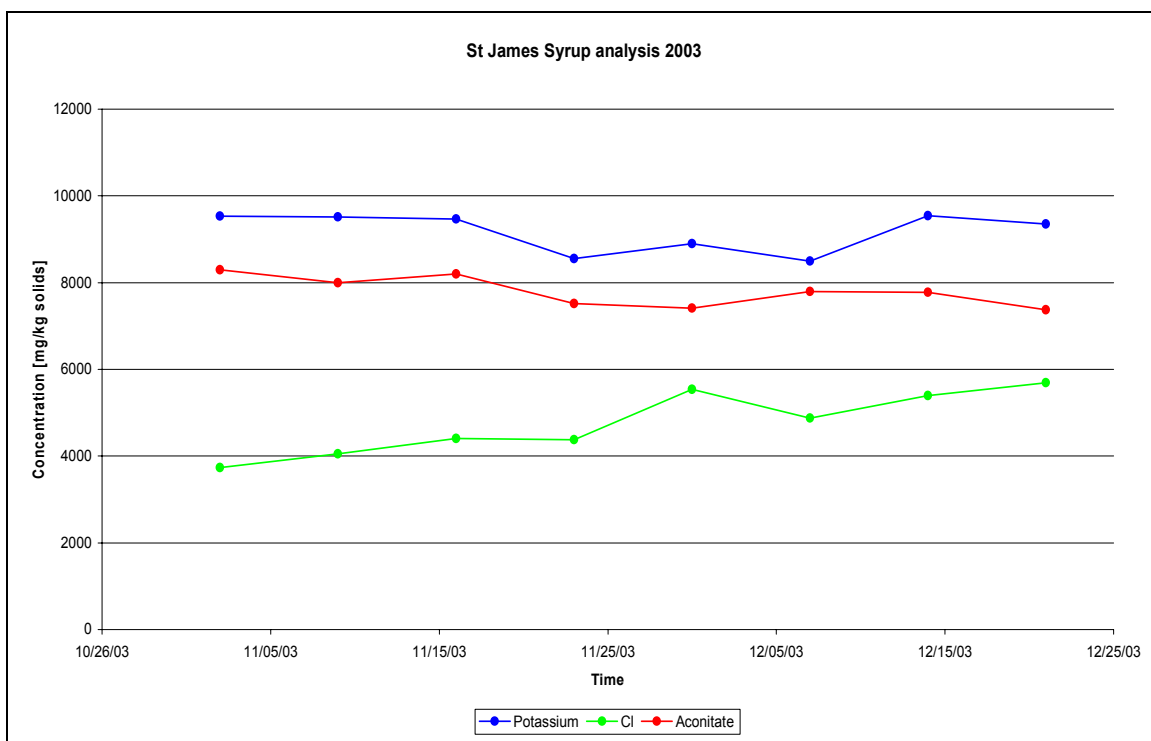


Figure 5.18: Syrup weekly composite ion analysis results.

It can be seen that there is no significant change in composition over the period tested for many of the components. It is harder to see the trends for some of the lower concentration components so the vertical scales of these components are increased in figures (5.19) through (5.22) to exaggerate the trends in lower concentration ion components.

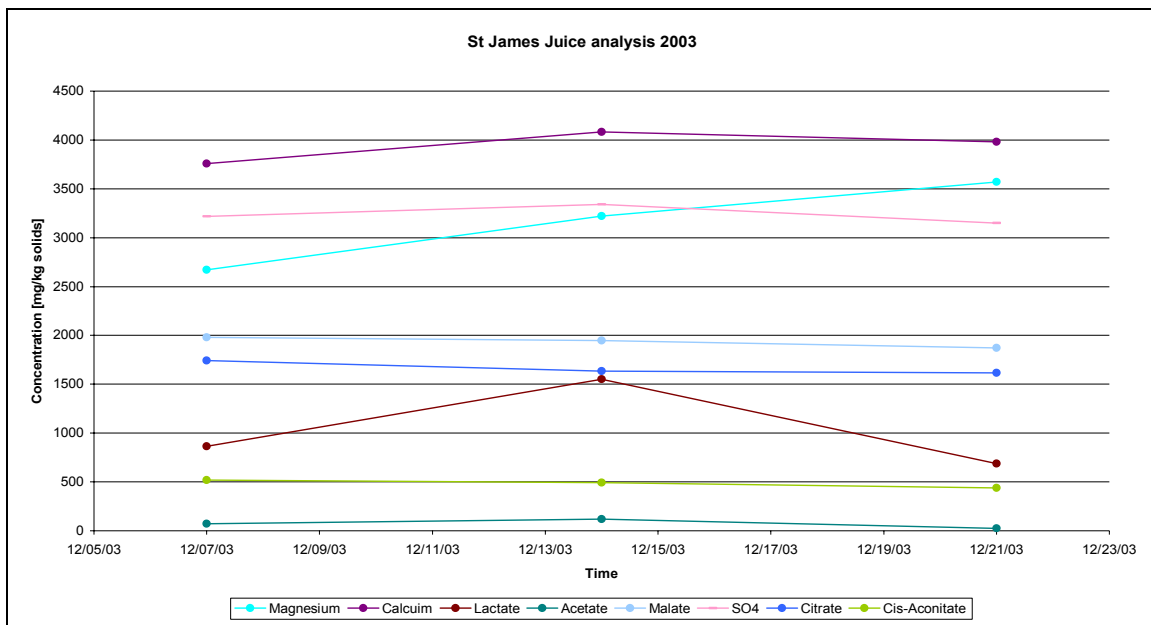


Figure 5.19: Clarified juice weekly composite ion analysis results expanded view.

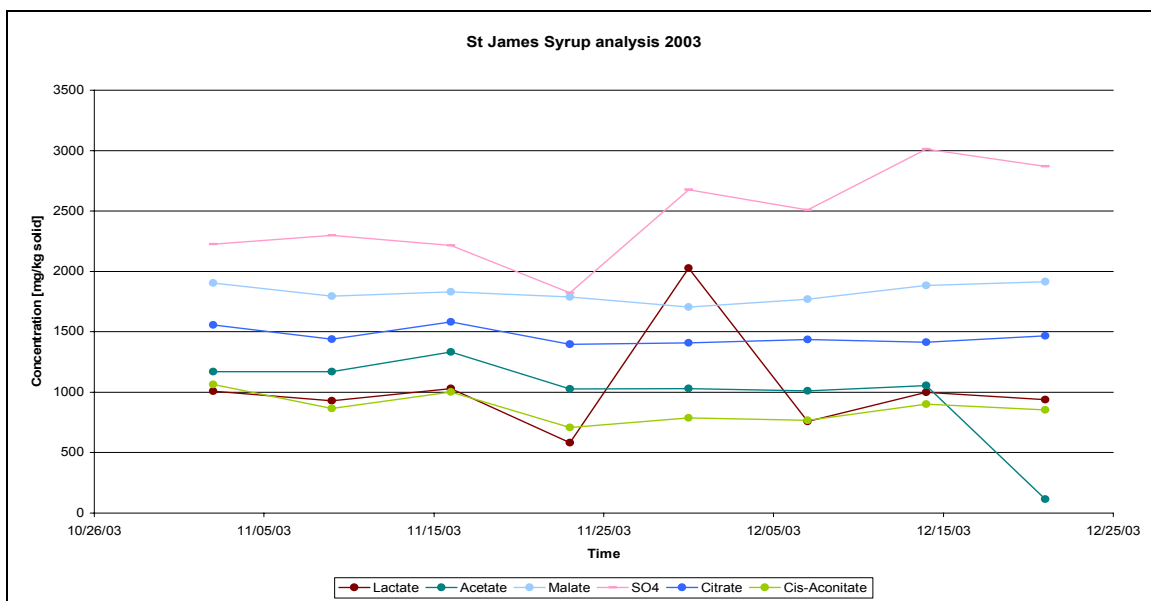


Figure 5.20: Syrup weekly composite ion analysis results expanded view.

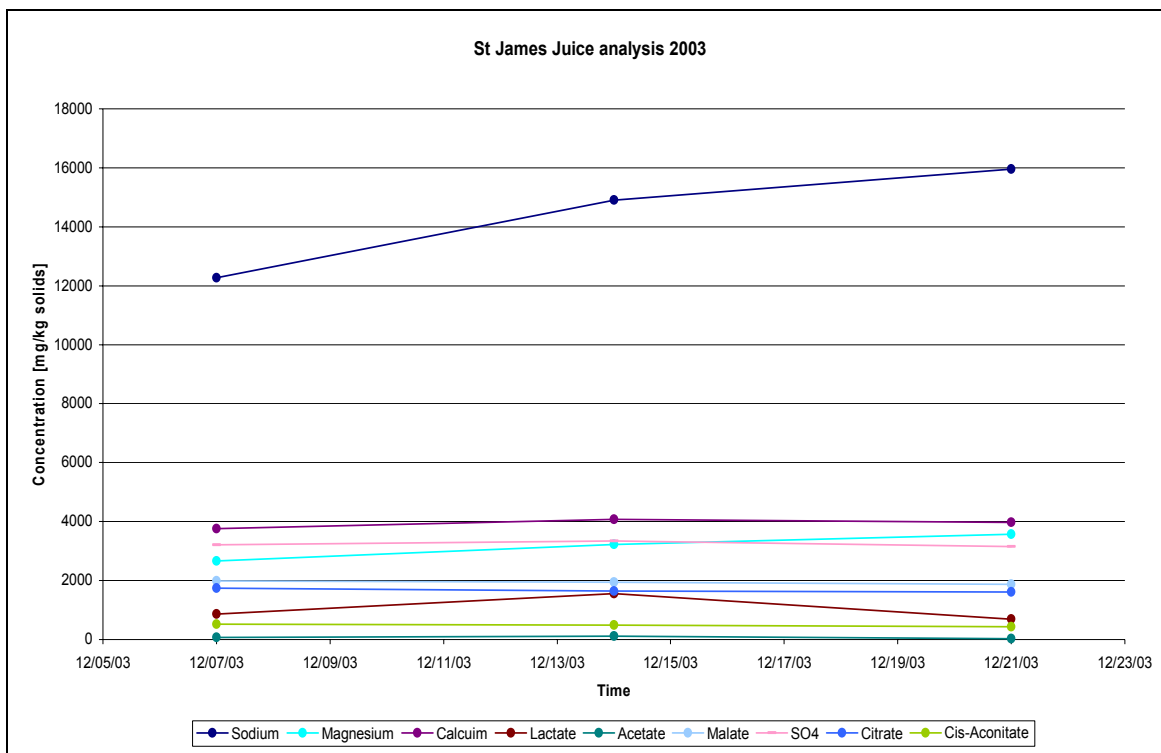


Figure 5.21: Clarified juice weekly composite ion analysis results expanded view.

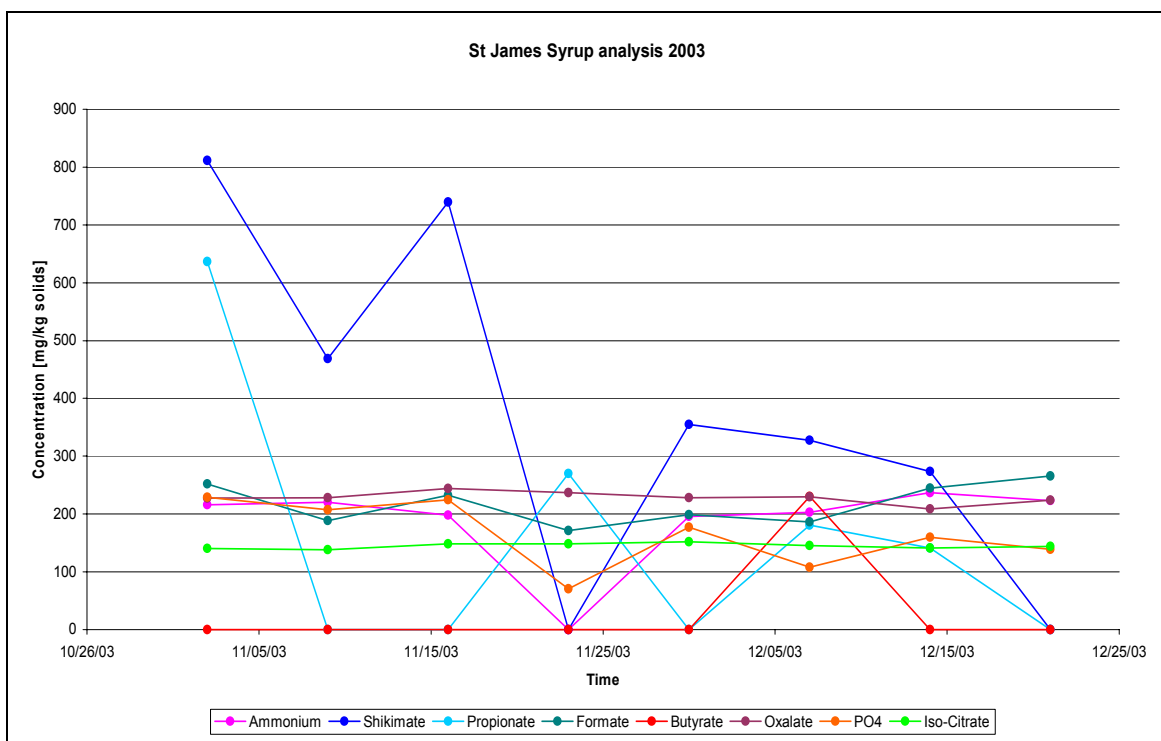


Figure 5.22: Syrup weekly composite ion analysis results expanded view.

The results in general show very little change over time, occasionally there is a spike in the component result for a few components but in general the trend is a constant concentration.

Since the concentrations were fairly constant, using an average flow over the time period when the mill was running and the average concentration of each component the accumulation of each component in the evaporator system can be computed. The computed accumulation is shown in figure (5.23). The calculation is based on the assumption that there is no ions carried over from the juice in the vapor stream and that the scale components are non-volatile. The computation was performed using differential equation form in MATLAB so that if a time dependant flow or concentration system was considered it could be easily modified for time dependant systems. The code for the calculation is shown in Appendix E.

The components that are generated in the evaporator station should show up as being on the below the x-axis and mass accumulating in the effect should show up above the axis. The sodium numbers were extremely high because the samples are preserved with a di-sodium salt and this skews the original value in the original sample. Sodium is not really of interest as all sodium salts should be soluble and so they should not deposit on the tube surface and should be a significant scaling component anyway.

Figure (5.23) shows a considerable accumulation of materials in the evaporators. The results of the other components indicate that there must be losses in some of the condensate lines due to carry over or that there is an error due to some other assumption. A significant source of error is the measurements from the HPLC themselves. The

concentrations of each component are extremely low (Only present in ppm) and so even a few ppm error in the analysis can make a very significant difference to the calculated accumulation in the effects.

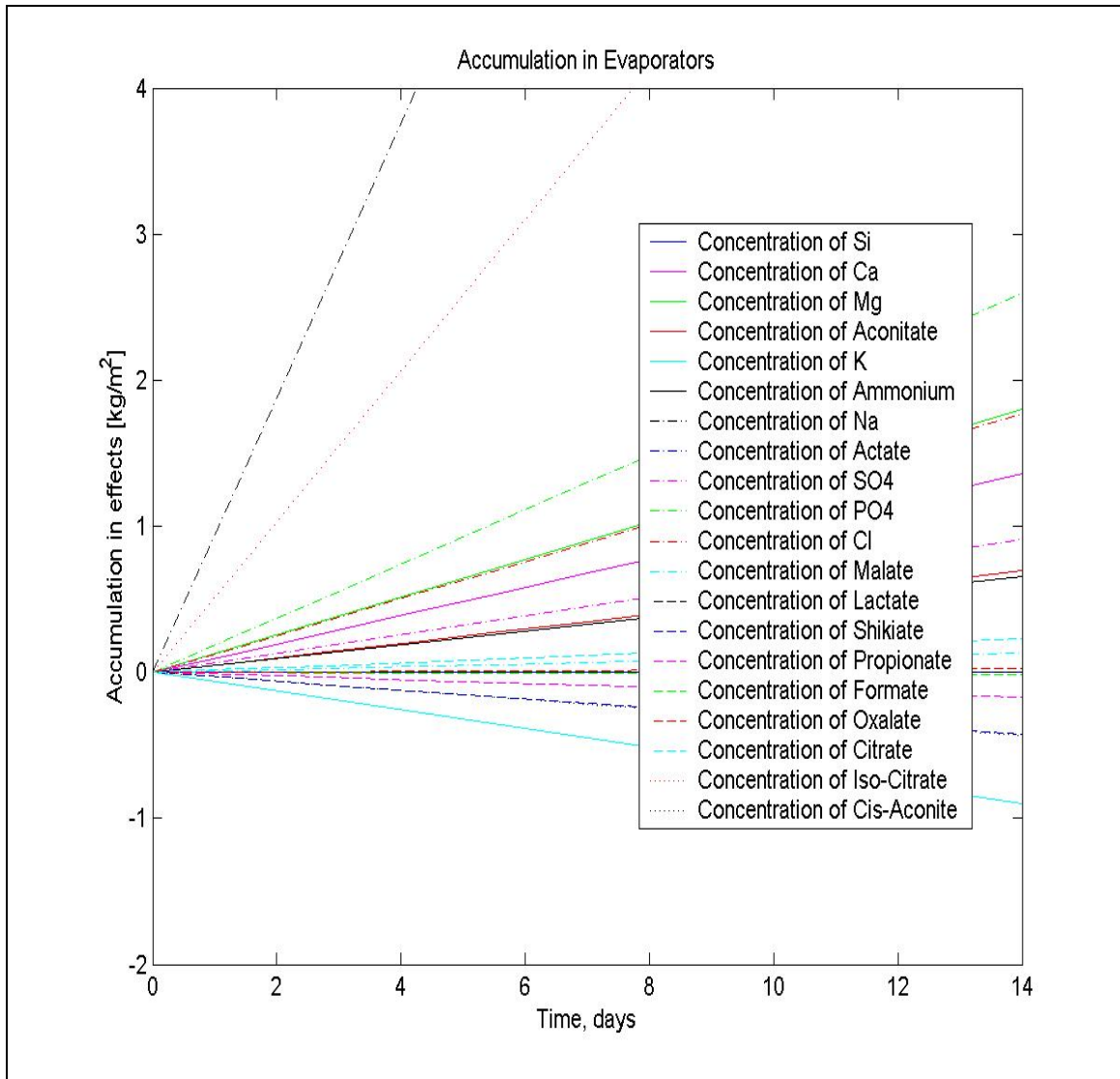


Figure 5.23: Accumulation in the evaporators based on average conditions.

The results for the cations and anions are very sensitive to small deviations in measured values as their concentrations are very low, this makes the accumulation figures less reliable to regress against.

5.3 Analysis of Heat Transfer Coefficient Data

5.3.1 Scaling Rates

The scaling rate is determined by plotting the inverse of the heat transfer coefficient squared as a function of time. When scaling occurs the heat transfer coefficient should decrease and as a result the inverse heat transfer coefficient should decrease, assuming scaling is the only effect affecting the heat transfer coefficient. If there is no scaling the inverse heat transfer coefficient should plot a straight line, the more significant the scaling the greater the slope of the trend in the heat transfer coefficient. As seen in figures (5.7) and (5.8) the final effect is the only effect with a significant scaling trend. The equation used for the regression is shown by equation (5.1), the regressed variable is C_3 .

$$\frac{1}{k^2} = \frac{1}{k_o^2} + C_3 t \quad (5.1)$$

The results for each clean cycle are shown in figures (5.24) to (5.27). As can be seen the first effects show very little scaling tendencies but the final effect shows significant scaling with time. The time is measured in days for equation (5.1). The template code for this regression is shown in appendix E. The inputs are the data in a matrix of four columns, one for each effect.

The last effect has a reasonably large amount of scatter in each case, and this is due in part to the magnitude of the heat transfer coefficient being small. The value is inverted and squared so even slight changes in the value when inverted and squared causes significant variance. This effect is not as significant in the first few effects as the magnitude of the heat transfer coefficients is significantly higher in these effects.

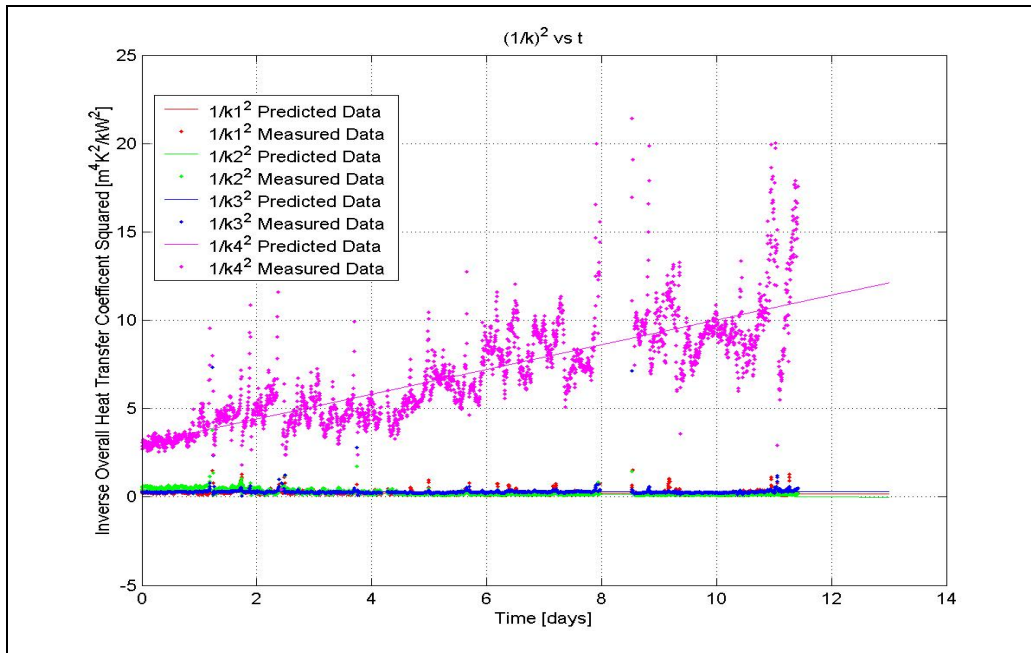


Figure 5.24: Regression for time dependence of heat transfer coefficients for the first data period.

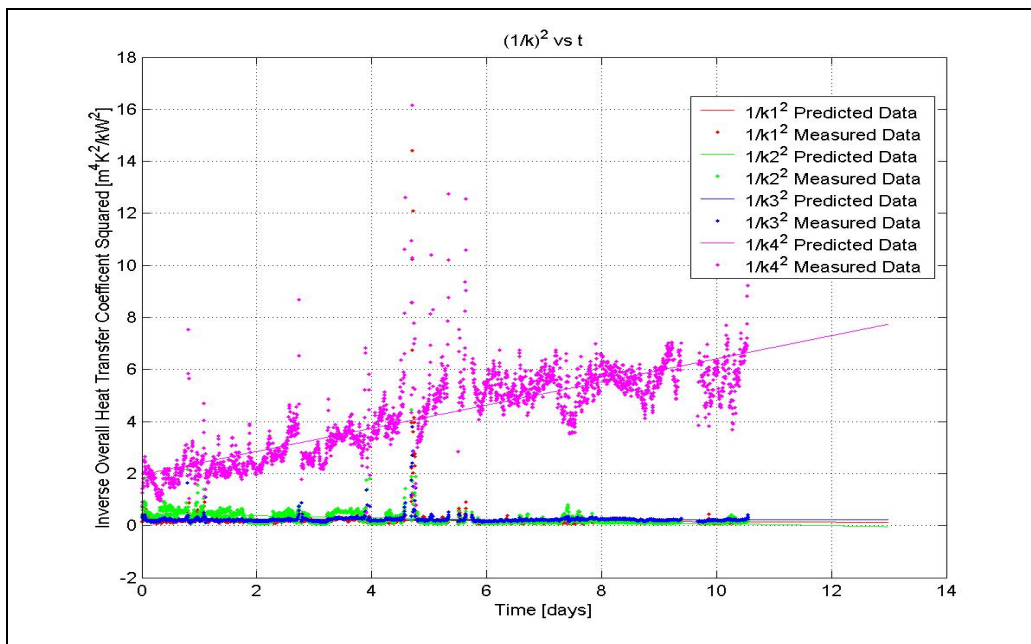


Figure 5.25: Regression for time dependence of heat transfer coefficients for the second data period.

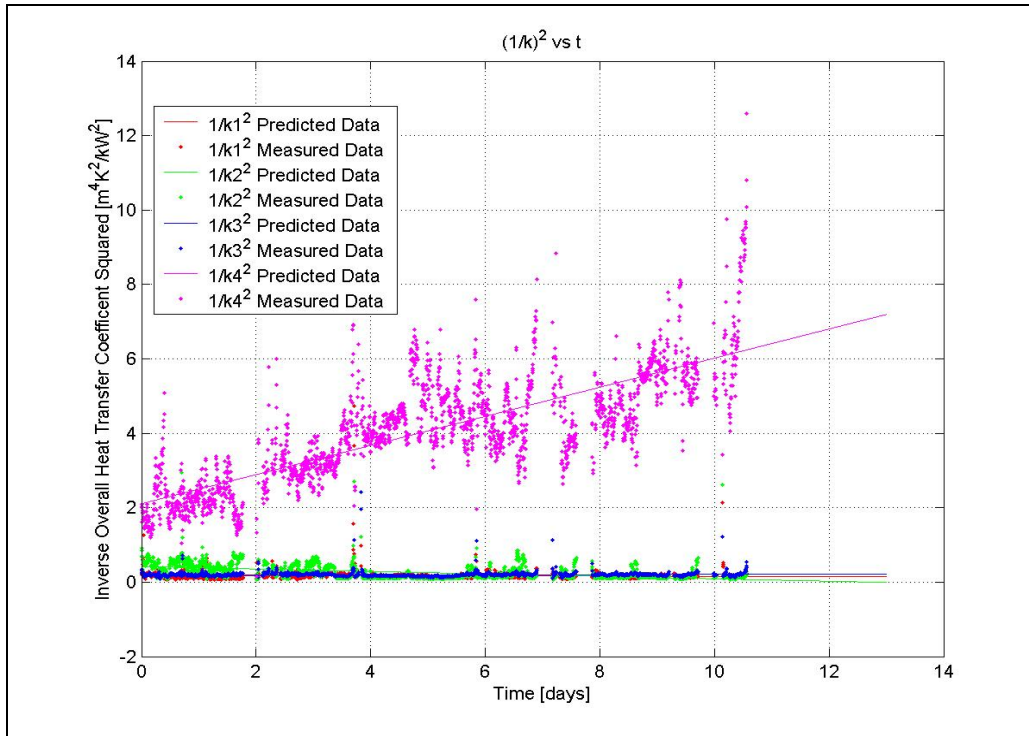


Figure 5.26: Regression for time dependence of heat transfer coefficients for the third data period.

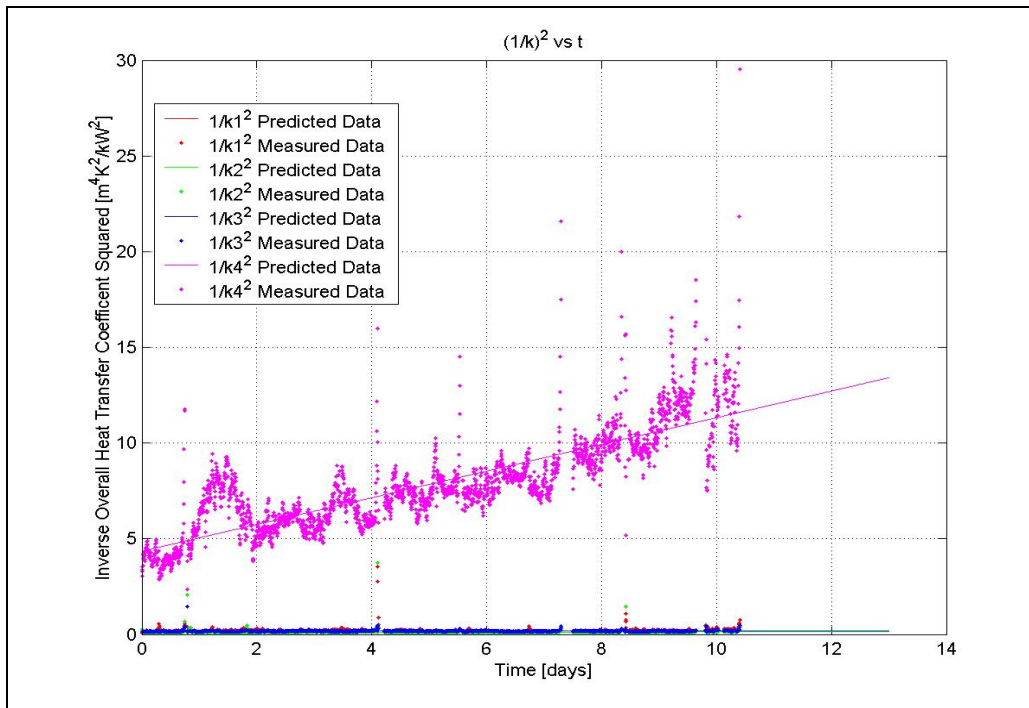


Figure 5.27: Regression for time dependence of heat transfer coefficients for the fourth data period.

The final effect had similar scaling rates for each data set, this is possible if the concentrations of key scaling components were kept constant and operating conditions were similar for each run. This would mean that the scaling rate for an effect would be expected to be constant. This data is reproduced in table (5.1) for easy comparison. The large scatter of points causes the R^2 value to be extremely low for a number of the runs. For the more accurate runs the value of the constant is close to 0.7. The low R^2 may be due to a larger number of outlying points and the initial heat transfer coefficient value seems to affect the scaling rate, for example in the first and forth runs the effect was already slightly scaled to begin with and shown in a high C_3 constant value. The second and third runs started out with a cleaner effect (higher heat transfer coefficient) and showed a lower constant for the regression.

Table 5.1: Regressed time dependant model constants.

	$1/k^2$ model constant C_3	R^2
First data period	0.700 ± 0.011	0.64
Second data period	0.445 ± 0.007	0.67
Third data period	0.394 ± 0.007	0.61
Forth data period	0.697 ± 0.010	0.68

If the data is regressed as equation (5.2) the results are very different numerically but the same trend for R^2 and where the constant values are highest persists in table (5.2).

$$\frac{1}{k} = \frac{1}{k_o} + C_2 t \quad (5.2)$$

Table 5.2: Regressed time dependant model constants.

	$1/k$ model constant C_2	R^2
First data period	0.134 ± 0.002	0.69
Second data period	0.115 ± 0.002	0.71
Third data period	0.100 ± 0.002	0.64
Forth data period	0.124 ± 0.002	0.71

5.3.2 Clean Heat Transfer Coefficient Prediction

The first twenty-four hours of heat transfer coefficient data after each clean was assumed to be “clean”. The data was used to plot the heat transfer coefficient as a function of a number of variables to generate a predictive heat transfer coefficient for the sugar mill Robert effect evaporators in Louisiana. The plot generated is shown in figure (5.28) for the regression of the data using equation (5.4).

$$k_o = 0.000118(100 - B)^{0.9113} T^{1.2882} \quad (5.4)$$

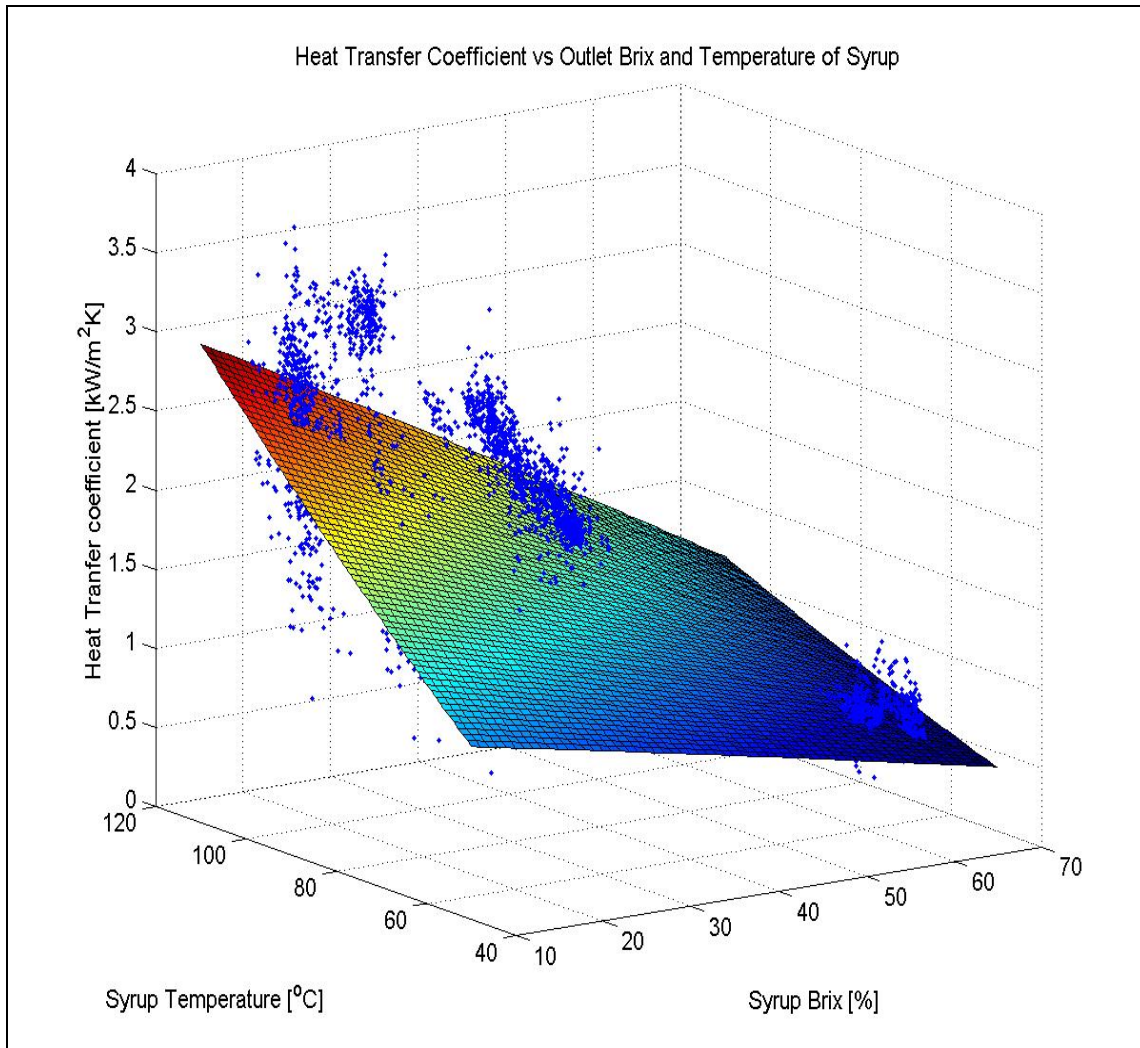


Figure 5.28: Regression for clean value of the heat transfer coefficients for the first twenty four hours per clean.

The data is regressed for a number of other models and the results and R^2 values are reproduced in Table 5.3. Some of the correlations are very good and a high value of R^2 is obtained, but in general the scatter of the data points is very high so the value of R^2 is low.

Table 5.3: Heat transfer coefficients as a function of temperature, Brix and viscosity regressed data

<u>Equation</u>	<u>Regressed constants</u>	<u>R^2</u>
$k_o = K \frac{Q^a}{\eta^b}$	$K = (114.7 \pm 50.9)e-6$ $a = 0.918 \pm 0.036$ $b = 0.500 \pm 0.004$	0.84
$k_o = K(100 - B_L)^a T_L^b$	$a = 0.911 \pm 0.046$ $b = 1.288 \pm 0.074$ $K = (118 \pm 20)e-6$	0.78
$k_o = K(100 - B)^a (T - 54 + 273.15)^b$	$K = (486 \pm 355)e-15$ $a = 1.00 \pm 0.04$ $b = 4.31 \pm 0.26$	0.78
$k_o = K \frac{T_L + 273.15}{B_L}$	$K = 0.132 \pm 0.001$	0.90
$k_o = K\mu^a$	$K = 1.433 \pm 0.006$ $a = -0.473 \pm 0.004$	0.81
$k_o = KT_L - a$	$K = 0.045 \pm 0.001$ $a = 2.042 \pm 0.043$	0.68

5.4 Scale

The scale from the final effect tubes is shown in figure (5.29). There are a number of clean tubes seen in the figure as the picture was taken after an attempt to clean the vessel was unsuccessful. The scale was particularly hard to remove and the residual scale after the clean with caustic soda and acid is seen clearly. Typically scale is removed by chemical means with the acid and caustic washes, but in this case the scale was not removed efficiently by these chemical-cleaning methods. Mechanical cleaning needed to be used to clean this particular effect of the evaporators. This method is not used

frequently in Louisiana typically as labor costs are high and the job is very time consuming and requires many man-hours to complete. Mechanical cleaning is a last resort for cleaning evaporators in high labor cost countries such as the United States of America. Some countries such as South Africa use mechanical cleaning in preference to chemical cleaning as labor costs are low and chemical costs are high.



Figure 5.29: Scale in the tubes of the final effect at the end of the season.

The significant scaling seen in figure (5.29) in this final effect caused the calculated heat transfer coefficient to be extremely low towards the end of the season.

CHAPTER 6. SUMMARY AND CONCLUSION

The correlations developed and found in literature are useful for a number of different applications and are easy to use. The correlations were regressed with data over the range of interest in a typical sugar mill evaporator train.

The Microsoft Excel® model developed performed well; there were some issues with running the model for the entire season due to equipment failure rather than failure on the part of the model or the controller. The computations are very sensitive to temperature so the RTD's needed to be calibrated and checked periodically to ensure they are operating correctly. Correct installation of these probes to prevent conduction errors is critical, this type of error occurred in the third effect calandria and had to be corrected with an offset correction until the probe could be repositioned to eliminate this error.

The model is based on minimal instrumentation as the system only uses two volumetric flow meters, one microwave Brix probe and nine RTD's, and would be extremely inexpensive for a mill to install. It is developing the model and coding the macros that require time and a good understanding of the system to perform the balances without causing a calculation iteration loop to be over or under specified.

Through evaluating the heat transfer coefficients online, an evaluation of the performance of individual effects was achieved. The results indicate that the final effect is the only effect with significant scaling issues and the first effects may not necessarily need to be cleaned as often as they currently are. This will save mills downtime and cleaning chemical costs.

The calculation effectively determined if a vessel was cleaned correctly during the cleaning cycle. Any vessels not cleaned correctly were noted because the heat transfer

coefficient for that effect did not return to the clean conditions. The heat transfer coefficients should return to the original values (before being scaled up) after a clean.

The collection of the heat transfer data allowed a model to be developed to describe fouling and how it proceeds with time. The use of a first principles model based on deposition and removal terms was attempted but due to the complexity of the system and the model chosen had to be based on empirical work performed before. The empirical model was broken down into two components, a time dependant part and a clean heat transfer coefficient value. The regressed parameters had a fairly low correlation coefficient to the original data and this is believed to be caused by noise in some of the measurements.

6.1 Recommendations for Future Work

The collection of more data will allow the regression of data to be more representative and allow more refined correlations to be generated. The current data is useful but the work generated would benefit from the inclusion of more data from a number of different sources in Louisiana not just the mill being studied.

Although a time dependent model of the heat transfer coefficient with time was generated with the limited data collected, the dependence of these constants on other operating conditions such as pH was not evaluated. Another significant question is if this time dependence value is unique for one mill and one season or if the regressed values are transferable to other mills in the region. There may even be variations in the scaling as a function of time during the season if for example there is more rain in a particular week than another and the significance of these variations should be recorded. Long-term scale composition and juice compositions should be recorded to track how these are

affecting heat transfer in the mills and to record if there are any changes occurring in mill operation to reduce scaling in the evaporators.

There have been changes to the feed distribution system on all the effects and this should increase the heat transfer coefficients calculated, this assumption should be validated.

The effectiveness of cleaning chemicals and cleaning chemical concentrations used in cleaning can be evaluated to optimize cleaning cocktails for evaporator cleaning.

Methods of scale prevention by improving clarification for example can be considered as an extension of this project. If the mill is already analyzing the clarified juice and the heat transfer coefficient an improvement in clarification should remove more scale forming components that will be noted in the clarified juice samples, and the juice should boil better so there should be an increase in heat transfer coefficient especially in the final effect. The improved syrup should also reduce pan-boiling times.

REFERENCES

- Abdulmuin, M. Z. and Ibrahim T. M. A. S. – *Formulation of steady-state and dynamic models for an evaporator* – Journal of the institution of engineers, Malay – Volume 37 – 1985 - pg 17 to 27.
- Badger W. L. and Banchero J. T. – *Introduction to chemical engineering* – McGraw-Hill book company - 1955
- Bott, T. B. – *Aspects of crystallization fouling* – Experimental thermal and fluid science – New York – Elsevier – 1997 – Vol. 14 – pg 356-360
- Bubnick, Z. – *Sugar Technologists Handbook* – Eighth Edition – Bartens – 1995.
- Chen, J. P. and Chou, C. C. – *Cane Sugar Handbook* – Twelfth Edition, Wiley and Sons Inc, ISBN 0-471-53037-9, 1993
- Daubert T. E. and Danner R. P. – *Data Compilation tables of Properties of Pure Compounds* – American Institute of Chemical Engineers – ISBN 0-8169-0341-7, 1985
- Deerr N., - *The history of sugar* – Volume 2 – Chapman and Hall Ltd. – 1950, pg 556 to 572.
- Epstein, N. – *Fouling: Technical Aspects - Fouling of Heat Transfer Equipment*, Somerscales and Knudsen, Eds., Hemisphere Publishing Company, WA (1981). ISBN 0-89116-199-6.
- Epstein, N. – *Fouling in heat exchangers - International heat transfer conference (6th)* – Toronto – Hemisphere Publishing – 1978 – pg 235 to 253
- Frantz J. F. – *An Apparatus for a Study of Scale Formation* – August 1956, Thesis, Louisiana State University, pg 7.
- Frederick, W.J. and Grace T.M., - *Scaling in Alkaline Spent Pulping Liquor Evaporators - Fouling of Heat Transfer Equipment*, Somerscales and Knudsen, Eds., Hemisphere Publishing Company, WA (1981). ISBN 0-89116-199-6.
- Gungor K. E. and Winterton R. H. S. – *A general correlation for flow boiling in tubes and annuli* – 1986, Pergamon Press Ltd, International Journal of Heat and Mass Transfer, Vol. 29, No. 3, pg 351-358.
- Gou S. Y., White E. T. and Wright P. G. – *Heat Transfer Coefficients For Natural Effect Circulation Evaporators*- 1983, Proceedings of the Australian Society of Sugar Cane Technologists, pg 237 to 244.

Godshall, Mary An and Wartelle, Lynda – *Composition of evaporator scale in Louisiana mills* – SPRI poster – 2002 - pg. 379-385.

Heluane H., Colombo M., Ingaramo A., Hernandez M. R. and Cesca – *Multiple Effect Evaporation in a sugar factory. A measured variables study* – Latin American Applied Research – Volume 31 - 2001 – pg 519 to 524.

Hoekstra R. G. – *A computer program for simulating and evaluating multiple effect evaporators in the sugar industry* – Proceedings of The South African Sugar Technologists' Association – June 1981, pg 43 to 50.

Honeywell – *SCM3000 Plus, Smart Coriolis Mass Flowmeter* – User's manual 34-CM-25-02, pg B1.

Honig P., - *Principles of Sugar Technology* – Volume 3 – Elsevier publishing company - 1963.

Hoy, J. W., Richard, C. A., Jackson, W. R. and Waguespack, H. L. Jr. – *Effects of Cultivars, Fungicides, and Fertilization at planting on yields obtained from whole stalk and Billet planting in Louisiana* – ASSCT - 2004

Hugot E. – *Handbook Of Cane Sugar Engineering* – Elsevier Publishing - 1960

Hussey P. S. – *A digital computer model of a multiple effect evaporator* – Proceedings of the South African Sugar Technologists' Association – June 1973 – pg 70 to 76.

Incopera, F. P. and DeWitt, D. P. – *Fundamentals of heat and mass transfer (Fifth edition)* – 2002, John Wiley and sons, ISBN 0-471-38650-2.

Kai Dunn and Teh Fu Yen - *Dissolution of Barium Sulfate Scale Deposits by Chelating Agents* - Environmental Science & Technology, 33 (16), 2821 -2824, 1999

Kern D. Q. – *Process Heat Transfer* – McGraw-Hill - 1950

Kern D. Q. – *Surface fouling...How to calculate limits* – Chemical Engineering Progress – Volume 55, number 6 – June 1959 – pg. 71 to 73.

Lilleboe D., - *2002/2003 Gilmore Sugar Manual* – Sugar publications – 2003, pg 58 to 60.

Madson R. F. – *A New Programme for Calculating Sugar Factory Energy Balances* – 1996, International Sugar Journal, Vol 98, No. 1167, pg 134 to 137.

Marto, P. J. and Nunn, R. H. – *Power Condenser Heat Transfer Technology (Computer Modeling/Design/Fouling)* – Hemisphere Publishing Corporation, ISBN 0-07-040662-6, 1981, pg. 375 to 459.

McCabe W. L. and Robinson C. S. – *Evaporator Scale Formation* – Industrial and Engineering Chemistry – May 1924 - pg 478 and 479

McCabe W. L. and Smith J. C. – *Unit Operations of Chemical Engineering* – McGraw-Hill book company - 1956

Minton, Paul E - *Handbook of Evaporation Technology* – Noyes Publishers – 1986 - Chapter 12 pg. 113 to 129

Morse, R. and Knudsen, J. – *Effect of alkalinity on the scaling of simulated cooling tower water* – The Canadian Journal of Chemical Engineering – Volume 55 – June 1977

Oufer, L., Knudsen, J. G. – *Modelling Chemical Reaction Fouling Under Sub-cooled Boiling Conditions* – AIChE Symposium Series – Heat Transfer Atlanta 1993 – No. 295 Vol. 89 - pg 308 to 313

Perry J. – *Chemical Engineers Handbook* – 1934, McGraw-Hill, First Edition, pg 829.

Reitzer, B. J. – *Rate of scale formation in tubular heat exchangers* – I & EC Process Design and Development – Vol. 3, No. 4 – October 1964 – pg 345 to 348.

Selman, R. N. and Plomley, E. M. – *Effect Performance* – ISSCT – 1950 – pg 696 to 704

Smith I. A. and Taylor L. A. W. – *Some Data on Heat Transfer in Multiple Effect Evaporators*- Proceedings of the South African Sugar Technologists' Association – June 1981 – pg 51 to 55

Snoad J – *Development of an on-line evaporator performance monitoring systems at Mulgrave mill* – Proceedings of Australian society of sugar cane technologists – 1997 – pg 485 to 492

Somerscales, E. F. C. and Knudsen G. K. – *Fouling of Heat Transfer equipment* - Proceedings of an International Conference on the Fouling of Heat Transfer Equipment, held at Rensselaer Polytechnic Institute Aug. 13-17 1979 - Hemisphere Pub. Corp. - 1981.

Taborek J., Aoki T., Ritter R. B., Palen J. W. and Knudsen J. G. – *Fouling: The major unresolved problem in heat transfer* – Chemical Engineering Progress – Vol. 68, No. 2- Feb. 1972 – pg 59 to 62

Taborek J., Aoki T., Ritter R. B., Palen J. W. and Knudsen J. G. – *Predictive methods for fouling behavior – Part 2* – Chemical Engineering Progress – Vol. 68, No. 7 – July 1972 – pg 69 to 78

Truong T., Anema S., Kirkpatrick K. and Chen H. - *The use of a heat flux sensor for in-line monitoring of fouling of non-heated surfaces* – Trans IChemE, Vol. 80, part C – December 2002 – pg 260 to 269

Ugrin E. and Urbicain M. J. – *Design and simulation of multiple effect evaporators* – Heat transfer engineering – Vol 20, No 4, pg 38 to 44.

Van der Pol P. W., Schweck H. and Schwartz T. – *Sugar Technology (Beet and Cane Sugar Manufacture)* – 1998, Bartens, ISBN 3-87040-065-X

Walthew, D. C. – *Communications from the sugar milling institute Number 159* – Evaporator fouling literature review – November 1994 – ISBN 1-86840-116-2

Wright P. G., Silva T. A. and Pennisi S. N. – *The SRI evaporator – A new Roberts Design* – Proceedings of the Australian Society of Sugar Cane Technology – Volume 25 – 2003

APPENDIX A EVAPORATOR MODEL MICROSOFT EXCEL® VBA CODE

A.1 Evaporator Model Microsoft Excel® VBA Code

The calculation for steam required is performed in Microsoft Excel®.

A.1.1 Startup Macro

The startup macro code is as follows, green is comments and black text is the code:

```
Sub Startup()
```

```
'%%%%%%%%%%%%%%%%%%%%%%%%%%%%%%%%%%%%%%%%%%%%%%%%%%%%%%%%%%%%%%%%%%%%%%%%  
'% St James Sugar Mill Evaporators  
'% Startup macro to initiate spreadsheet  
'% Updated 13 July 2004  
'% Revision 1.02  
'% Revised by David Solberg  
'%%%%%%%%%%%%%%%%%%%%%%%%%%%%%%%%%%%%%%%%%%%%%%%%%%%%%%%%%%%%%%%%%%%%%%%%  
  
'%%%%%%%%%%%%%%%%%%%%%%%%%%%%%%%%%%%%%%%%%%%%%%%%%%%%%%%%%%%%%%%%%%%%%%%%  
'% First insert initial guesses  
'%%%%%%%%%%%%%%%%%%%%%%%%%%%%%%%%%%%%%%%%%%%%%%%%%%%%%%%%%%%%%%%%%%%%%%%%
```

```
'Select the correct worksheet  
Worksheets("Model").Select
```

```
'Steam flow estimate  
Range("F36").Select  
ActiveCell.FormulaR1C1 = "11"
```

```
'Initial guesses first effect  
'Feed Brix estimate  
Range("F44").Select  
ActiveCell.FormulaR1C1 = "15"  
'Guess for boiling liquid temperature  
Range("F54").Select  
ActiveCell.FormulaR1C1 = "106"  
'Guess for vapor generated temperature  
Range("F57").Select  
ActiveCell.FormulaR1C1 = "105"  
'Guess for vapor mass flow (same as steam)  
Range("F58").Select  
ActiveCell.Formula = "=F44"
```

```
'Initial guesses second effect  
'Guess for boiling liquid temperature  
Range("L54").Select  
ActiveCell.FormulaR1C1 = "99"
```

```
'Guess for vapor generated temperature
Range("L57").Select
ActiveCell.FormulaR1C1 = "97"
'Guess for vapor mass flow (same as steam)
Range("L58").Select
ActiveCell.Formula = "=F44"
```

```
'Initail guesses third effect
'Guess for boiling liquid temperature
Range("R54").Select
ActiveCell.FormulaR1C1 = "92"
'Guess for vapor generated temperature
Range("R57").Select
ActiveCell.FormulaR1C1 = "89"
'Guess for vapor mass flow (same as steam)
Range("R58").Select
ActiveCell.Formula = "=F44"
```

```
'Initail guesses final effect
'Guess for boiling liquid temperature
Range("X54").Select
ActiveCell.FormulaR1C1 = "67"
'Guess for vapor generated temperature
Range("X57").Select
ActiveCell.FormulaR1C1 = "60"
'Guess for vapor mass flow (same as steam)
Range("X58").Select
ActiveCell.Formula = "=F44"
```

```
%%%%%%%%%%
'% Reinsert computations
%%%%%%%%%%
```

```
'Better guess for steam flow
Range("F36").Select
ActiveCell.Formula = "=(C23-W20)/4"
ActiveCell.Copy
ActiveCell.PasteSpecial (xlPasteValues)
```

```
'Insert formulae first effect
'Brix feed calculation
Range("F44").Select
ActiveCell.Formula = "=(W20*W21)/C23"
'Boiling juice temperature
Range("F54").Select
ActiveCell.Formula = "=F57+F52+F53"
'Vapor generated temperature
Range("F57").Select
ActiveCell.Formula = "=F62-F63"
'Vapor generated mass flow
Range("F58").Select
ActiveCell.Formula = "=(F47*F43+F40-F41-F64*F65)/F59"
```

```
'Insert formulae second effect
'Boiling juice temperature
Range("L54").Select
```



```

ActiveCell.Formula = "=L57+L52+L53"
'Vapor generated temperature
Range("L57").Select
ActiveCell.Formula = "=L62-L63"
'Vapor generated mass flow
Range("L58").Select
ActiveCell.Formula = "=(L47*L43+L40-L41-L64*L65)/L59"

'Insert formulae third effect
'Boiling juice temperature
Range("R54").Select
ActiveCell.Formula = "=R57+R52+R53"
'Vapor generated temperature
Range("R57").Select
ActiveCell.Formula = "=R62-R63"
'Vapor generated mass flow
Range("R58").Select
ActiveCell.Formula = "=(R47*R43+R40-R41-R64*R65)/R59"

'Insert formulae final effect
'Boiling juice temperature
Range("X54").Select
ActiveCell.Formula = "=X57+X52+X53"
'Vapor generated temperature
Range("X57").Select
ActiveCell.Formula = "=X62-X63"
'Vapor generated mass flow
Range("X58").Select
ActiveCell.Formula = "=(X47*X43+X40-X41-X64*X65)/X59"

'Reselect "ON"/"OFF" cell
Range("B2").Select

```

End Sub

A.1.2 Solver Iteration Code

The auto code used for iterating steam flow using solver is as below where again code in green is for comments and black text is the code.

‘This section of the code checks for any changes to the work book, if a change is detected the code will immediately check cell B2. If the change has occurred in cell B2 the next section of code “Workbook_Open()” is called to check if the value of B2 is changed to initiate the solver routine. The code will do nothing if any cell besides B2 is changed.

```
Private Sub Workbook_SheetChange(ByVal Sh As Object, ByVal Target As Range)
```

```

'%%%%%%%%%%
'% If changes are made in the sheet check
'% to see if user wants to run solver loops
'% if so run Workbook_Open code
'%%%%%%%%%%

```

```

If Intersect(Target, Range("B2")) Is Nothing Then
    Exit Sub
Else
    Call Workbook_Open
End If
End Sub

```

‘This is the “Workbook_Open()” section of the code, this function is called when the workbook is opened or if it is called by the routine from the workbook change function.

```
Private Sub Workbook_Open()
```

```

'%%%%%%%%%%%%%%
'% St James Sugar Mill Evaporators
'% Code that runs the macro..
'% Updated 13 July 2004
'% Revision 1.02
'% Revised by David Solberg
'%%%%%%%%%%%%%%

'%%%%%%%%%%%%%%
'% First check if code should run on sheet
'% opening and initialize counter
'%%%%%%%%%%%%%%

```

‘This section of code is used to initiate the Restart counter (set it equal to 0) and assign the variable Number the value of cell B2.

```

Number = Worksheets("Model").Range("B2")
Number = Range("B2").Value
Restart = 0

```

‘This condition checks if cell B2 is set to allow the computation to run or not.

```
Do While Number < 1
```

‘The computation runs until this counter “Restart” reaches 20 then the computation runs code similar to the startup code is run to ensure there are no errors in the spreadsheet, any errors are corrected by resetting the spreadsheet.

```
Do While Restart < 20
```

```
'Increment counter for reset of sheet
```

```
Restart = Restart + 1
```

‘The calculate command just ensures looped cells are iterated for and will force computations for all circular referenced cells.

```
Calculate
```

```

'%%%%%%%%%%%%%%
'% Timer break for solver
'%%%%%%%%%%%%%%

```

‘The five second delay in the code is initiated here, the timer command is the time since midnight in seconds. There is also a small section of code that corrects for the possibility of problems with the code getting into an infinite loop that it cannot get out of at midnight. The code adds five seconds to the current timer value then does nothing until the timer reaches the current time plus five seconds then it exits the loop and runs the solver routine.

```
'Use timer funtion (Time in secs since midnight)
```

```
Start = timer
```

```

'Five second delay
Delay = 5
Total = Start + Delay
'Need to correct midnight roll over errors, if timer value is close to midnight the new time is set to 10
If Total < 86390 Then
Else: Total = 10
End If
'The 5 sec delay...
Do While timer < Total
    DoEvents
Loop

'Keep visible if it is set to go "OFF"
Number = Worksheets("Model").Range("B2")
Number = Range("B2").Value
If Number < 1 Then
    Application.Visible = False
Else
    Application.Visible = True
End If

'%%%%%%%%%%%%%%
'%    Start calculations after break
'%%%%%%%%%%%%%%

'Select the correct worksheet
Worksheets("Model").Select

'Check the circular references are calculated.
Calculate

'%%%%%%%%%%%%%%
'% Fix values of inputs to prevent them changing
'% while solver is converging to a solution
'%%%%%%%%%%%%%%

'First effect
'Steam temperature inlet
Range("B14").Select
ActiveCell.Formula = "='Process Data'!C6"
ActiveCell.Copy
ActiveCell.PasteSpecial (xlPasteValues)
'Juice inlet temperature
Range("C22").Select
ActiveCell.Formula = "='Process Data'!C5"
ActiveCell.Copy
ActiveCell.PasteSpecial (xlPasteValues)
'Juice inlet flow
Range("C26").Select
ActiveCell.Formula = "='Process Data'!C14"
ActiveCell.Copy
ActiveCell.PasteSpecial (xlPasteValues)
'Syrup temperature
Range("G22").Select
ActiveCell.Formula = "='Process Data'!C10"
ActiveCell.Copy

```

ActiveCell.PasteSpecial (xlPasteValues)

'Second effect

'Steam temperature inlet

Range("H14").Select

ActiveCell.Formula = "='Process Data'!C7"

ActiveCell.Copy

ActiveCell.PasteSpecial (xlPasteValues)

'Syrup temperature

Range("L22").Select

ActiveCell.Formula = "='Process Data'!C11"

ActiveCell.Copy

ActiveCell.PasteSpecial (xlPasteValues)

'Third effect

'Steam temperature inlet

Range("M14").Select

ActiveCell.Formula = "='Process Data'!C8"

ActiveCell.Copy

ActiveCell.PasteSpecial (xlPasteValues)

'Syrup temperature

Range("Q22").Select

ActiveCell.Formula = "='Process Data'!C12"

ActiveCell.Copy

ActiveCell.PasteSpecial (xlPasteValues)

'Forth effect

'Steam temperature inlet

Range("R14").Select

ActiveCell.Formula = "='Process Data'!C9"

ActiveCell.Copy

ActiveCell.PasteSpecial (xlPasteValues)

'Syrup temperature

Range("W24").Select

ActiveCell.Formula = "='Process Data'!C13"

ActiveCell.Copy

ActiveCell.PasteSpecial (xlPasteValues)

'Syrup Brix

Range("W21").Select

ActiveCell.Formula = "='Process Data'!C16"

ActiveCell.Copy

ActiveCell.PasteSpecial (xlPasteValues)

'Syrup flow

Range("W23").Select

ActiveCell.Formula = "='Process Data'!C15"

ActiveCell.Copy

ActiveCell.PasteSpecial (xlPasteValues)

'Reselect "ON"/"OFF" cell

Range("B2").Select

%%%%%%%%%%

% Initiate solver routine

%%%%%%%%%%

'The solver routine code.

```

'Reset solver to ensure there is no memory storage of data from previous runs (causes errors).
SolverReset
'Sets the options in the solver options box.
SolverOptions MaxTime:=60, Iterations:=10, Precision:=0.00000001, AssumeLinear:=False,
StepThru:=False, Estimates:=1, Derivatives:=2, SearchOption:=2, IntTolerance:=0.0000000000000001,
Scaling:=False
'Runs solver by setting a sum of squares cell value equal to zero by changing the steam supply flow rate.
SolverOk SetCell:="$X$75", MaxMinVal:=3, ValueOf:=0, ByChange:="$F$36"
'Closes the solver results dialog box and selects to keep the solver solution
SolverSolve UserFinish:=True, ShowRef:=True
'Exit the solver routine
SolverFinish

'Again check the circular reference values are iterated for
Calculate

'Check user has not changed code run option to see if the calculation needs to exit the subroutine
'***** WILL ONLY BREAK OUT OF LOOP *****
'***** AFTER 20 ITTERATIONS *****
Number = Worksheets("Model").Range("B2")

'Loops the above code until the reset counter reaches 20 then it will skip to the code below.
Loop

'%%%%%%%%%%%%%%
'% After 20 loops reinitialize
'% spreadsheet and run solver
'%%%%%%%%%%%%%%

'Select the correct worksheet
Worksheets("Model").Select

'Call startup macro to ensure system running ok
Call Startup

'%%%%%%%%%%%%%%
'% Fix values of inputs to prevent them changing
'% while solver is converging to a solution
'%%%%%%%%%%%%%%

'First effect
'Steam temperature inlet
Range("B14").Select
ActiveCell.Formula = "='Process Data'!C6"
ActiveCell.Copy
ActiveCell.PasteSpecial (xlPasteValues)
'Juice inlet temperature
Range("C22").Select
ActiveCell.Formula = "='Process Data'!C5"
ActiveCell.Copy
ActiveCell.PasteSpecial (xlPasteValues)
'Juice inlet flow
Range("C26").Select
ActiveCell.Formula = "='Process Data'!C14"
ActiveCell.Copy
ActiveCell.PasteSpecial (xlPasteValues)

```

```
'Syrup temperature
Range("G22").Select
ActiveCell.Formula = "='Process Data'!C10"
ActiveCell.Copy
ActiveCell.PasteSpecial (xlPasteValues)
```

```
'Second effect
'Steam temperature inlet
Range("H14").Select
ActiveCell.Formula = "='Process Data'!C7"
ActiveCell.Copy
ActiveCell.PasteSpecial (xlPasteValues)
'Syrup temperature
Range("L22").Select
ActiveCell.Formula = "='Process Data'!C11"
ActiveCell.Copy
ActiveCell.PasteSpecial (xlPasteValues)
```

```
'Third effect
'Steam temperature inlet
Range("M14").Select
ActiveCell.Formula = "='Process Data'!C8"
ActiveCell.Copy
ActiveCell.PasteSpecial (xlPasteValues)
'Syrup temperature
Range("Q22").Select
ActiveCell.Formula = "='Process Data'!C12"
ActiveCell.Copy
ActiveCell.PasteSpecial (xlPasteValues)
```

```
'Forth effect
'Steam temperature inlet
Range("R14").Select
ActiveCell.Formula = "='Process Data'!C9"
ActiveCell.Copy
ActiveCell.PasteSpecial (xlPasteValues)
'Syrup temperature
Range("W24").Select
ActiveCell.Formula = "='Process Data'!C13"
ActiveCell.Copy
ActiveCell.PasteSpecial (xlPasteValues)
'Syrup Brix
Range("W21").Select
ActiveCell.Formula = "='Process Data'!C16"
ActiveCell.Copy
ActiveCell.PasteSpecial (xlPasteValues)
'Syrup flow
Range("W23").Select
ActiveCell.Formula = "='Process Data'!C15"
ActiveCell.Copy
ActiveCell.PasteSpecial (xlPasteValues)
```

```
'Reselect "ON"/"OFF" cell
Range("B2").Select
```

```
Application.Visible = True
```

```

%%%%%%%%%%%%%%%%%%%%%%%%%%%%%%%%%%%%%%%%%%%%%%%%%%%%%%%%%%%%%%%%%%%%%%%%
'% Initiate solver routine
%%%%%%%%%%%%%%%%%%%%%%%%%%%%%%%%%%%%%%%%%%%%%%%%%%%%%%%%%%%%%%%%%%%%%%%%

Calculate

'Initiate solver routine
SolverReset
SolverOptions MaxTime:=60, Iterations:=10, Precision:=0.00000001, AssumeLinear:=False,
StepThru:=False, Estimates:=1, Derivatives:=2, SearchOption:=2, IntTolerance:=0.0000000000000001,
Scaling:=False
SolverOk SetCell:="$X$75", MaxMinVal:=3, ValueOf:=0, ByChange:="$F$36"
SolverSolve UserFinish:=True, ShowRef:=True
SolverFinish

Calculate

'Reinitialize counter to zero
Restart = 0

'Check user has not changed code run option
Number = Worksheets("Model").Range("B2")

Loop

End Sub

```

A.2 Code to Run Data After it Has Been Logged and Needs to be Rerun.

The data collected from the controller may need to be rerun if there are errors say in a measurement which needs to be corrected, to rerun the data more code was generated that will select data from a spreadsheet and run it in the model then paste important data in the columns. The calculation takes data from a spreadsheet called “6min avg” to the model spreadsheet called “Dave” where the solver is run and the iterated result sent back to the “6min avg” sheet. This code is run by running the macro “rundave”.

```

Sub rundave()

For n = 4 To 16521

'Select worksheet
Worksheets("Model").Select

'Get input values..
'Juice

```

```

Worksheets("Model").Range("c22").Select
ActiveCell.Formula = "="&6min avg"!K" & n & ""
'Cal 1
Worksheets("Model").Range("b14").Select
ActiveCell.Formula = "="&6min avg"!L" & n & ""
'Cal 2
Worksheets("Model").Range("h14").Select
ActiveCell.Formula = "="&6min avg"!m" & n & ""
'Cal 3
Worksheets("Model").Range("m14").Select
ActiveCell.Formula = "="&6min avg"!n" & n & "+1.4"
'Cal 4
Worksheets("Model").Range("r14").Select
ActiveCell.Formula = "="&6min avg"!o" & n & ""
'Juice 1
Worksheets("Model").Range("G22").Select
ActiveCell.Formula = "="&6min avg"!p" & n & ""
'Juice 2
Worksheets("Model").Range("L22").Select
ActiveCell.Formula = "="&6min avg"!q" & n & ""
'Juice 3
Worksheets("Model").Range("Q22").Select
ActiveCell.Formula = "="&6min avg"!r" & n & ""
'Juice 4
Worksheets("Model").Range("W24").Select
ActiveCell.Formula = "="&6min avg"!s" & n & ""
'Flow in
Worksheets("Model").Range("c26").Select
ActiveCell.Formula = "="&6min avg"!E" & n & ""
'Flow out
Worksheets("Model").Range("W23").Select
ActiveCell.Formula = "="&6min avg"!F" & n & ""
'Brix out
Worksheets("Model").Range("W21").Select
ActiveCell.Formula = "="&6min avg"!C" & n & ""
'Check Brix correct
If ActiveCell.Value < 40 Then
    ActiveCell.Formula = "=66"
Else

End If

```

'Startup macro to ensure system running ok

'Feed Brix estimate

```

Worksheets("Model").Range("c24").Select
ActiveCell.FormulaR1C1 = "15"

```

'Reinsert computation

'Brix feed calculation

```

Worksheets("Model").Range("c24").Select
ActiveCell.Formula = "=(W20*W21)/C23"

```

'Steam estimate

```

Worksheets("Model").Range("f36").Select
ActiveCell.FormulaR1C1 = "8"

```


ActiveCell.Copy
ActiveCell.PasteSpecial (xlPasteValues)

'Initial guesses first effect

Worksheets("Model").Range("f54").Select
ActiveCell.FormulaR1C1 = "103"
Worksheets("Model").Range("f57").Select
ActiveCell.FormulaR1C1 = "102"
Worksheets("Model").Range("f58").Select
ActiveCell.FormulaR1C1 = "10"

'Initail guesses second effect

Worksheets("Model").Range("l54").Select
ActiveCell.FormulaR1C1 = "97"
Worksheets("Model").Range("l57").Select
ActiveCell.FormulaR1C1 = "95"
Worksheets("Model").Range("l58").Select
ActiveCell.FormulaR1C1 = "10.5"

'Initail guesses third effect

Worksheets("Model").Range("r54").Select
ActiveCell.FormulaR1C1 = "90"
Worksheets("Model").Range("r57").Select
ActiveCell.FormulaR1C1 = "87"
Worksheets("Model").Range("r58").Select
ActiveCell.FormulaR1C1 = "11"

'Initail guesses final effect

Worksheets("Model").Range("x54").Select
ActiveCell.FormulaR1C1 = "67"
Worksheets("Model").Range("x57").Select
ActiveCell.FormulaR1C1 = "60"
Worksheets("Model").Range("x58").Select
ActiveCell.FormulaR1C1 = "11"

'Reinsert computation

'Brix feed calculation

Worksheets("Model").Range("c24").Select
ActiveCell.Formula = "=(W20*W21)/C23"

'Insert formulae first effect

Worksheets("Model").Range("f58").Select
ActiveCell.Formula = "=(F47*F43+F40-F41-F63*F64)/F59"
Worksheets("Model").Range("f57").Select
ActiveCell.Formula = "=F61-F62"
Worksheets("Model").Range("f54").Select
ActiveCell.Formula = "=F57+F52+F53"

'Insert formulae second effect

Worksheets("Model").Range("l58").Select
ActiveCell.Formula = "=(l47*l43+l40-l41-l63*l64)/l59"
Worksheets("Model").Range("l57").Select
ActiveCell.Formula = "=l61-l62"
Worksheets("Model").Range("l54").Select
ActiveCell.Formula = "=L57+L52+L53"

'Insert formulae third effect

```
Worksheets("Model").Range("r58").Select
ActiveCell.Formula = "=(r47*r43+r40-r41-r63*r64)/r59"
Worksheets("Model").Range("r57").Select
ActiveCell.Formula = "=r61-r62"
Worksheets("Model").Range("r54").Select
ActiveCell.Formula = "=R57+R52+R53"
```

'Insert formulae final effect

```
Worksheets("Model").Range("x57").Select
ActiveCell.Formula = "=x61-x62"
Worksheets("Model").Range("x54").Select
ActiveCell.Formula = "=X57+X52+X53"
Worksheets("Model").Range("x58").Select
ActiveCell.Formula = "=(X47*X43+X40-X41-X63*X64)/X59"
```

'Steam estimate

```
Worksheets("Model").Range("f36").Select
ActiveCell.Formula = "=(C23-W20)/4"
ActiveCell.Copy
ActiveCell.PasteSpecial (xlPasteValues)
```

Calculate

SolverReset

```
SolverOptions MaxTime:=60, Iterations:=100, Precision:=0.00000001, AssumeLinear:=False,
StepThru:=False, Estimates:=1, Derivatives:=2, SearchOption:=2, IntTolerance:=0.0000000001,
Scaling:=False
SolverOk SetCell:="$X$74", MaxMinVal:=2, ByChange:="$F$36"
SolverSolve UserFinish:=True, ShowRef:=True
SolverFinish
```

Calculate

SolverReset

```
SolverOptions MaxTime:=60, Iterations:=100, Precision:=0.000000001, AssumeLinear:=False,
StepThru:=False, Estimates:=1, Derivatives:=2, SearchOption:=2, IntTolerance:=0.0000000001,
Scaling:=False
SolverOk SetCell:="$X$74", MaxMinVal:=3, ValueOf:=0, ByChange:="$F$36"
SolverSolve UserFinish:=True, ShowRef:=True
SolverFinish
```

'Put answers back in spreadsheet...

'Select worksheet

```
Worksheets("6min avg").Select
```

'k1

```
Worksheets("6min avg").Range("T" & n & "").Select
ActiveCell.Value = "=Model!F34"
ActiveCell.Copy
ActiveCell.PasteSpecial (xlPasteValues)
```

'k2

```
Worksheets("6min avg").Range("U" & n & "").Select
ActiveCell.Value = "=Model!L34"
```

```
ActiveCell.Copy  
ActiveCell.PasteSpecial (xlPasteValues)
```

'k3

```
Worksheets("6min avg").Range("V" & n & "").Select  
ActiveCell.Value = "="&"Model"!R34"  
ActiveCell.Copy  
ActiveCell.PasteSpecial (xlPasteValues)
```

'k4

```
Worksheets("6min avg").Range("W" & n & "").Select  
ActiveCell.Value = "="&"Model"!X34"  
ActiveCell.Copy  
ActiveCell.PasteSpecial (xlPasteValues)
```

'error

```
Worksheets("6min avg").Range("X" & n & "").Select  
ActiveCell.Value = "="&"Model"!X74"  
ActiveCell.Copy  
ActiveCell.PasteSpecial (xlPasteValues)
```

'steam flow

```
Worksheets("6min avg").Range("Y" & n & "").Select  
ActiveCell.Value = "="&"Model"!F36"  
ActiveCell.Copy  
ActiveCell.PasteSpecial (xlPasteValues)
```

'Feed Brix

```
Worksheets("6min avg").Range("Z" & n & "").Select  
ActiveCell.Value = "="&"Model"!C24"  
ActiveCell.Copy  
ActiveCell.PasteSpecial (xlPasteValues)
```

'Brix 1

```
Worksheets("6min avg").Range("AA" & n & "").Select  
ActiveCell.Value = "="&"Model"!G23"  
ActiveCell.Copy  
ActiveCell.PasteSpecial (xlPasteValues)
```

'Brix 2

```
Worksheets("6min avg").Range("AB" & n & "").Select  
ActiveCell.Value = "="&"Model"!L23"  
ActiveCell.Copy  
ActiveCell.PasteSpecial (xlPasteValues)
```

'Brix 3

```
Worksheets("6min avg").Range("AC" & n & "").Select  
ActiveCell.Value = "="&"Model"!Q23"  
ActiveCell.Copy  
ActiveCell.PasteSpecial (xlPasteValues)
```

'DP1-2

```
Worksheets("6min avg").Range("AD" & n & "").Select  
ActiveCell.Value = "="&"Model"!H7"  
ActiveCell.Copy  
ActiveCell.PasteSpecial (xlPasteValues)
```

'DP2-3

```
Worksheets("6min avg").Range("AE" & n & "").Select  
ActiveCell.Value = "=" & Model & "!M7"  
ActiveCell.Copy  
ActiveCell.PasteSpecial (xlPasteValues)
```

'DP3-4

```
Worksheets("6min avg").Range("AF" & n & "").Select  
ActiveCell.Value = "=" & Model & "!R7"  
ActiveCell.Copy  
ActiveCell.PasteSpecial (xlPasteValues)
```

'PV1

```
Worksheets("6min avg").Range("AG" & n & "").Select  
ActiveCell.Value = "=" & Model & "!F4"  
ActiveCell.Copy  
ActiveCell.PasteSpecial (xlPasteValues)
```

'PV2

```
Worksheets("6min avg").Range("AH" & n & "").Select  
ActiveCell.Value = "=" & Model & "!K4"  
ActiveCell.Copy  
ActiveCell.PasteSpecial (xlPasteValues)
```

'PV3

```
Worksheets("6min avg").Range("AI" & n & "").Select  
ActiveCell.Value = "=" & Model & "!P4"  
ActiveCell.Copy  
ActiveCell.PasteSpecial (xlPasteValues)
```

'PV4

```
Worksheets("6min avg").Range("AJ" & n & "").Select  
ActiveCell.Value = "=" & Model & "!T4"  
ActiveCell.Copy  
ActiveCell.PasteSpecial (xlPasteValues)
```

'PS1

```
Worksheets("6min avg").Range("AK" & n & "").Select  
ActiveCell.Value = "=" & Model & "!B15"  
ActiveCell.Copy  
ActiveCell.PasteSpecial (xlPasteValues)
```

'PS2

```
Worksheets("6min avg").Range("AL" & n & "").Select  
ActiveCell.Value = "=" & Model & "!H16"  
ActiveCell.Copy  
ActiveCell.PasteSpecial (xlPasteValues)
```

'PS3

```
Worksheets("6min avg").Range("AM" & n & "").Select  
ActiveCell.Value = "=" & Model & "!M16"  
ActiveCell.Copy  
ActiveCell.PasteSpecial (xlPasteValues)
```

'PS4

```
Worksheets("6min avg").Range("AN" & n & "").Select
ActiveCell.Value = "=" & Model & "!R16"
ActiveCell.Copy
ActiveCell.PasteSpecial (xlPasteValues)
```

'DT1

```
Worksheets("6min avg").Range("AO" & n & "").Select
ActiveCell.Value = "=" & Model & "!F55"
ActiveCell.Copy
ActiveCell.PasteSpecial (xlPasteValues)
```

'DT2

```
Worksheets("6min avg").Range("AP" & n & "").Select
ActiveCell.Value = "=" & Model & "!L55"
ActiveCell.Copy
ActiveCell.PasteSpecial (xlPasteValues)
```

'DT3

```
Worksheets("6min avg").Range("AQ" & n & "").Select
ActiveCell.Value = "=" & Model & "!R55"
ActiveCell.Copy
ActiveCell.PasteSpecial (xlPasteValues)
```

'DT4

```
Worksheets("6min avg").Range("AR" & n & "").Select
ActiveCell.Value = "=" & Model & "!X55"
ActiveCell.Copy
ActiveCell.PasteSpecial (xlPasteValues)
```

'Juice

```
Worksheets("6min avg").Range("As" & n & "").Select
ActiveCell.Value = "=" & Model & "!c23"
ActiveCell.Copy
ActiveCell.PasteSpecial (xlPasteValues)
```

'Syrup

```
Worksheets("6min avg").Range("At" & n & "").Select
ActiveCell.Value = "=" & Model & "!w20"
ActiveCell.Copy
ActiveCell.PasteSpecial (xlPasteValues)
```

Next n

End Sub

APPENDIX B CALCULATION OF BOILING POINT RISE DUE TO HYDROSTATIC HEAD

B.1 Calculation of Boiling Point Rise Due to Hydrostatic Head

The Antoine equation is used to calculate the pressure and temperature conditions of saturated steam. The following drawing assists in explaining this computation:

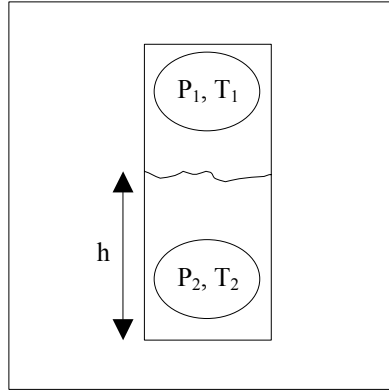


Figure B.1: Pressures and temperatures in the evaporator vessel.

The juice boils at a temperature T_2 due to the pressure P_2 . The pressure P_2 is higher than the vapor pressure P_1 because of the pressure exerted by the juice above it. The boiling point elevation is the difference in temperature between T_1 and T_2 .

$$\text{Boiling point elevation due to hydrostatic head} = T_2 - T_1 \quad (\text{B.1})$$

The computation is performed by assuming the liquid is only water and then computing the boiling point rise.

The Antoine equation used is:

$$\ln\left(\frac{P^{Sat}}{0.1333224}\right) = 18.3036 - \frac{3816.44}{T^{sat} - 46.13} \quad (\text{B.2})$$

Where P^{sat} is in kPa and T^{sat} is in K.

The pressure P_2 is computed as follows:

$$P_2 = P_1 + \rho g(z/2) \quad (B.3)$$

Rearranging equation (B.2) and substituting in equation (B.3) then solving for T_2 :

$$T_2 = 46.13 - \frac{3816.44}{-18.3036 + \ln\left(\frac{P_1 + \rho g(z/2)}{0.1333224}\right)} \quad (B.4)$$

Since T_1 is known, equation (B.1) is used to find the boiling point rise (BPR) due to the hydrostatic head

$$T_{BPR-HydrostaticHead} = 46.13 - \frac{3816.44}{-18.3036 + \ln\left(\frac{P_1 + \rho g(z/2)}{0.1333224}\right)} - T_1 \quad (B.5)$$

Where T_1 is in K.

A note on units:

The term $\rho g(z/2)$ has the correct units (kPa) if the following units are used:

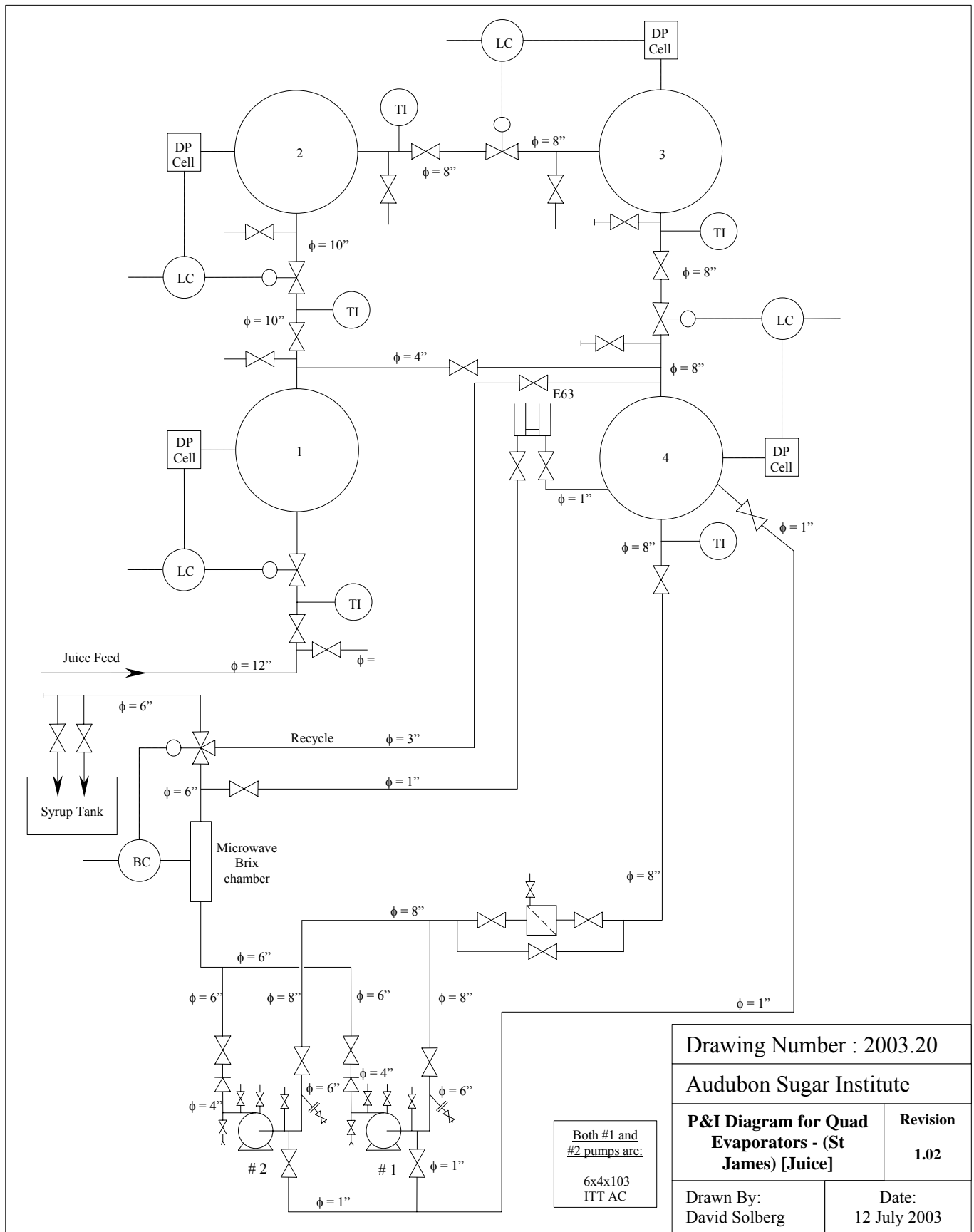
- z is the juice level in meters. (A value of $\frac{1}{2}$ of the liquid level is used to find the average boiling point rise in the vessel, as the rise is higher at the base of the liquid level than at the surface.)
- ρ is the specific gravity of the juice in the vessel. (If the density in kg/m^3 is used the pressure in Pa is obtained so dividing the term by 1000 to get kPa naturally yields the specific gravity.)
- g is the gravitational constant 9.81m/s^2 .

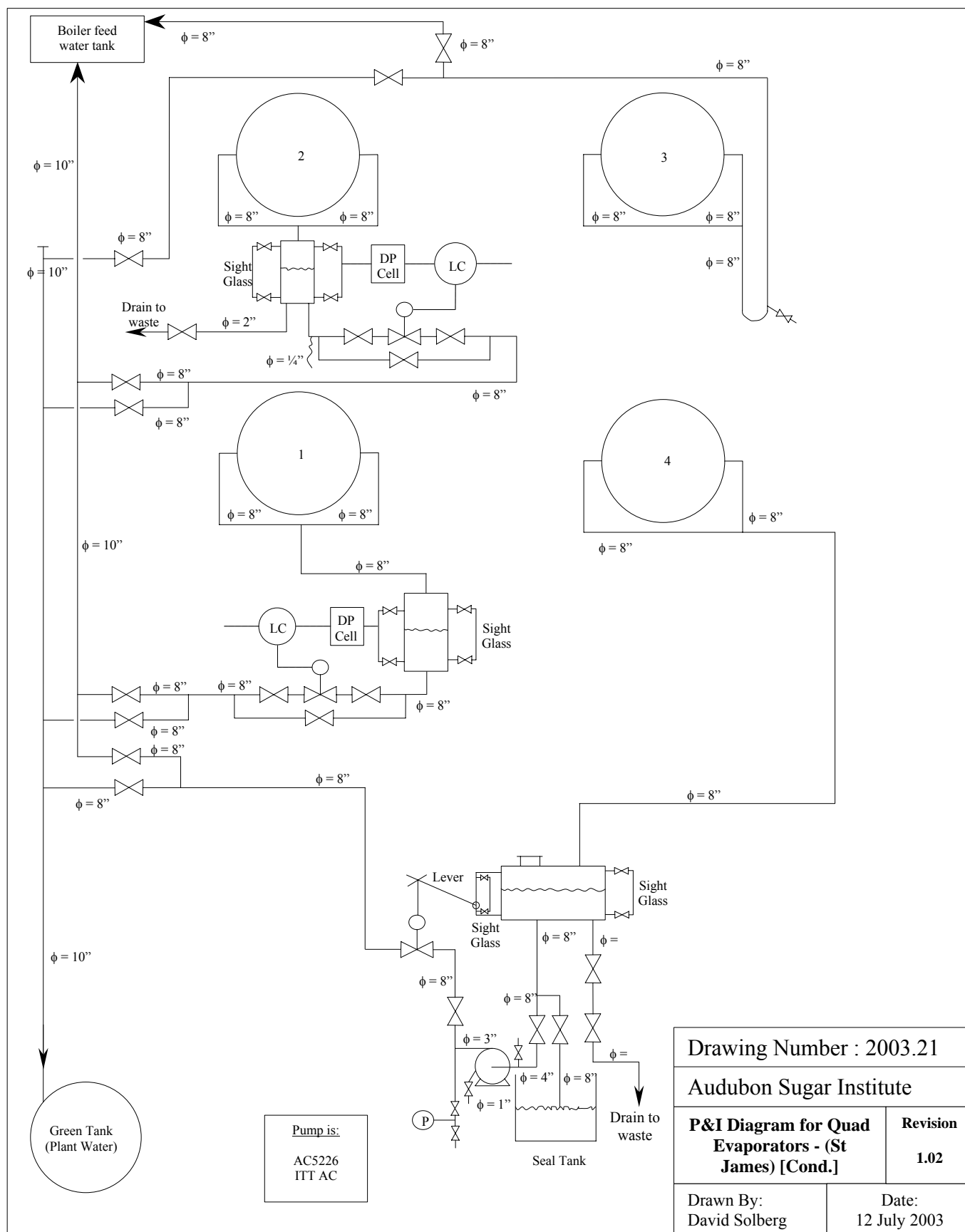
APPENDIX C P&I DIAGRAMS FOR ST JAMES MILL QUADRUPLE EVAPORATOR TRAIN

C.1 P&I Diagrams for St James Mill Quadruple Evaporator Train

The diagrams are shown on the next few pages in the following order for the quadruple effect evaporator at St James:

1. The juice flow system
2. The condensate flow system
3. The steam flow system
4. Vessel drainage for cleaning
5. Vacuum breakage system
6. Acid addition system
7. The water flow system
8. The water and juice flow systems superimposed
9. All cleaning systems superimposed
10. The steam and vapor generated system colored





Drawing Number : 2003.21

Audubon Sugar Institute

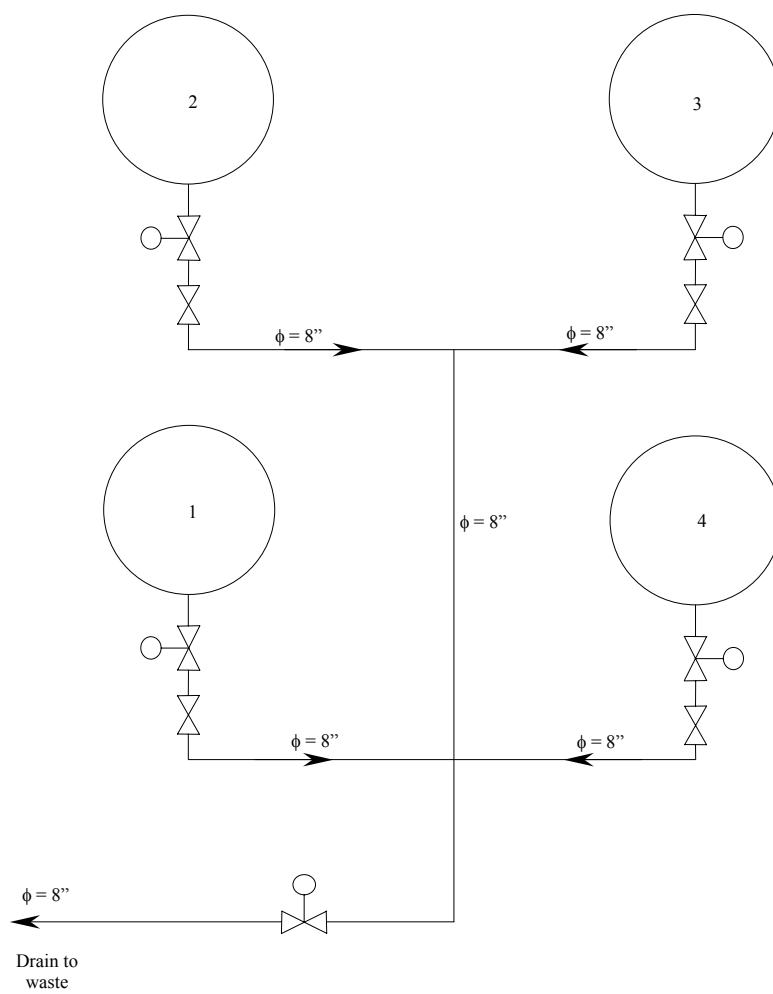
**P&I Diagram for Quad
Evaporators - (St
James) [Cond.]**

**Revision
1.02**

Drawn By:
David Solberg

Date:
12 July 2003





Drawing Number : 2003.22

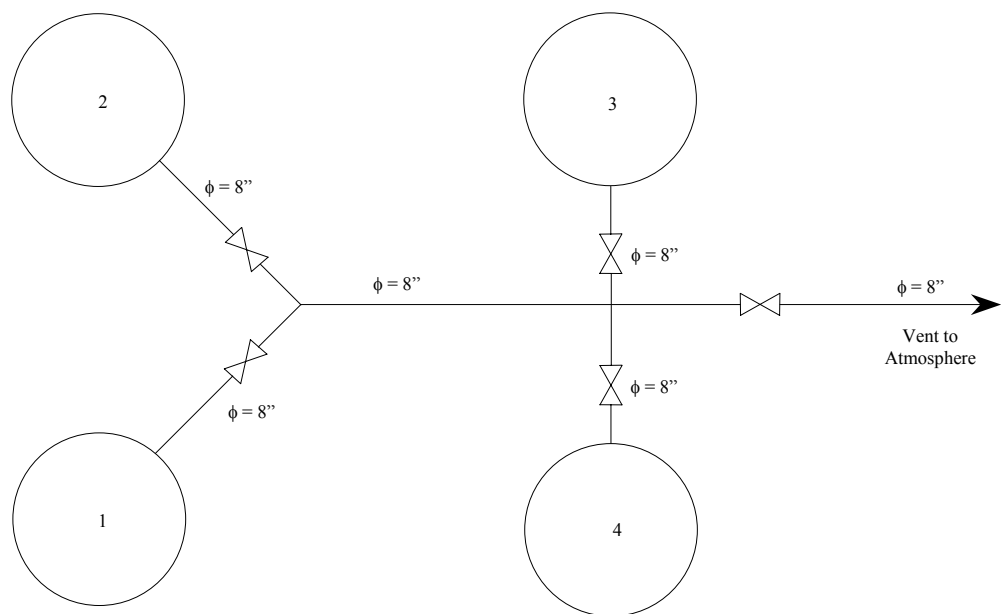
Audubon Sugar Institute

**P&I Diagram for Quad
Evaporators - (St
James) [Cleaning]**

**Revision
1.02**

Drawn By:
David Solberg

Date:
12 July 2003



Drawing Number : 2003.24

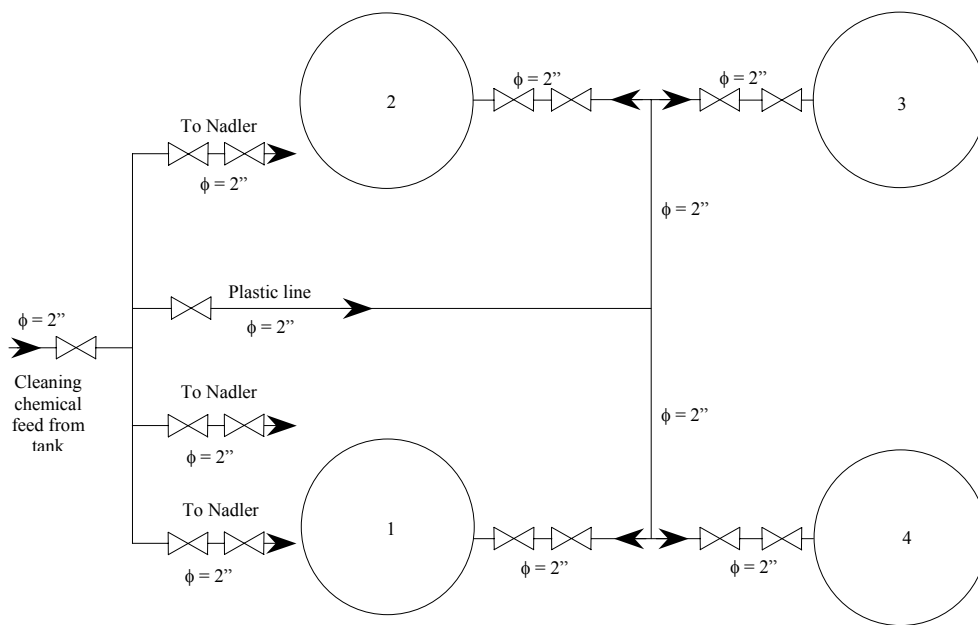
Audubon Sugar Institute

**P&I Diagram for Quad
Evaporators - (St
James) [Vac Break]**

**Revision
1.02**

Drawn By:
David Solberg

Date:
12 July 2003



Drawing Number : 2003.25

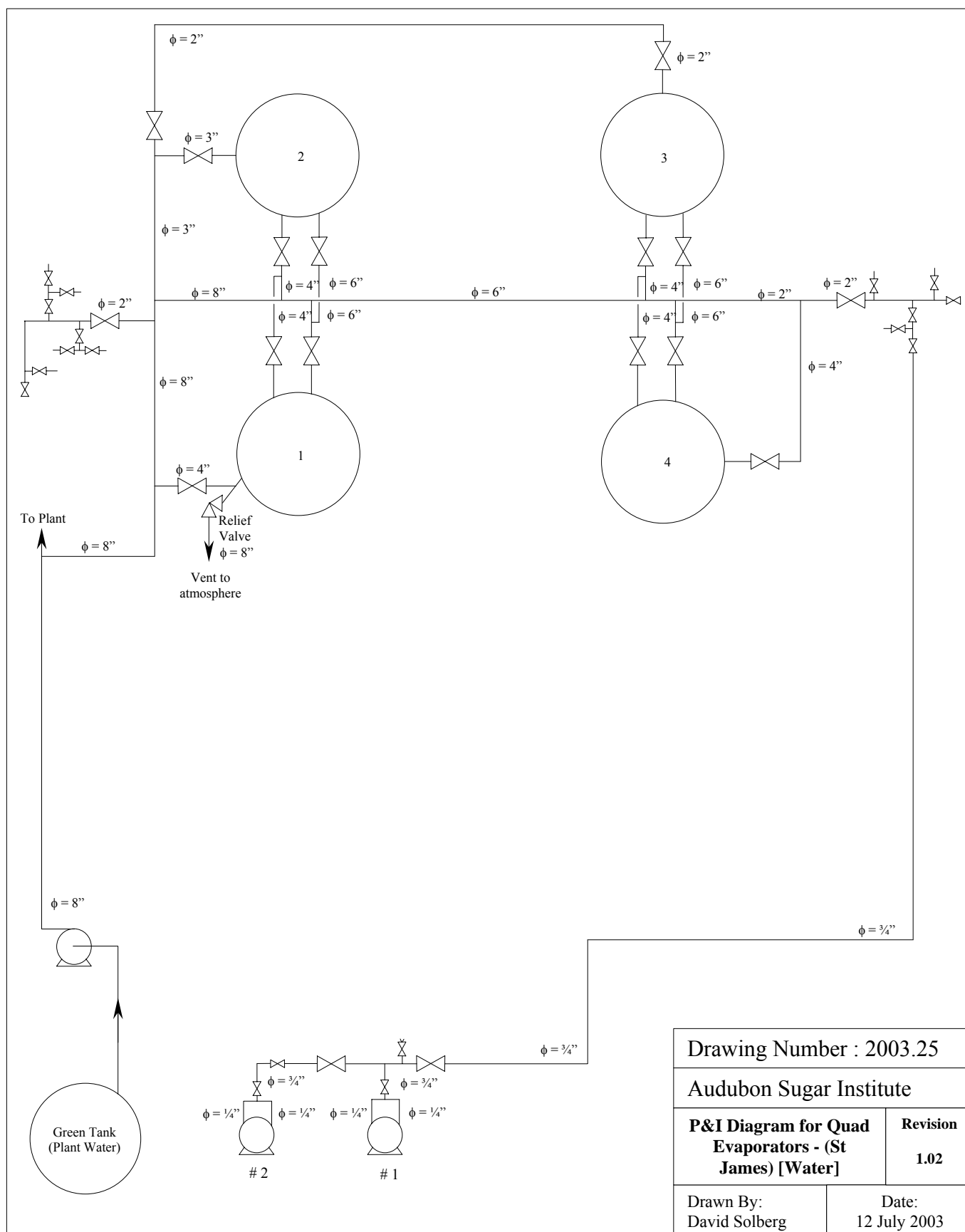
Audubon Sugar Institute

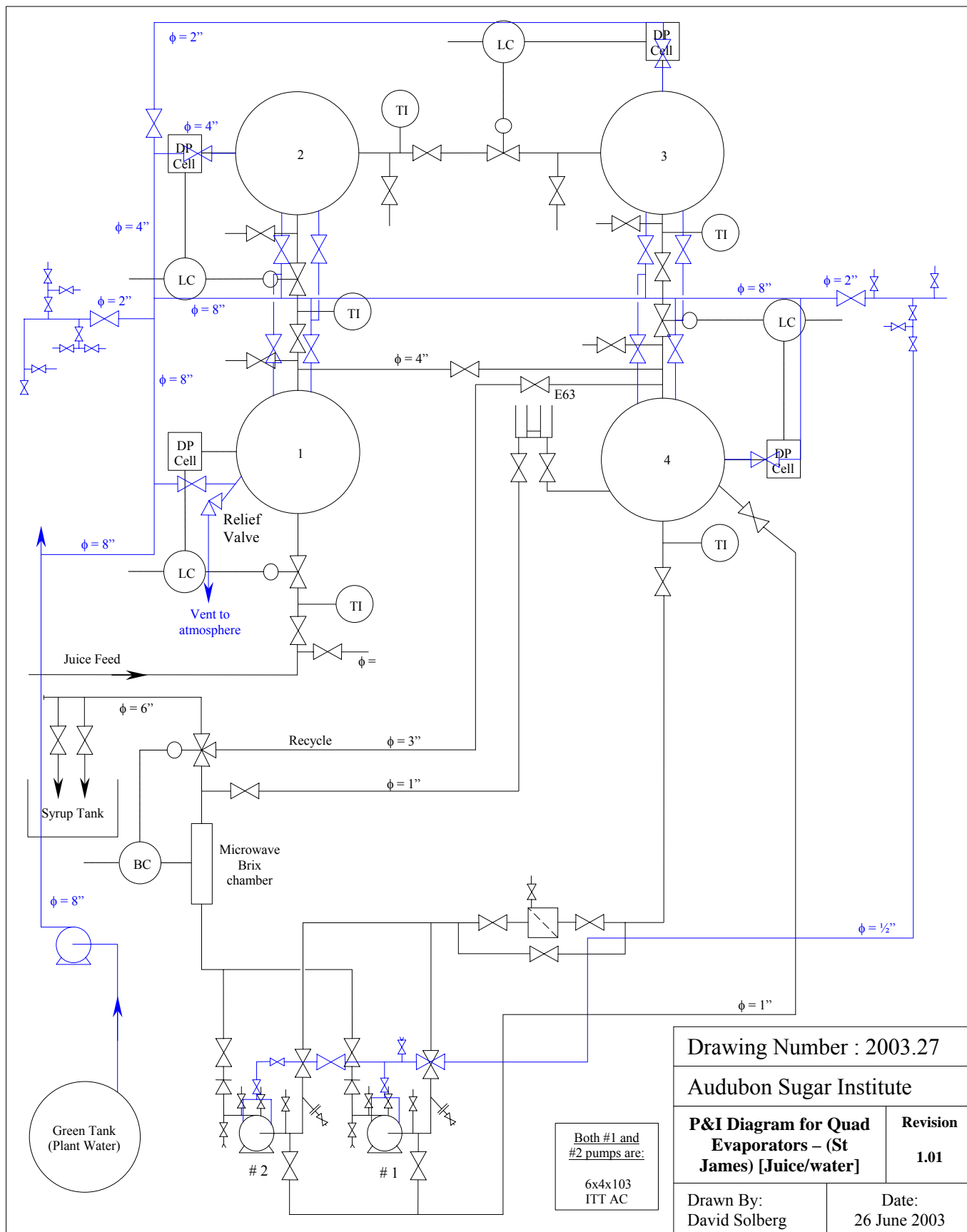
**P&I Diagram for Quad
Evaporators - (St
James) [Cleaning]**

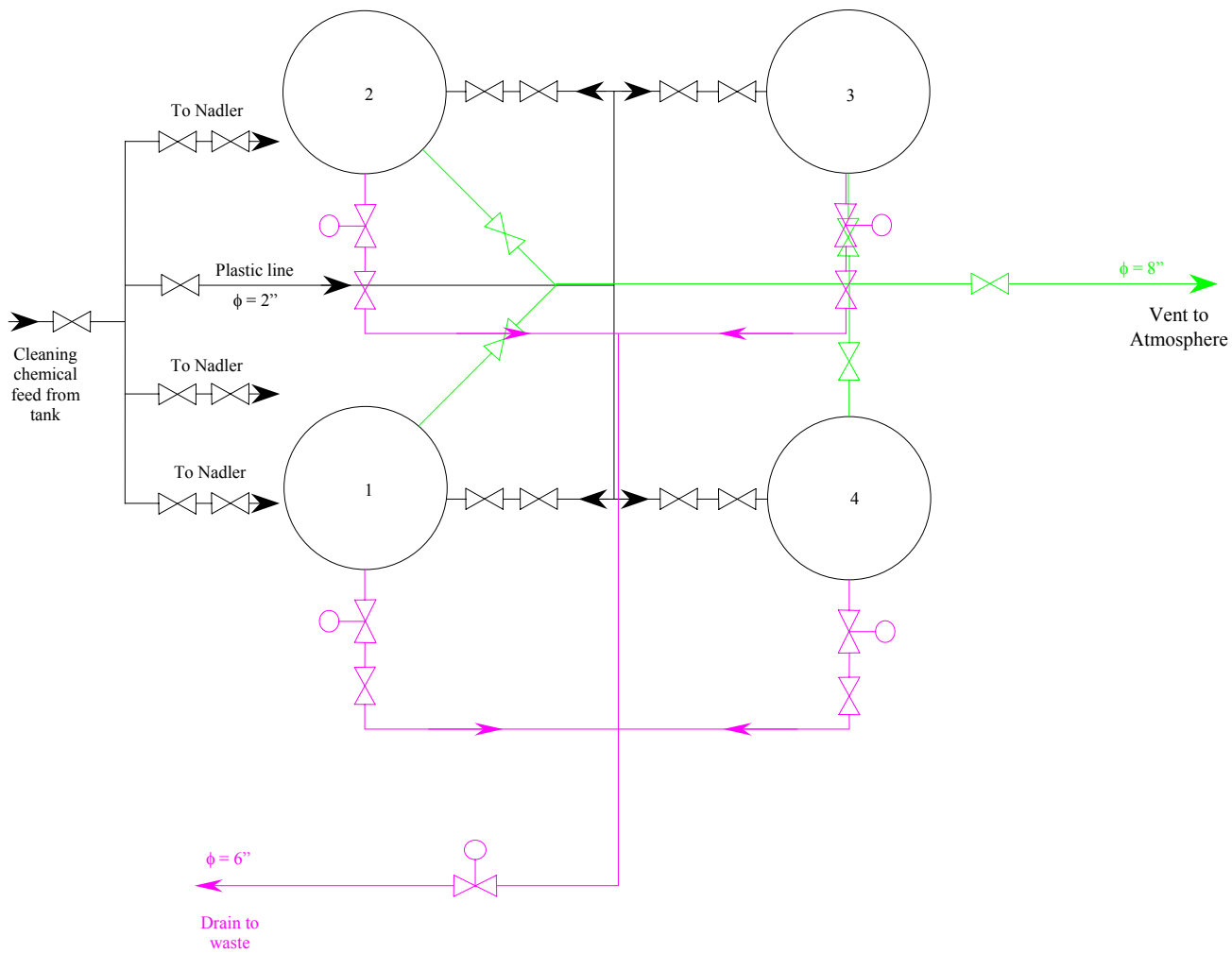
**Revision
1.02**

Drawn By:
David Solberg

Date:
12 July 2003







Drawing Number : 2003.26

Audubon Sugar Institute

**P&I Diagram for Quad
Evaporators - (St
James) [Cleaning]**

**Revision
1.01**

Drawn By:
David Solberg

Date:
26 June 2003

APPENDIX D CONTROLLER LABEL AND TAG VARIABLES USED AT ST JAMES

D.1 Controller Label and Tag Variables Used at St James

Variable	Description (Process Variables)
TT-001	Juice inlet temperature [$^{\circ}\text{C}$]
TT-002	First body steam temperature [$^{\circ}\text{C}$]
TT-003	Second body steam temperature [$^{\circ}\text{C}$]
TT-004	Third body steam temperature [$^{\circ}\text{C}$]
TT-005	Forth body steam temperature [$^{\circ}\text{C}$]
TT-006	First body “syrup” temperature [$^{\circ}\text{C}$]
TT-007	Second body “syrup” temperature [$^{\circ}\text{C}$]
TT-008	Third body “syrup” temperature [$^{\circ}\text{C}$]
TT-009	Forth body “syrup” temperature [$^{\circ}\text{C}$]
FT-001	Volumetric juice flow to final effect [m^3/s]
FT-002	Volumetric syrup flow out final effect [m^3/s]
BT-001	Brix of final syrup [%]
Variable	Description (Set Point Variables)
HTCV1	Heat transfer coefficient for vessel 1 [$\text{kW}/\text{m}^2\text{K}$]
HTCV2	Heat transfer coefficient for vessel 2 [$\text{kW}/\text{m}^2\text{K}$]
HTCV3	Heat transfer coefficient for vessel 3 [$\text{kW}/\text{m}^2\text{K}$]
HTCV4	Heat transfer coefficient for vessel 4 [$\text{kW}/\text{m}^2\text{K}$]
ERROR	Sum of squares error in the mass and energy balance

APPENDIX E SCALE MODEL CODE

E.1 Scale Model Code

E.1.1 Accumulation of Materials in the Evaporators

Model.m

```
% St James Evaporator flows for 2003
% Scale model based on concentrations of majorscale components
% Started 25 March 2004
% By David Solberg
% Last Update 26 March 2004
% REVISION 1.01

close all          % Closes all figures that are open
clear all          % Clear all variables
clc                % Clear workspace

%Define global variables

global Fin_Pre Cain_Pre Cbin_Pre Ccin_Pre Cdin_Pre Cein_Pre Cfin_Pre Cgin_Pre Chin_Pre Ciin_Pre
Cjin_Pre Ckin_Pre Clin_Pre Cmin_Pre Cnin_Pre Coin_Pre Cpin_Pre Cqin_Pre Crin_Pre Csin_Pre
Ctin_Pre
global Fout_4 Caout_4 Cbout_4 Ccout_4 Cdout_4 Ceout_4 Cfout_4 Cgout_4 Chout_4 Ciout_4 Cjout_4
Ckout_4 Clout_4 Cmout_4 Cnout_4 Coout_4 Cpout_4 Cqout_4 Crout_4 Csout_4 Ctout_4

%Define flows

Fst_1  = 12.158;    %Steam flow into first effect [kg/s]

Fin_1  = 67.113;    %Juice flow into the first effect [kg/s]
Fout_1 = 55.111;    %Syrup flow out the first effect [kg/s]
Fv_1   = Fin_1 - Fout_1; %Vapor flow out first effect [kg/s]
Bxin_1 = 15.806;    %Brix in the first effect [%]
Bxout_1 = 19.237;   %Brix out the first effect [%]

Fin_2  = Fout_1;    %Juice flow into the second effect [kg/s]
Fout_2 = 42.787;    %Syrup flow out the second effect [kg/s]
Fv_2   = Fin_2 - Fout_2; %Vapor flow out second effect [kg/s]
Bxin_2 = Bxout_1;   %Brix in the second effect [%]
Bxout_2 = 24.761;   %Brix out the second effect [%]

Fin_3  = Fout_2;    %Juice flow into the second effect [kg/s]
Fout_3 = 30.258;    %Syrup flow out the third effect [kg/s]
Fv_3   = Fin_3 - Fout_3; %Vapor flow out third effect [kg/s]
Bxin_3 = Bxout_2;   %Brix in the third effect [%]
Bxout_3 = 34.992;   %Brix out the third effect [%]

Fin_4  = Fout_3;    %Juice flow into forth effect [kg/s]
```

```

Fout_4 = 16.897;      %Syrup flow out the forth effect [kg/s]
Fv_4 = Fin_4 - Fout_4; %Vapor flow out forth effect [kg/s]
Bxin_4 = Bxout_3;     %Brix in the forth effect [%]
Bxout_4 = 62.792;     %Brix out the forth effect [%]

Fout_Pre = Fin_1;     %Syrup flow out the pre [kg/s]
Bxout_Pre = Bxin_1;   %Brix out the pre [%]
Bxin_Pre = 13.25;     %Brix in the pre [%]
Fin_Pre = Fin_1*(Bxout_Pre/Bxin_Pre); %Calculated flow into the pre [kg/s]
Fv_Pre = Fin_Pre-Fout_Pre; %Vapor flow out the pre [kg/s]

Exh_Pre = Fv_Pre;     %Rilleaux steam usage for pre [kg/s]

```

% Concentration of components % Concentrations in feed

```

Cain_Pre = 0.00;      % Concentration of Si [mg/kg]
Cbin_Pre = 502.53;    % Concentration of Ca [mg/kg]
Ccin_Pre = 403.44;    % Concentration of Mg [mg/kg]
Cdin_Pre = 1068.58;   % Concentration of Aconite [mg/kg]
Cein_Pre = 1062.09;   % Concentration of K [mg/kg]
Cfin_Pre = 97.51;     % Concentration of Ammonium [mg/kg]
Cgin_Pre = 1837.76;   % Concentration of Na [mg/kg]
Chin_Pre = 131.52;    % Concentration of Actate [mg/kg]
Ciin_Pre = 412.21;    % Concentration of SO4 [mg/kg]
Cjin_Pre = 313.68;    % Concentration of PO4 [mg/kg]
Ckin_Pre = 801.33;    % Concentration of Cl [mg/kg]
Clin_Pre = 246.21;    % Concentration of Malate [mg/kg]
Cmin_Pre = 131.52;    % Concentration of Lactate [mg/kg]
Cnin_Pre = 0;         % Concentration of Shikimate [mg/kg]
Coin_Pre = 0;         % Concentration of Propionate [mg/kg]
Cpin_Pre = 25.85;     % Concentration of Formate [mg/kg]
Cqin_Pre = 31.96;     % Concentration of Oxalate [mg/kg]
Crin_Pre = 211.88;    % Concentration of Citrate [mg/kg]
Csin_Pre = 834.09;    % Concentration of Iso-Citrate [mg/kg]
Ctin_Pre = 61.47;     % Concentration of Cis-Aconitate [mg/kg]

```

%Concentrations out Syrup

```

Caout_4 = 0.00;      % Concentration of Si [mg/kg]
Cbout_4 = 1656.02;    % Concentration of Ca [mg/kg]
Ccout_4 = 948.21;     % Concentration of Mg [mg/kg]
Cdout_4 = 4691.74;    % Concentration of Aconitate [mg/kg]
Ceout_4 = 5512.78;    % Concentration of K [mg/kg]
Cfout_4 = 111.70;     % Concentration of Ammonium [mg/kg]
Cgout_4 = 1488.20;    % Concentration of Na [mg/kg]
Chout_4 = 624.38;     % Concentration of Actate [mg/kg]
Ciout_4 = 1468.59;    % Concentration of SO4 [mg/kg]
Cjout_4 = 99.43;      % Concentration of PO4 [mg/kg]
Ckout_4 = 2850.64;    % Concentration of Cl [mg/kg]
Clout_4 = 1096.02;    % Concentration of Malate [mg/kg]
Cmout_4 = 624.38;     % Concentration of Lactate [mg/kg]
Cnout_4 = 227.47;     % Concentration of Shikiate [mg/kg]
Coout_4 = 92.72;      % Concentration of Propionate [mg/kg]
Cpout_4 = 130.51;     % Concentration of Formate [mg/kg]
Cqout_4 = 137.64;     % Concentration of Oxalate [mg/kg]

```

```
Crout_4 = 880.27;    % Concentration of Citrate [mg/kg]
Csout_4 = 87.03;    % Concentration of Iso-Citrate [mg/kg]
Ctout_4 = 522.96;    % Concentration of Cis-Aconite [mg/kg]
```

```
% Calculate accumulation in the effects (Total)
```

```
%% ##### Change units to get to days!!!!#####
```

```
[t,c] = ode23s('rhsode1',[0 14],[0 0 0 0 0 0 0 0 0 0 0 0 0 0 0 0]); %Run for 14 days
```

```
% Plot results
```

```
figure(1)
plot(t,c(:,1),'b');
hold on;
plot(t,c(:,2),'m');
plot(t,c(:,3),'g');
plot(t,c(:,4),'r');
plot(t,c(:,5),'c');
plot(t,c(:,6),'k');
plot(t,c(:,7),'-k');
plot(t,c(:,8),'-b');
plot(t,c(:,9),'-m');
plot(t,c(:,10),'-g');
plot(t,c(:,11),'-r');
plot(t,c(:,12),'-c');
plot(t,c(:,13),'--k');
plot(t,c(:,14),'--b');
plot(t,c(:,15),'--m');
plot(t,c(:,16),'--g');
plot(t,c(:,17),'--r');
plot(t,c(:,18),'--c');
plot(t,c(:,19),'r');
plot(t,c(:,20),'k');
legend('Concentration of Si','Concentration of Ca','Concentration of Mg','Concentration of
Aconitate','Concentration of K','Concentration of Ammonium','Concentration of Na','Concentration of
Actate','Concentration of SO4','Concentration of PO4','Concentration of Cl', 'Concentration of
Malate','Concentration of Lactate','Concentration of Shikiate','Concentration of Propionate','Concentration
of Formate','Concentration of Oxalate','Concentration of Citrate','Concentration of Iso-
Citrate','Concentration of Cis-Aconite',0);
axis([0 14 -10000 30000])
title('Accumulation in Evaporators')
xlabel('Time, days');
ylabel('Accumulation in effects [kg]')
```

```
%#####%
%                                                    %
%           Fitting data to the model                %
%                                                    %
%#####%
```

```
[t,c] = ode23s('rhsode1',[0 14],[0 0 0 0 0 0 0 0 0 0 0 0 0 0 0 0]); %Run for 14 days
```

```
rhsode.m
```

```
function dcdt = rhsode1(t,c);
```

```
ca = c(1);  
cb = c(2);  
cc = c(3);  
cd = c(4);  
ce = c(5);  
cf = c(6);  
cg = c(7);  
ch = c(8);  
ci = c(9);  
cj = c(10);  
ck = c(11);  
cl = c(12);  
cm = c(13);  
cn = c(14);  
co = c(15);  
cp = c(16);  
cq = c(17);  
cr = c(18);  
cs = c(19);  
ct = c(20);
```

```
global Fin_Pre  
global Cain_Pre  
global Cbin_Pre  
global Ccin_Pre  
global Cdin_Pre  
global Cein_Pre  
global Cfin_Pre  
global Cgin_Pre  
global Chin_Pre  
global Ciin_Pre  
global Cjin_Pre  
global Ckin_Pre  
global Clin_Pre  
global Cmin_Pre  
global Cnin_Pre  
global Coin_Pre  
global Cpin_Pre  
global Cqin_Pre  
global Crin_Pre  
global Csin_Pre  
global Ctin_Pre
```

```
global Fout_4  
global Caout_4  
global Cbout_4  
global Ccout_4  
global Cdout_4  
global Ceout_4  
global Cfout_4  
global Cgout_4  
global Chout_4  
global Ciout_4  
global Cjout_4
```

```

global Ckout_4
global Clout_4
global Cmout_4
global Cnout_4
global Coout_4
global Cpout_4
global Cqout_4
global Crout_4
global Csout_4
global Ctout_4

```

```

dcadt = (86400/1000000)*(Fin_Pre*Cain_Pre-Fout_4*Caout_4);
dcbdt = (86400/1000000)*(Fin_Pre*Cbin_Pre-Fout_4*Cbout_4);
dccdt = (86400/1000000)*(Fin_Pre*Ccin_Pre-Fout_4*Ccout_4);
dcddt = (86400/1000000)*(Fin_Pre*Cdin_Pre-Fout_4*Cdout_4);
dcedt = (86400/1000000)*(Fin_Pre*Cein_Pre-Fout_4*Ceout_4);
dcfdt = (86400/1000000)*(Fin_Pre*Cfin_Pre-Fout_4*Cfout_4);
dcgdt = (86400/1000000)*(Fin_Pre*Cgin_Pre-Fout_4*Cgout_4);
dchdt = (86400/1000000)*(Fin_Pre*Chin_Pre-Fout_4*Chout_4);
dcidt = (86400/1000000)*(Fin_Pre*Ciin_Pre-Fout_4*Ciout_4);
dcjdt = (86400/1000000)*(Fin_Pre*Cjin_Pre-Fout_4*Cjout_4);
dckdt = (86400/1000000)*(Fin_Pre*Ckin_Pre-Fout_4*Ckout_4);
dcldt = (86400/1000000)*(Fin_Pre*Clin_Pre-Fout_4*Clout_4);
dcmdt = (86400/1000000)*(Fin_Pre*Cmin_Pre-Fout_4*Cmout_4);
dcndt = (86400/1000000)*(Fin_Pre*Cnin_Pre-Fout_4*Cnout_4);
dcodt = (86400/1000000)*(Fin_Pre*Coin_Pre-Fout_4*Coout_4);
dcpdt = (86400/1000000)*(Fin_Pre*Cpin_Pre-Fout_4*Cpout_4);
dcqdt = (86400/1000000)*(Fin_Pre*Cqin_Pre-Fout_4*Cqout_4);
dcrdt = (86400/1000000)*(Fin_Pre*Crin_Pre-Fout_4*Crout_4);
dcsdt = (86400/1000000)*(Fin_Pre*Csin_Pre-Fout_4*Csout_4);
dctdt = (86400/1000000)*(Fin_Pre*Ctin_Pre-Fout_4*Ctout_4);

```

```

dcdt =
[dcadt;dcbdt;dccdt;dcddt;dcedt;dcfdt;dcgdt;dchdt;dcidt;dcjdt;dckdt;dcldt;dcmdt;dcndt;dcodt;dcpdt;dcqdt;dc
rdt;dcsdt;dctdt];

```

E.1.2 Time Dependant Scale Constant Regression

The template file below has empty matrices for the heat transfer coefficients, Brix, temperatures and time, once this data is imported the code is run to compute the time dependant constants. The matrix input handles all four effects so is a four column and n row matrix, where n is the number of variable points used per effect. Data is fitted using a least squares method.

Template.m

```
clc
```


148

```

r=1./k;
s=r.*r;
X2 = [ones(size(td)) td]; % Linear plot assumed
a3 = X2\s % Regressed value
T2 = (0:steps:12-steps)'; % Test model to 12 days
Y2 = [ones(size(T2)) T2]*a3; % Verify model
figure (6)
plot(T2,Y2(:,1),'-r',td,s(:,1),'r',T2,Y2(:,2),'-g',td,s(:,2),'g',T2,Y2(:,3),'-b',td,s(:,3),'b',T2,Y2(:,4),'-
m',td,s(:,4),'m'), grid on
legend('1/k1^2 Predicted Data','1/k1^2 Measured Data','1/k2^2 Predicted Data','1/k2^2 Measured
Data','1/k3^2 Predicted Data','1/k3^2 Measured Data','1/k4^2 Predicted Data','1/k4^2 Measured Data',0);
title('(1/k)^2 vs t')
xlabel('Time [days]');
ylabel('Inverse Overall Heat Transfer Coefficient Squared [m^4K^2/kW^2]')

% Check k predictions
Yy1=(1./Y2).^0.5;
Ty1=T2;

% Find R squareds for each fit
N = size(k);
kmean = sum(k)./N(1,1);
R(:,1) = Yy1(:,1) - kmean(1,1);
R(:,2) = Yy1(:,2) - kmean(1,2);
R(:,3) = Yy1(:,3) - kmean(1,3);
R(:,4) = Yy1(:,4) - kmean(1,4);
SR = R.^2;
SSR = sum(SR);
error_in_k_mean(:,1) = k(:,1) - kmean(1,1);
error_in_k_mean(:,2) = k(:,2) - kmean(1,2);
error_in_k_mean(:,3) = k(:,3) - kmean(1,3);
error_in_k_mean(:,4) = k(:,4) - kmean(1,4);
STO = error_in_k_mean.^2;
SSTO = sum(STO);
rsquared = SSR./SSTO

```

E.1.3 Clean Heat Transfer Coefficient Regression

The template file below has empty matrices for the heat transfer coefficients, Brix and temperatures, once this data is imported the code is run to compute the clean heat transfer coefficient values. The matrix inputs take separate data for each effect, so each vector is a one column and n row vector, where n is the number of variable points used per effect. The vector data from each effect is then combined into a single vector that is used for subsequent computations. Data is fitted using a least squares method.

Regressforko.m

```
clc
clear all
close all

k1=[];

k2=[];

k3=[];

k4=[];

B0=[];

B1=[];

B2=[];

B3=[];

B4=[];

T1j=[];

T2j=[];

T3j=[];

T4j=[];

for n=1:943
    k(n,1)=k1(n,1);
end
for n=944:1886
    k(n,1)=k2(n-943,1);
end
for n=1887:2829
    k(n,1)=k3(n-1886,1);
end
for n=2830:3772
    k(n,1)=k4(n-2829,1);
end

for n=1:943
    B(n,1)=B1(n,1);
end
for n=944:1886
    B(n,1)=B2(n-943,1);
end
for n=1887:2829
    B(n,1)=B3(n-1886,1);
end
for n=2830:3772
```

```

    B(n,1)=B4(n-2829,1);
end

for n=1:943
    Tj(n,1)=T1j(n,1);
end
for n=944:1886
    Tj(n,1)=T2j(n-943,1);
end
for n=1887:2829
    Tj(n,1)=T3j(n-1886,1);
end
for n=2830:3772
    Tj(n,1)=T4j(n-2829,1);
end

%#####
%          Variables Used                                %
%#####
%                                                    %
% ki = Measured Heat Transfer Coefficient (Vessel i)    %
% Bi = Brix fed to effect i+1                            %
% Tij = Syrup temperature                                %
%                                                    %
%#####%

x1=log(k);
x2=log(100-B);
x3=log(Tj);

%Regress as y = ao + a1x2 + a2x3
W = [ones(size(x2)) x2 x3];
b = W\x1
%Check model max error
Klg = W*b;
K = exp(Klg);

error = max(abs(K - k));
errorinK=k-K;

% Find R squareds for each fit
N=size(k);
kmean=sum(k)./N(1,1);
R = K-kmean;
SR = R.^2;
SSR = sum(SR);
error_in_k_mean = k - kmean;
STO = error_in_k_mean.^2;
SSTO = sum(STO);
rsquared = SSR./SSTO

```

APPENDIX F PROPERTY CORRELATION EQUATIONS

F.1 Property Correlation Equations

F.1.1 Pressure and Temperature

The correlations for the parameters in the model were verified and tested for their validity over the specified range used in the mill. The data for saturated steam conditions were taken from saturated steam tables in the sugar technologists handbook by Van De Pol et al. The transcribed tabular data of pressure against pressure is represented graphically below in figure F.1.

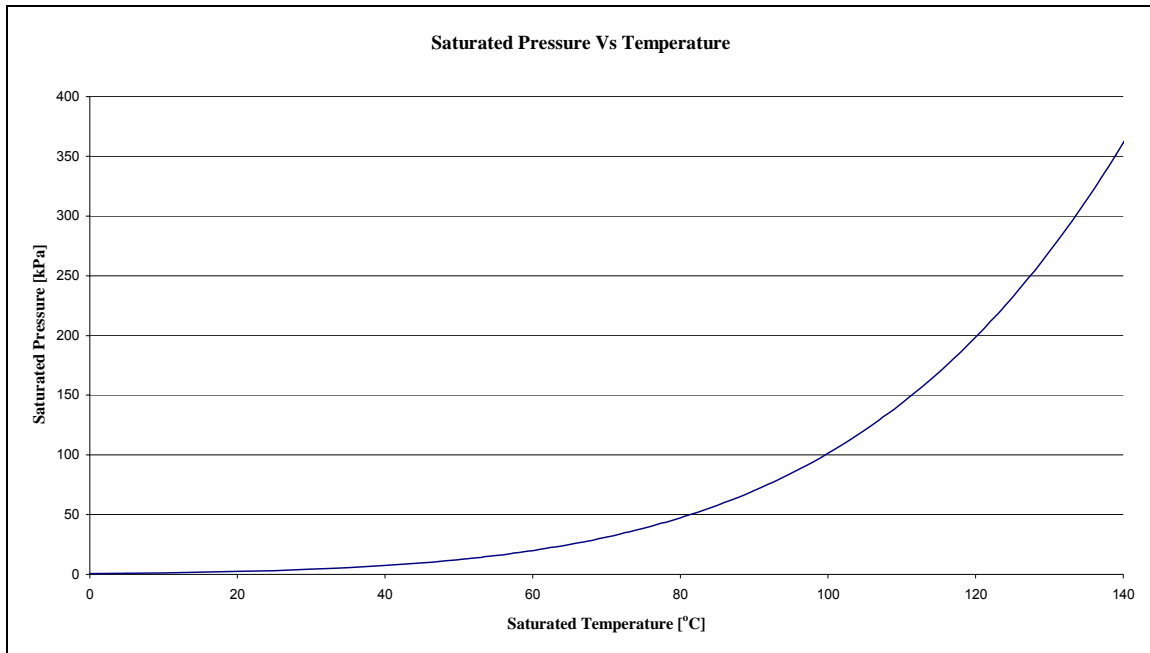


Figure F.1: Saturated steam pressure related to saturated steam temperatures from steam tables.

Since the pressure and temperature behavior is essentially exponential the accuracy of temperature and pressure interrelationships are vital. The next figure shown (figure F.2) indicates the error in the correlated saturated pressure as a function of the

saturated pressure. Figure F.2 shows the deviation between the measured and correlation values for a given saturated temperature. The equation used to produces a pressure in kPa from a temperature in K is shown as follows:

$$\ln(P^{Sat}) = 0.1333224 \left(18.3036 - \frac{3816.44}{T^{Sat} - 46.13} \right) \quad (F.1)$$

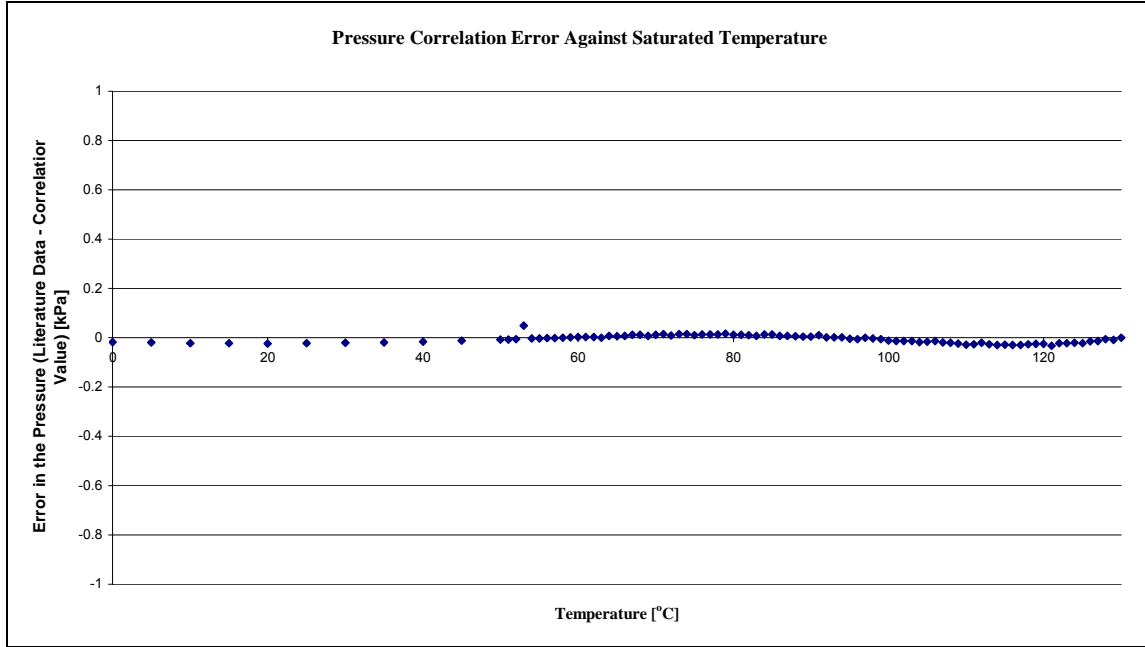


Figure F.2: Error between saturated pressure and temperature for saturated steam correlation used in modeling.

There is a correlation given in the correlations by Daubert and Danner which works fairly well (with an accuracy of less than 1% error) for the same calculation but, if a sum of squares of the error from steam table value pressures in Pascal for the temperature range of 0°C to 145°C is used, the sum of squares for the Daubert correlation compared to that for equation (F.1) is worse by a factor of around 25. The Antoine type equation in F.1 is more applicable for the temperature range of interest. The other steam properties are correlated as a function of the saturated temperature, for example the latent heat that is discussed next.

F.1.2 Latent Heat

There are slight discrepancies in the steam table between the latent heat presented and the values computed from subtracting the steam and water enthalpies from one another at the same saturated temperature together, the difference between these values is shown in figure F.3. In general this error is very small, the outliers may be due to typographic errors.

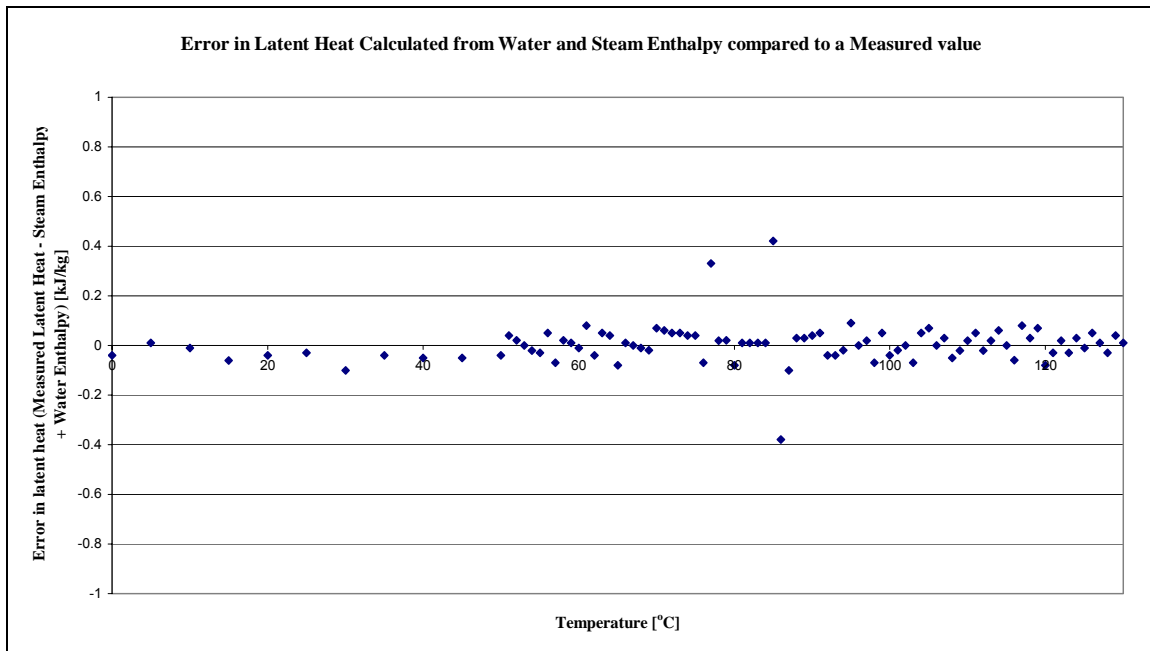


Figure F.3: Error in latent heat measured value and that computed from steam and water properties at the same saturated temperature.

When the correlation derived in equation F.2 is used, it shows good correlation between the measured and calculated values as seen in figure F.4. The scatter of the error data in figure F.4 is also good as it is not showing any significant upward or downward trend and is scattered about the zero line. The correlation used was simply a cubic polynomial fitted to literature data. The latent heat is in kJ/kg and the temperature is inputted as °C.

$$\lambda = -0.0000138T^{\text{sat}^3} + 0.00061T^{\text{sat}^2} - 2.3698T^{\text{sat}} + 2501.6 \quad (\text{F.2})$$

Again when compared over the 0°C to 145°C is used, the sum of squares for the Daubert correlation, again with an accuracy of less than 1% error, compare to that for equation F.2 is worse by a factor of around 200. The fitting curve depicted by equation F.2 to literature data is shown in figure F.5. The R^2 value of one indicates a good fit of the data by the correlation.

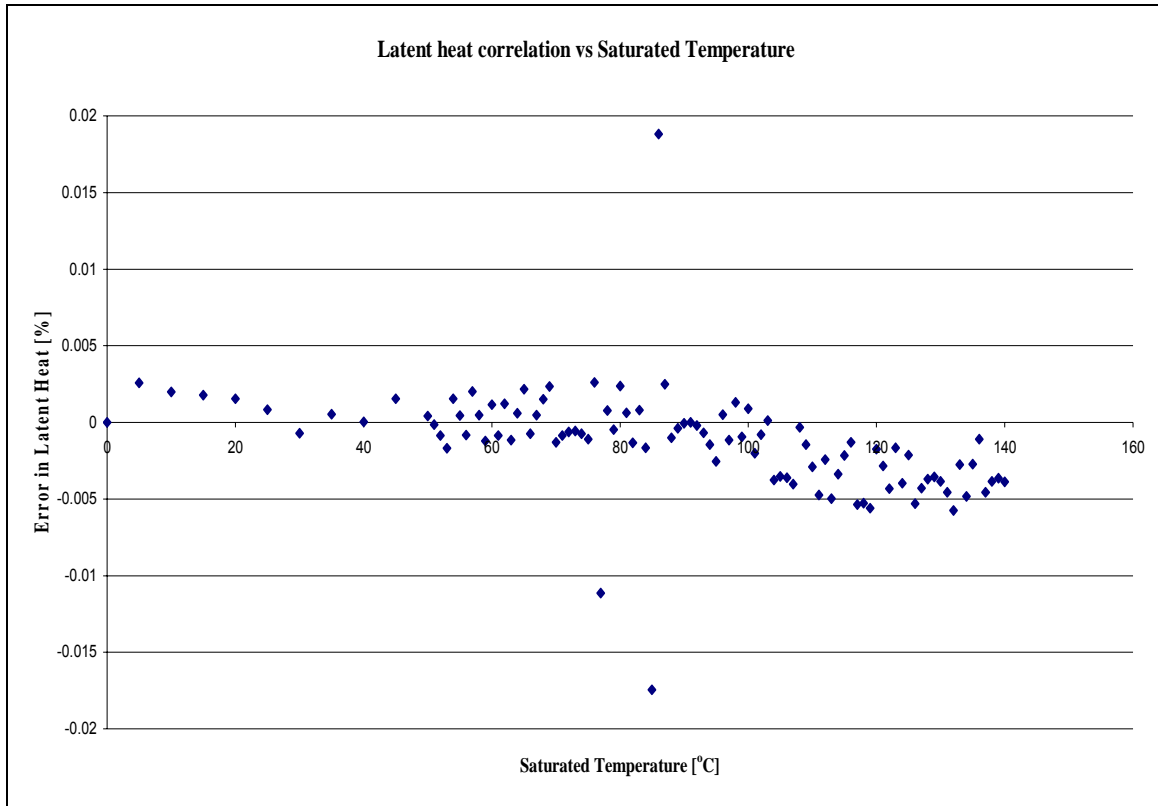


Figure F.4: Error in latent heat correlation from equation F.2 as a function of saturated temperature.

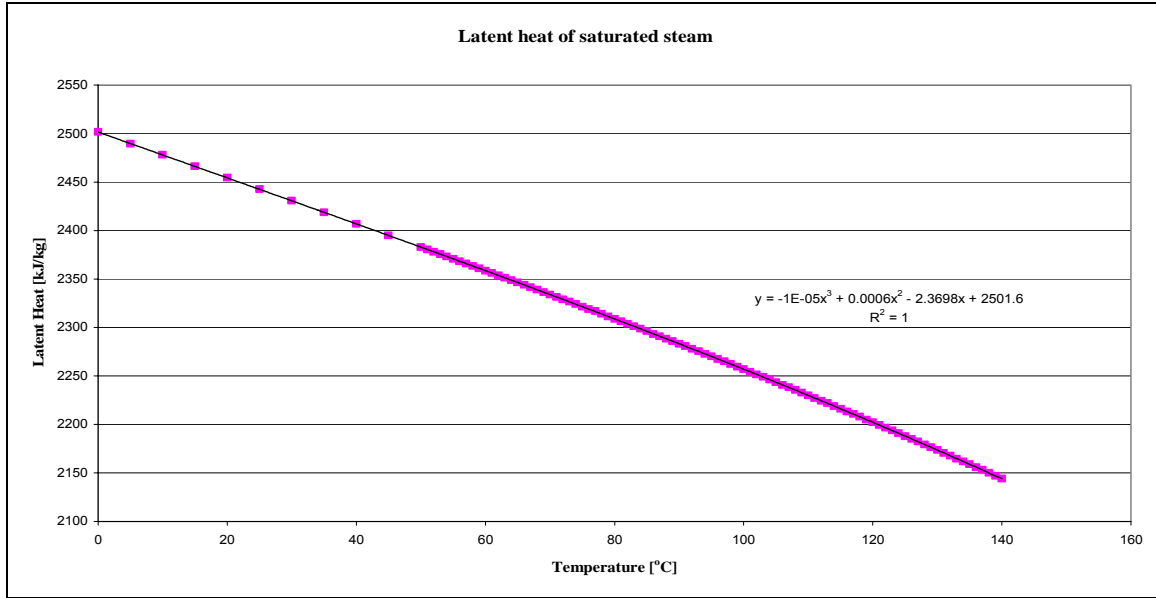


Figure F.5: The fitting of the polynomial in equation F.2 to literature latent heat data.

F.1.3 Steam Enthalpy

The steam or saturated water vapor enthalpy is also correlated using a polynomial fit to literature data. The fitting of the data is shown in figure F.6 and the error in the correlation used is shown in figure F.7.

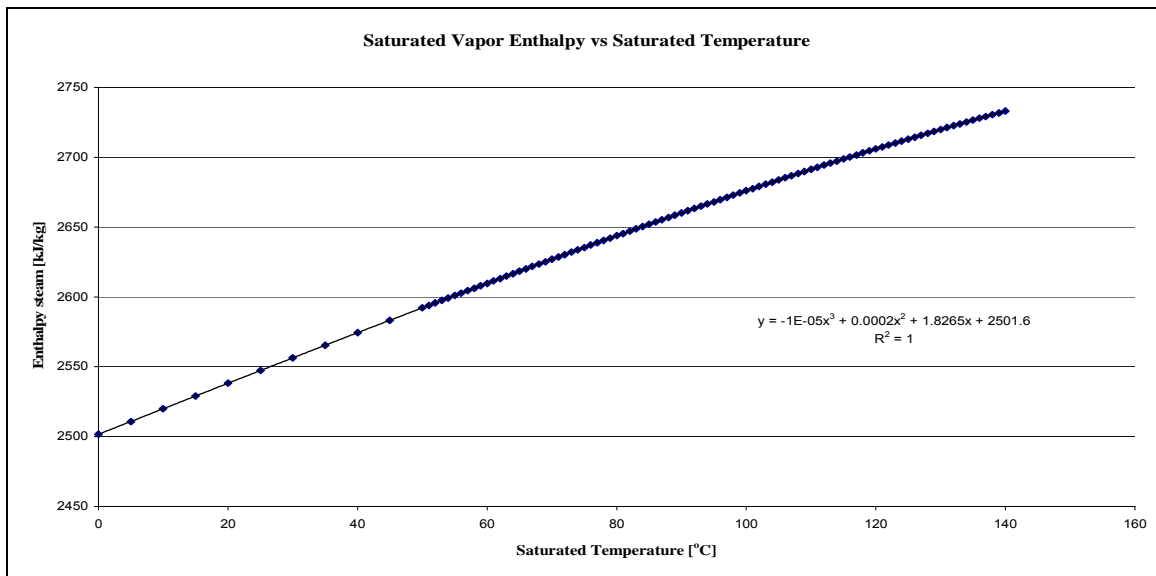


Figure F.6: The fitting of the polynomial in equation F.3 to literature vapor enthalpy data.

The equation generated for the correlation is shown in equation F.3. The vapor enthalpy is in kJ/kg and the temperature is inputted as °C.

$$H_v = -0.0000101T^{\text{sat}^3} + 0.000199T^{\text{sat}^2} + 1.8265T^{\text{sat}} + 2501.6 \quad (\text{F.3})$$

Even though the polynomial fit generates an R^2 value of one the error between measured and correlation predictions is not as good as the latent heat as there is not a good scatter of the data about the zero position. The error is however limited to less than 0.01% over the region of interest so can be used without sacrificing accuracy of model predictions significantly.

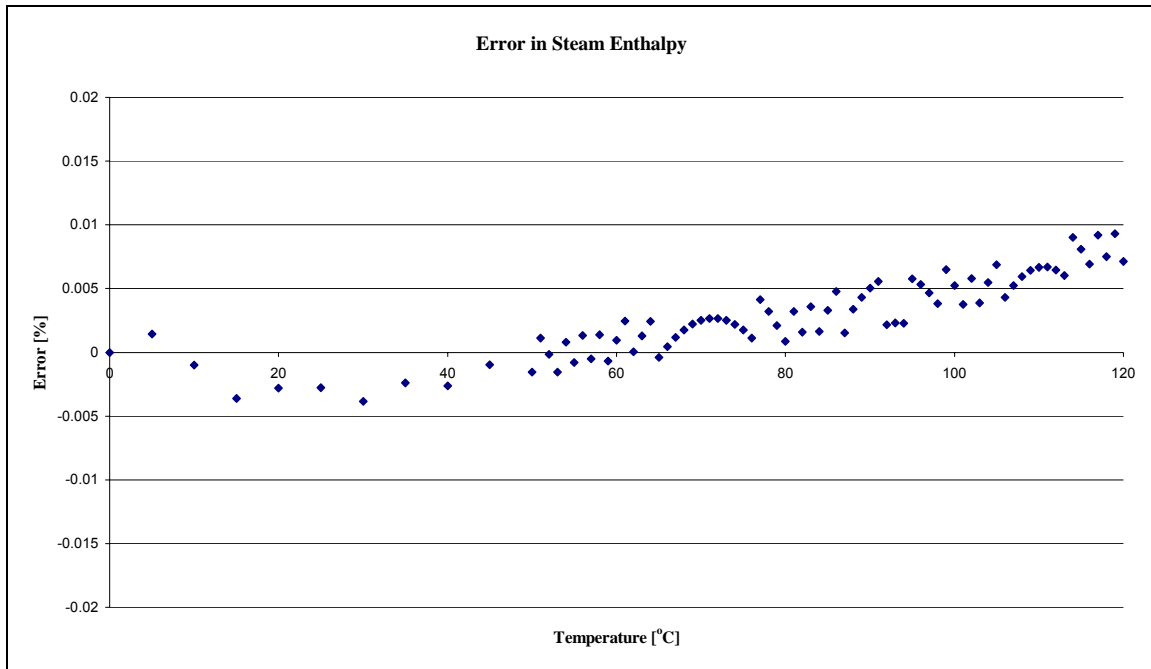


Figure F.7: Error in steam enthalpy correlation from equation F.3 as a function of saturated temperature.

F.1.4 Juice and Syrup Specific Enthalpy

The specific enthalpy of the juice and syrup for each evaporator effect was computed using the correlation from Van Der Pol et al. in their handbook. The equation

is shown below in equation (F.4) and is valid for any dissolved solids content greater than zero.

$$h = T(4.1868 - Bx*(0.0297 - 4.6E - 5*q) + 3.75E - 5*Bx*T) \quad (F.4)$$

The same equation is used for juice and syrup, the correlation is extrapolated for temperatures above 100°C.

F.1.5 Juice and Syrup Density

The density correlations are taken from the sugar technologists manual and are composed of two components, one to account for the density of pure sucrose solutions and another part to account for impurities in technical solutions. The pure solution correlation is valid for 0 to 100°C and includes a term of dissolved solids (w_s) which is approximated as Brix in the model calculations at the mill. The correlation for pure sucrose is based on measurements between 10 and 80°C with dissolved solids contents up to 60%, all other higher and lower values interpolated.

The data from the sugar technologist's handbook agrees well with the data used to generate Brix from density and temperature data by Honeywell for their Coriolis mass flow meter. The density correlation also agrees with published data in Chen and Chou (1993).

$$\rho = \rho_w + p_1 + p_2 + p_3 + p_4 + p_5 \quad (F.5)$$

$$\rho_w = (q + q_1 + q_2)/q_3 \quad (F.6)$$

$$q = 999.83952 + 16.952577*t - 7.9905127*10^{-3}*t^2 \quad (F.7)$$

$$q_1 = -46.241757*10^{-6}*t^3 + 105.84601*10^{-9}*t^4 \quad (F.8)$$

$$q_2 = -281.03006*10^{-12}*t^5 \quad (F.9)$$

$$q_3 = 1 + 16.887236*10^{-3}*t \quad (F.10)$$

$$w = w_s/100 \quad (F.11)$$

$$\tau = (t-20)/100 \quad (F.12)$$

$$p_1 = b_1*w + b_2*w^2 + b_3*w^3 + b_4*w^4 + b_5*w^5 + b_6*w^6 \quad (F.13)$$

$$p_2 = (b_{11}*w + b_{12}*w^2 + b_{13}*w^3 + b_{14}*w^4 + b_{15}*w^5)*\tau \quad (F.14)$$

$$p_3 = (b_{21}*w + b_{22}*w^2 + b_{23}*w^3 + b_{24}*w^4)*\tau^2 \quad (F.15)$$

$$p_4 = (b_{31}*w + b_{32}*w^2 + b_{33}*w^3)*\tau^3 \quad (F.16)$$

$$p_5 = (b_{41}*w + b_{42}*w^2)*\tau^4 \quad (F.17)$$

$$b_1 = 385.1761 \quad (F.18)$$

$$b_2 = 135.3705 \quad (F.19)$$

$$b_3 = 40.9299 \quad (F.20)$$

$$b_4 = -3.9643 \quad (F.21)$$

$$b_5 = 13.4853 \quad (F.22)$$

$$b_6 = -17.2890 \quad (F.23)$$

$$b_{11} = -46.2720 \quad (F.24)$$

$$b_{12} = -7.1720 \quad (F.25)$$

$$b_{13} = 1.1597 \quad (F.26)$$

$$b_{14} = 5.1126 \quad (F.27)$$

$$b_{15} = 17.5254 \quad (F.28)$$

$$b_{21} = 59.7712 \quad (F.29)$$

$$b_{22} = 7.2491 \quad (F.30)$$

$$b_{23} = 12.3630 \quad (F.31)$$

$$b_{24} = -35.4791 \quad (F.32)$$

$$b_{31} = -47.2207 \quad (F.33)$$

$$b_{32} = -21.6977 \quad (F.34)$$

$$b_{33} = 27.6301 \quad (F.35)$$

$$b_{41} = 18.3184 \quad (F.36)$$

$$b_{42} = 12.3081 \quad (F.37)$$

For pure solutions in the temperature range 100 to 150°C another correlation has to be used. The correlation for pure sucrose at these elevated temperatures is based on measurements between 100 and 140°C with dissolved solids contents up to 30%, all other higher values interpolated.

$$\rho = A + B*t + C*t^2 \quad (F.38)$$

$$A = 1008.79 + 3.80029*w_s + 0.0190338*w_s^2 \quad (F.39)$$

$$B = -0.288221 - 0.0020088*w_s - 0.0000769467*w_s^2 \quad (F.40)$$

$$C = -0.00215765 + 0.00000724506*w_s + 0.000000408157*w_s^2 \quad (F.41)$$

For technical solutions:

Values greater than 69% for w_{DS} (Brix) are extrapolated. q is the purity as a percentage.

$$\rho = \rho_p + \Delta\rho \quad (F.42)$$

$\Delta\rho$ is the difference in densities between pure and technical (real) sucrose solutions.

$$\Delta\rho = -1 + \exp[(-6.927*10^{-6}*w_{DS}^2 - 1.165*10^{-4}*w_{DS})*(q-100)] \quad (F.43)$$

A correlation that is simpler for density that can be applied to sugar solutions is as shown in equation (F.44). This equation is only valid for a low temperature range and when the temperature increases to above about 90°C to 100°C the correlation becomes invalid and thus cannot be used in the model as the feed temperature is around 115°C so using this correlation would cause erroneous densities and throw the model computations out.

$$\rho = 1000 \left(1 + \frac{B * (B + 200)}{54000} \right) \left(1 - 0.036 \frac{(T - 20)}{(160 - T)} \right) \quad (\text{F.44})$$

F.2 Other Correlations Used

F.2.1 Boiling Point Elevation

The boiling point elevation is a function of Brix, temperature and purity, attempts have been made to try reduce the number of variables in this equation and this has resulted in the popular and simplified form of Hugot (1986) as seen in equation (F.45).

$$BPE_{Brix} = \frac{2B}{100 - B} \quad (\text{F.45})$$

This equation is fairly accurate for low Brix systems but at higher Brix the purity and temperature of the system have a much larger effect on the boiling point elevation. The correlation could be used with reasonable accuracy for the first few effects but the last effect requires a correlation that will correct for temperature and purity. In figure F.8 the effect of temperature are clearly shown as a function of Brix for a fixed purity of 90%, the diagram also indicates the downfall of equation (F.45) as a plot is included in the figure.

If the effect of purity is considered then a plot such as figure F.9 can be drawn up. The temperature is fixed at 80°C for this evaluation. It can be seen that the purity also has a rather large effect on the boiling point elevation but the effect is more marked under the last effect conditions. The effect of purity is not as significant as the temperature effect but still needs to be accounted for especially at higher Brix conditions.

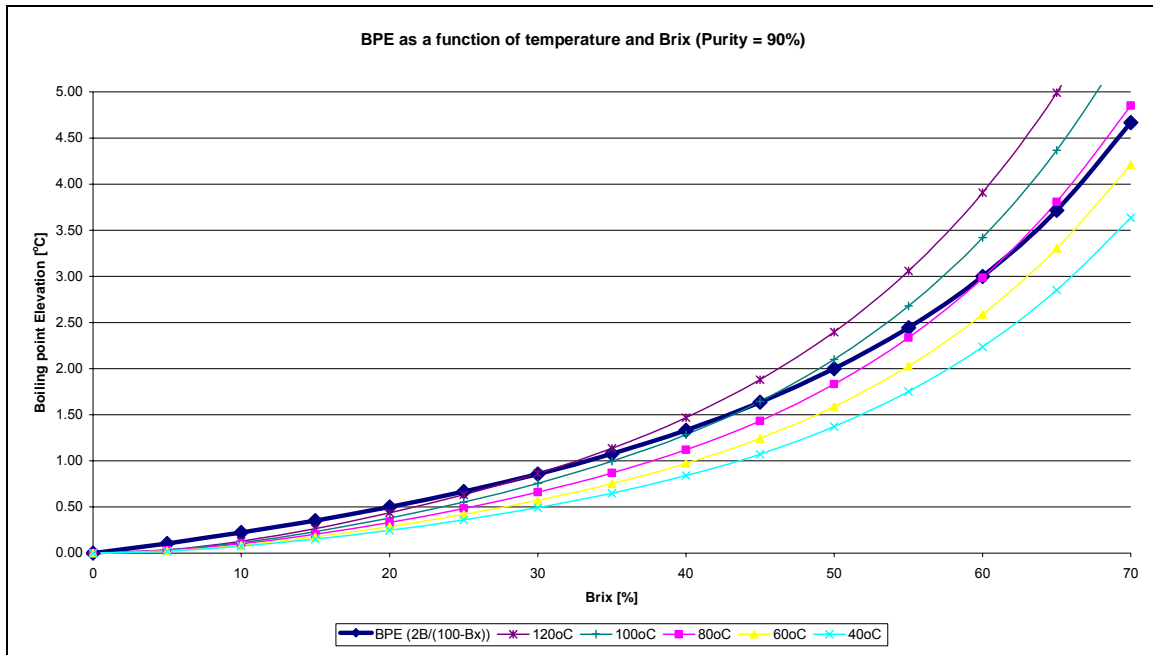


Figure F.8: Boiling point elevation as a function of temperature at a purity of 90%.

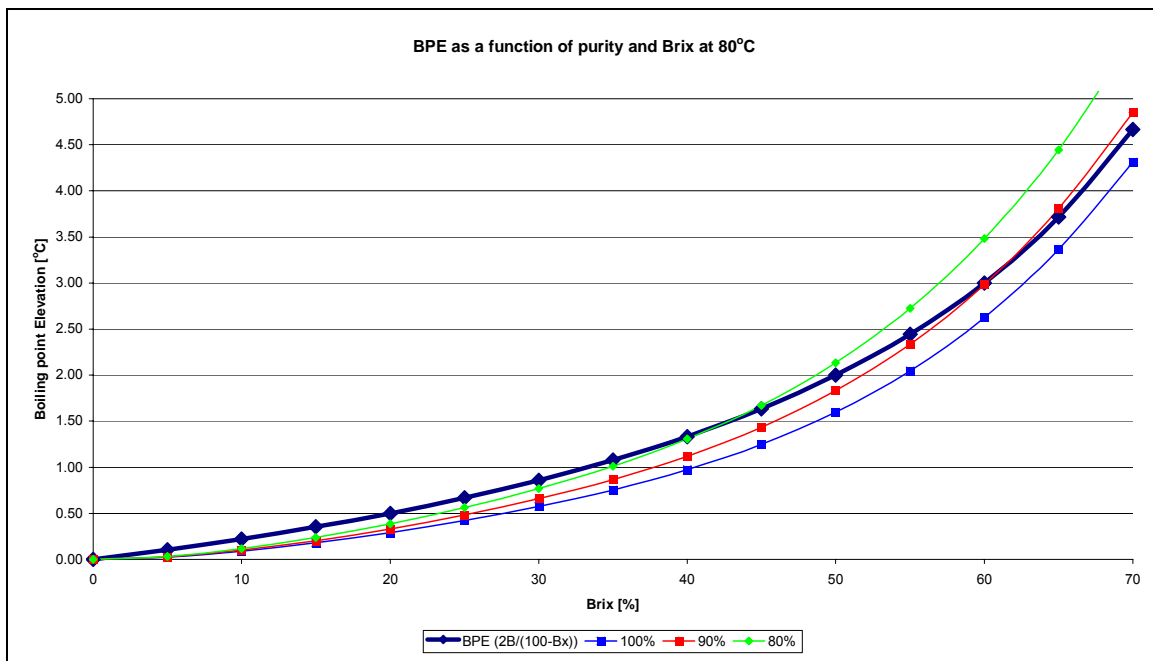


Figure F.9: Boiling point elevation as a function of purity at a temperature of 80°C.

The equations used in the simulation utilize purity, temperature and Brix effects and are shown in the next few sets of equations. The equations are derived for 0 to 60 Brix solutions.

$$\Delta T_{BPE-Brix} = a \cdot B^2 \frac{(273+T)^2}{(374.3-T)^{0.38}} (b \cdot (B-k)^2 + c) \quad (F.46)$$

The terms a, b, c and k are seen below:

$$k = 40 \quad (F.47)$$

$$a = 1.59515E-4 - 2.00092E-6q + 8.01933E-9q^2 \quad (F.48)$$

$$b = 1.84440E-6 - 3.04380E-8q + 1.72958E-10q^2 \quad (F.49)$$

$$c = 1.08062E-3 + 2.89645E-6q - 3.01416E-8q^2 \quad (F.50)$$

APPENDIX G ELECTROMAGNETIC FLOW METER SIZING AT ST JAMES

G.1 Electromagnetic Flow Meter Sizing at St James

G.1.1 Sizing the Meters

The mill had at their disposal meters of the following sizes: 4", 8" and 10" (The 6" meter was used on another section of the mill). Ultra Mag® makes the electromagnetic flow meters. The operating ranges are as follows for the units available:

4" meter: 8 to 1,440 GPM

8" meter: 33 to 5,636 GPM

10" meter: 52 to 8,864 GPM

The calculations indicate that the 4" meter would be sufficient for the syrup out flow measurement and the 8" meter would be capable of recording the juice feed rate to the evaporator sets. The calculations were based on the 2001 season data from the Gilmore Sugar Manual 2002/2003. The calculated juice flow to the heaters is around 1039 GPM based on the 2002/2003 season. On a mill tour there were indications that this actual flow varied from 1000 to 1400 GPM. For the calculations consider the low flow of this range as a minimum value to work with. (The chosen meters are slightly larger than the ideal sizing so the maximum flow on the meters should not be a problem but one must ensure that the meter is clear of the minimum flow limit.).

The heater juice has a Brix of 16.65 (density is $\pm 1065 \text{ kg/m}^3$) according to the data from previous seasons; this juice is then fed to the pre-evaporators before being passed to the quadruple effect. The Brix of the feed to the quad effect for which the control is to be installed was not known when the mill was visited so an assumption

needs to be made as to it's Brix. There will not be a significant Brix change over the pre-evaporators, so assuming the Brix is about 18 feeding the quad effect the flow calculations will be as follows:

$$\text{Density at 18 Brix} = \pm 1071 \text{ kg/m}^3$$

$$\text{Density at 60 Brix} = \pm 1285 \text{ kg/m}^3$$

$$\text{Density at 12 Brix} = \pm 1045 \text{ kg/m}^3$$

$$\begin{aligned}\text{Flow to evaporators} &= (16.65/18) * (1065/1071) * 1000 \text{ GPM} \\ &= 920 \text{ GPM [Within the 8" meter range of 33 to 5,636 GPM]} \\ (\text{lower 20\% of the maximum scale and velocity in meter} &= 1.79 \text{ m/s})\end{aligned}$$

$$\begin{aligned}\text{Flow out evaporators} &= (18/60) * (1071/1285) * 920 \text{ GPM} \\ &= 230 \text{ GPM [Within the 4" meter range of 8 to 1,440 GPM]} \\ (\text{Lower 16\% of the maximum scale and velocity in meter} &= 1.79 \text{ m/s})\end{aligned}$$

As seen with comparing the ranges these flows are a little on the low end of the scale but in the case of increased flow and plant expansions the meters will not have to be replaced and can handle much increased flow rates.

G.1.2 Installation Options of the Electromagnetic Flow Meters:

To prevent flash errors (two phase flow) the following arrangements can possibly be used. The increased pressure due to the hydrostatic head acting on the feed should suppress flashing (if present) and ensure only liquid flow in the pipe. The optimum installation is shown in figure G.1.

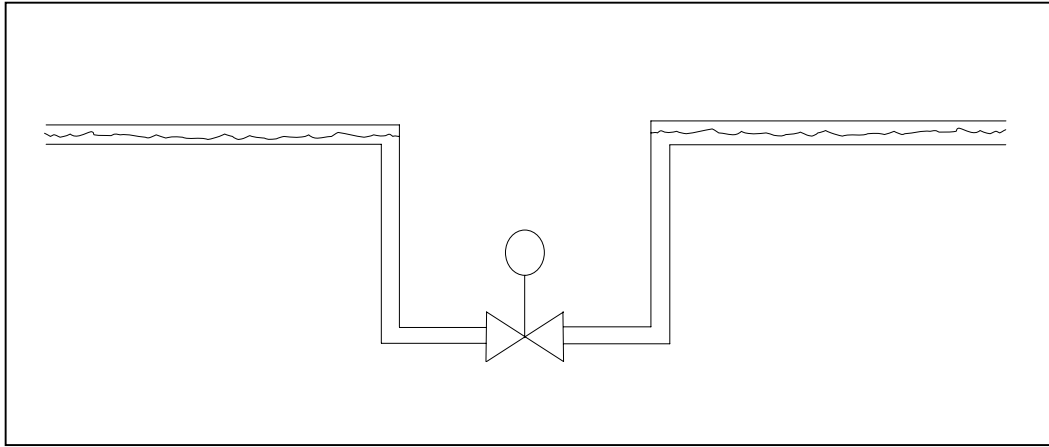


Figure G.1: Installation of a flow meter to ensure single phase flow on the pipe section containing the meter.

The meters can also be installed horizontally or vertically but there may be errors if there is two phase fluid flow, if the liquid starts to flash. The flashing amount will depend on the conditions from the pre-evaporator to the first of the quadruple effect units. The installed units, because of their locations, could not easily have the liquid trap installed as shown in figure G.1, so necessitating them to be installed as in figure G.2.

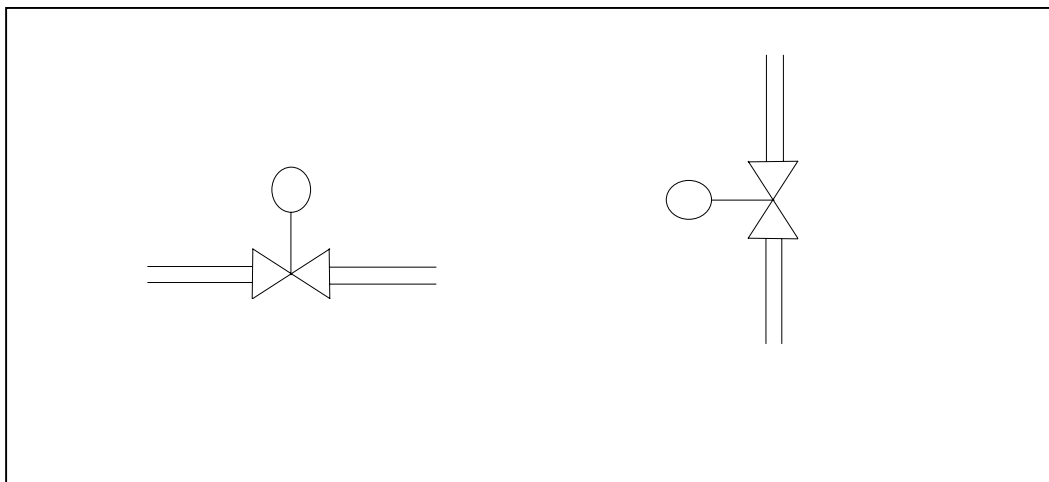


Figure G.2: Horizontal alignment (left) and vertical alignment (right) for the mag flow meters used at St James.

APPENDIX H RTD CALIBRATION

H.1 RTD Calibration

The RTD's were calibrated by placing them in a beaker of water and then the beaker was stirred while being heated. A calibrated thermometer was placed in the water to record the actual water temperature. When the thermometer reached each degree marking the reading taken by that RTD was recorded from the controller along with the calibrated thermometer temperature. This was performed until the water began to boil at 100°C. The heat was then removed and the temperature recorded on each degree Celsius while the water cooled from both the controller and thermometer. The results here show a slight hysteresis effect but as can be seen the RTD's appear extremely accurate. The setup used is shown in figure (H.1).



Figure H.1: The calibration of RTD's using a heated beaker and calibrated thermometers.

The resulting calibration curves for each RTD are shown next along with the tag of each probe.

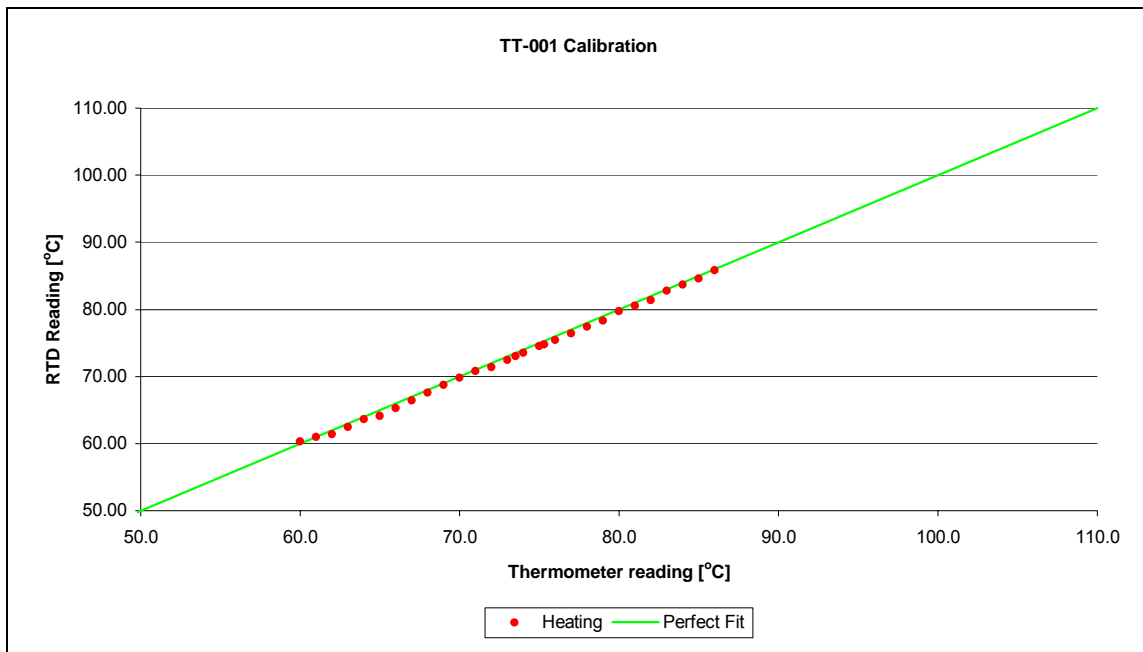


Figure H.2: The calibration curve of RTD TT-001.

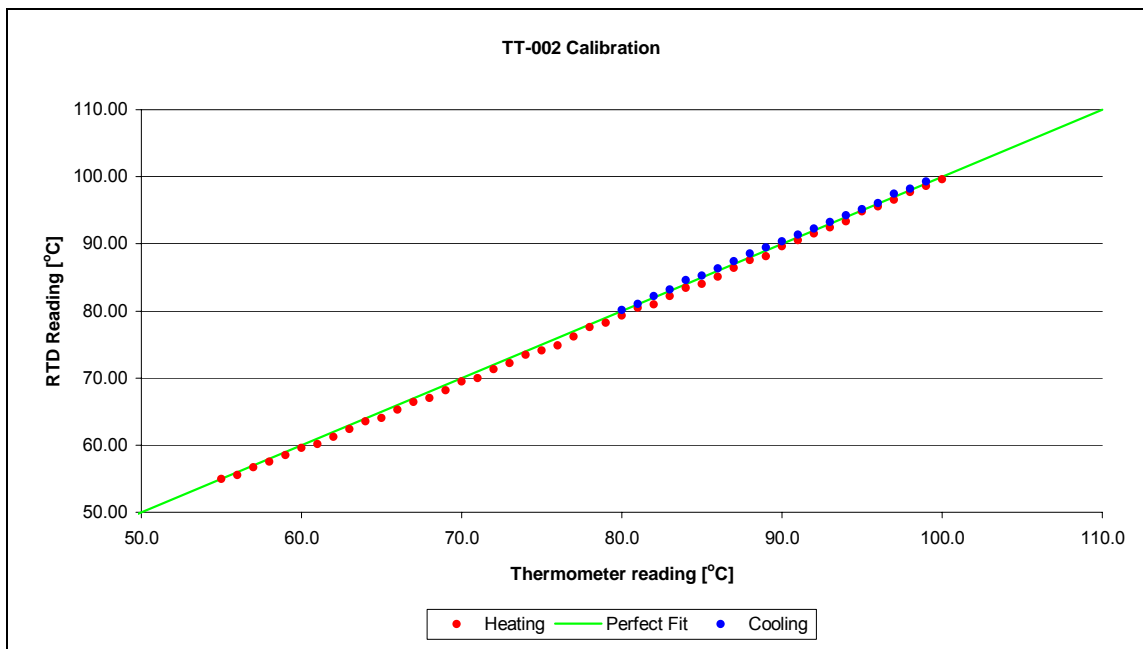


Figure H.3: The calibration curve of RTD TT-002.

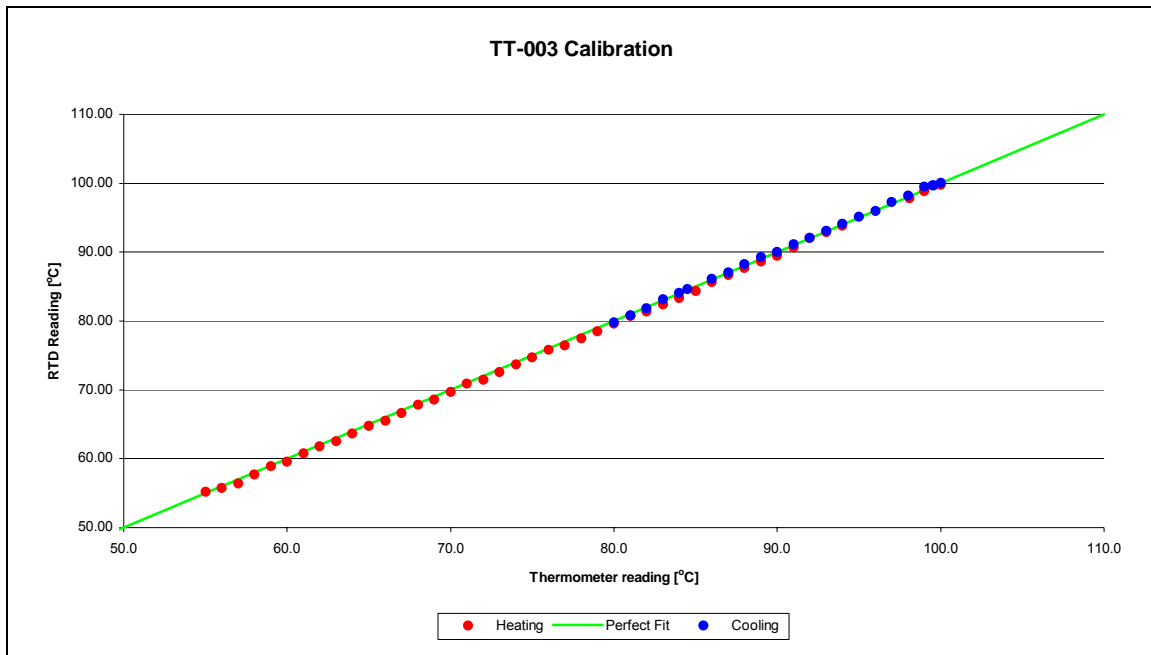


Figure H.4: The calibration curve of RTD TT-003.

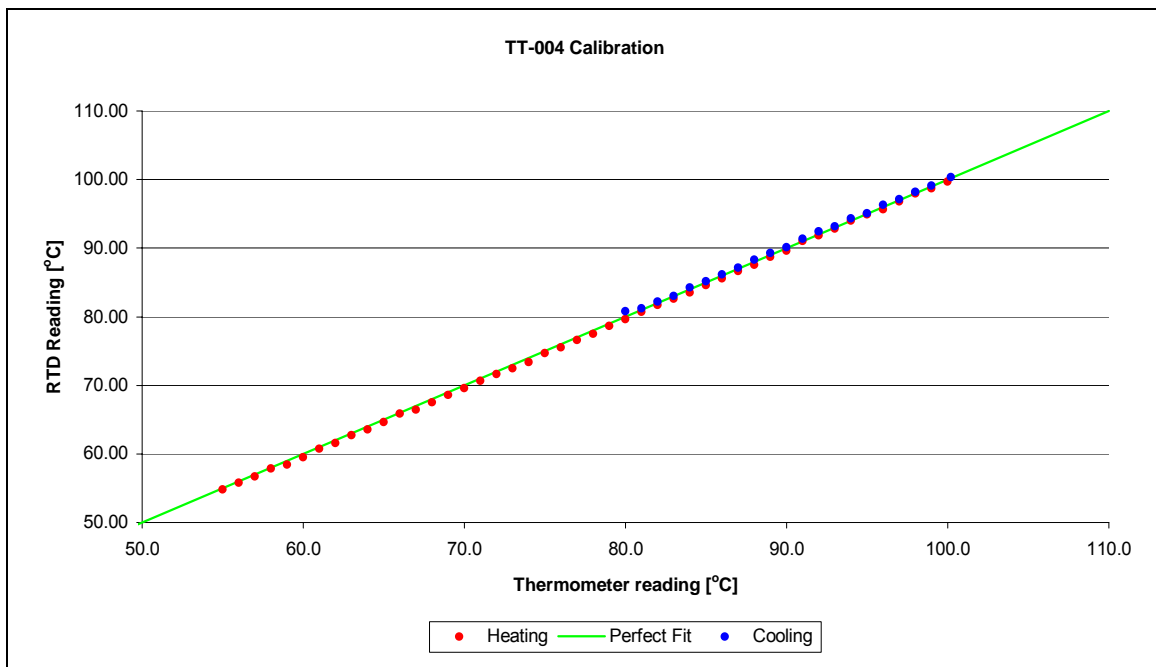


Figure H.5: The calibration curve of RTD TT-004.

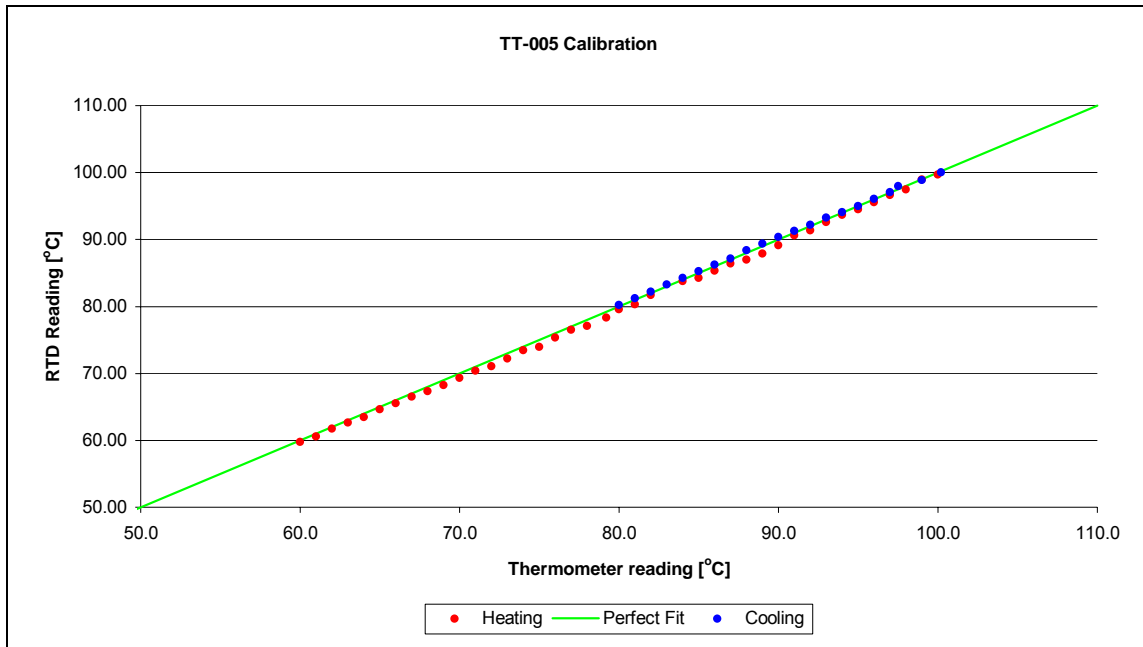


Figure H.6: The calibration curve of RTD TT-005.

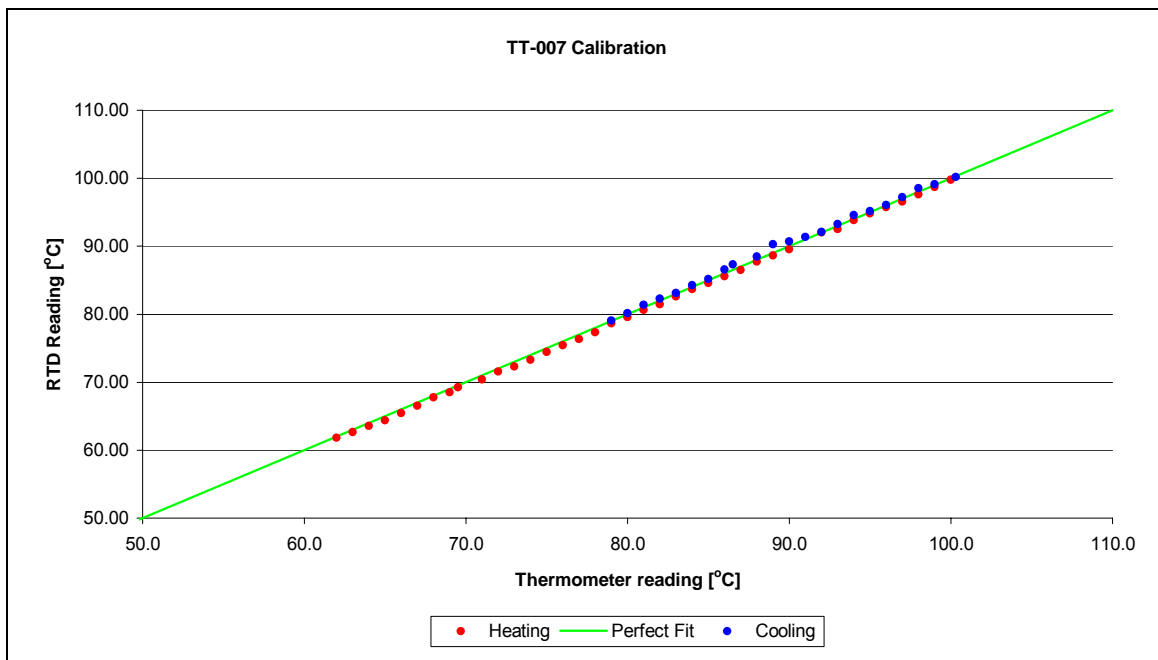


Figure H.7: The calibration curve of RTD TT-007.

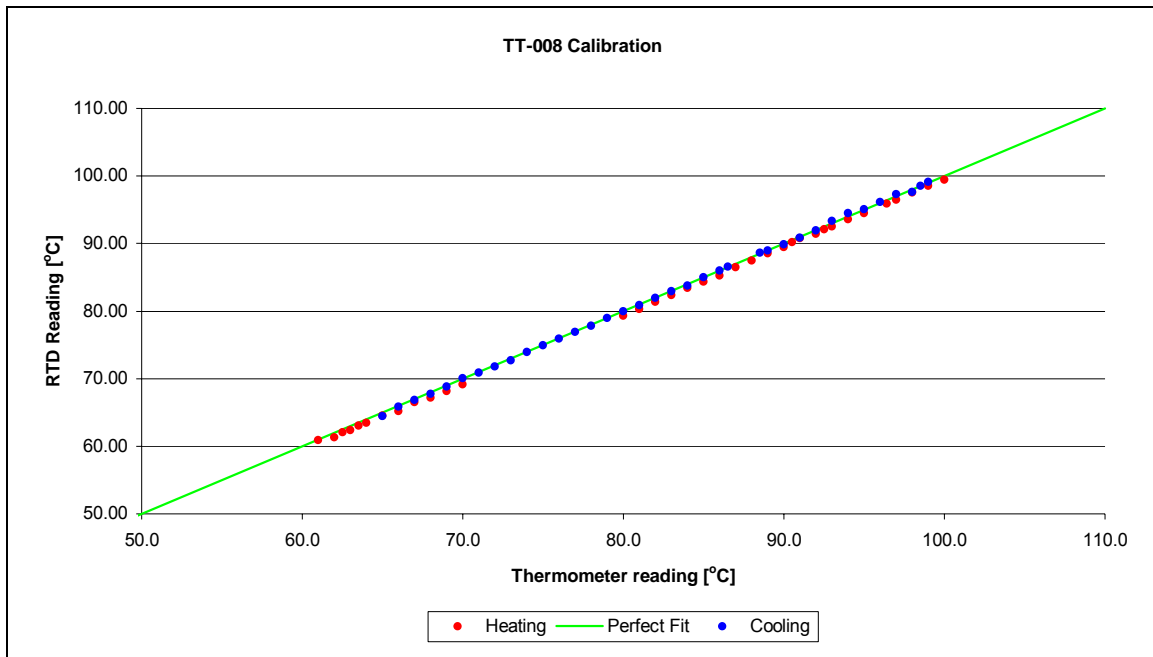


Figure H.8: The calibration curve of RTD TT-008.

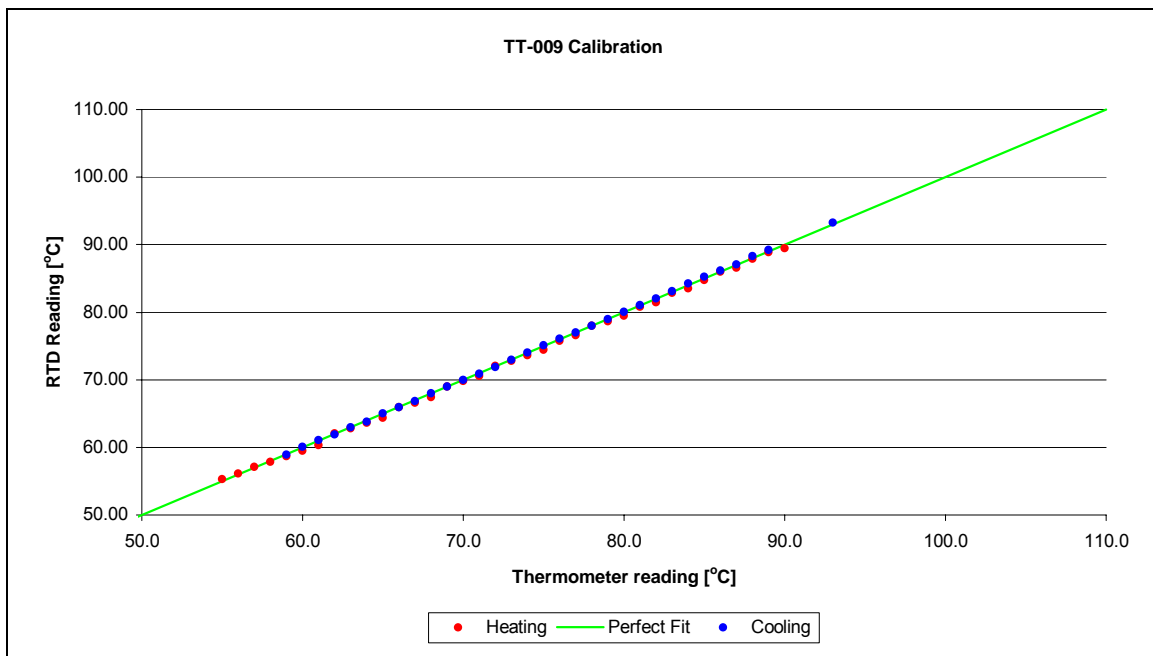


Figure H.9: The calibration curve of RTD TT-009.

The temperatures of the calandria were checked while the mill was operating, the pressure was recorded in the calandria using a manometer and assuming saturated conditions this was converted to a saturated temperature. The temperature recorded on

the controller is compared to the result from the saturated pressure and comparisons were made. The results are shown in table H.1 and the results show that only the third effect calandria has a significant error of 1.4°C.

Table H.1: The calibration of the calandria RTD's based on saturated steam pressure.

Location	Vessel side height [in]	Atm side height [in]	P (g) [in Hg]	P (abs) [in Hg]	P [kPa]	T calc [°C]	T recorded [°C]	ΔT [°C]
T _{S2}	-6.0	6.2	12.2	42.121	142.639	109.87	109.78	0.10
T _{S2}	-6.7	6.7	13.4	43.321	146.703	110.71	110.63	0.08
T _{V2}	-2.6	2.8	5.4	35.321	119.611	104.72	105.16	-0.44
T _{S3}	-3	3.1	6.1	36.021	121.982	105.29	103.89	1.40
T _{S3}	-2.9	3.2	6.1	36.021	121.982	105.29	103.67	1.62
T _{S3}	-2.5	2.7	5.2	35.121	118.934	104.55	103.18	1.37
T _{V3}	0.9	-0.7	-1.6	28.321	95.907	98.47	98.89	-0.42
T _{V3}	0.9	-0.7	-1.6	28.321	95.907	98.47	98.85	-0.38
T _{S4}	1	-0.8	-1.8	28.121	95.229	98.27	98.52	-0.24
T _{S4}	1.1	-0.9	-2.0	27.921	94.552	98.07	98.60	-0.52
T _{S4}	1.2	-0.95	-2.2	27.771	94.044	97.93	98.26	-0.33
T _{V4}	-	-	-23.9	6.021	20.390	60.50	61.40	-0.90
T _{V4}	-	-	-23.8	6.121	20.729	60.86	61.40	-0.54

VITA

David Timothy Solberg was born on 29 February 1980, in Mhangura, Zimbabwe. He attended Lomagundi College Preparatory School before moving to St John's College in Harare, Zimbabwe, and left high school in 1998. He attended the University of Natal, Durban campus in South Africa for four years to obtain a bachelor's degree in chemical engineering in 2002. In 2003 he was offered a graduate assistantship with Audubon Sugar Institute to further his studies and obtain a master's degree in chemical engineering with a minor in sugar process engineering at Louisiana State University in the United States of America.

He is an Associate Member of the British Institute of Chemical Engineers and is a member of the Golden Key Honor Society.